

INFORMATION TO USERS

This was produced from a copy of a document sent to us for microfilming. While the most advanced technological means to photograph and reproduce this document have been used, the quality is heavily dependent upon the quality of the material submitted.

The following explanation of techniques is provided to help you understand markings or notations which may appear on this reproduction.

1. The sign or "target" for pages apparently lacking from the document photographed is "Missing Page(s)". If it was possible to obtain the missing page(s) or section, they are spliced into the film along with adjacent pages. This may have necessitated cutting through an image and duplicating adjacent pages to assure you of complete continuity.
2. When an image on the film is obliterated with a round black mark it is an indication that the film inspector noticed either blurred copy because of movement during exposure, or duplicate copy. Unless we meant to delete copyrighted materials that should not have been filmed, you will find a good image of the page in the adjacent frame.
3. When a map, drawing or chart, etc., is part of the material being photographed the photographer has followed a definite method in "sectioning" the material. It is customary to begin filming at the upper left hand corner of a large sheet and to continue from left to right in equal sections with small overlaps. If necessary, sectioning is continued again—beginning below the first row and continuing on until complete.
4. For any illustrations that cannot be reproduced satisfactorily by xerography, photographic prints can be purchased at additional cost and tipped into your xerographic copy. Requests can be made to our Dissertations Customer Services Department.
5. Some pages in any document may have indistinct print. In all cases we have filmed the best available copy.

University
Microfilms
International

300 N. ZEEB ROAD, ANN ARBOR, MI 48106
18 BEDFORD ROW, LONDON WC1R 4EJ, ENGLAND

8027530

SATAKE, AKIO

NUMERICAL ANALYSIS OF CERTAIN CONSTRAINED OPTIMIZATION
PROBLEMS IN NONLINEAR MECHANICS

The University of Oklahoma

PH.D.

1980

University
Microfilms
International

300 N. Zeeb Road, Ann Arbor, MI 48106

18 Bedford Row, London WC1R 4EJ, England

THE UNIVERSITY OF OKLAHOMA
GRADUATE COLLEGE

NUMERICAL ANALYSIS OF CERTAIN CONSTRAINED OPTIMIZATION PROBLEMS
IN NONLINEAR MECHANICS

A DISSERTATION
SUBMITTED TO THE GRADUATE FACULTY
in partial fulfillment of the requirements for the
degree of
DOCTOR OF PHILOSOPHY

BY
AKIO SATAKE
Norman, Oklahoma
1980

NUMERICAL ANALYSIS OF CERTAIN CONSTRAINED OPTIMIZATION PROBLEMS
IN NONLINEAR MECHANICS

APPROVED BY

J. N. Reddy
J. N. Reddy, Ph.D.
(Co-Chairman)

Y. K. Sasaki
Y. K. Sasaki, Ph.D.
(Co-Chairman)

C. W. Bert
C. W. Bert, Ph.D.

M. L. Rasmussen
M. L. Rasmussen, Ph.D.

L. W. White
L. W. White, Ph.D.

DEDICATION

I would like to dedicate this work to my wife, Michiko.

ACKNOWLEDGMENTS

First of all, I wish to express my sincere gratitude and appreciation to Dr. J. N. Reddy for his constant encouragement, counsel, but most importantly for his stimulation of my research interests. My gratitude is extended to Dr. Y. K. Sasaki for his guidance and influence on my academic attitude as well as my philosophy. Without their advice, this dissertation could not have been completed.

I am very grateful to Dr. C. W. Bert for his continual willingness to help my research, and to Dr. M. L. Rasmussen for his superb teaching in analytical and physical aspects.

A special thanks is due to Dr. L. W. White for his strong interest in my dissertation, and to Dr. M. Kawahara, the professor of Chuo University, Tokyo, for his constant support. Thanks also to Mrs. Chris Viney who helped in proofreading and Mrs. Betty Sudduth for her superb typing.

The results reported herein were obtained during an investigation supported by ARCO, Chevron, U.S.A., Exxon and General Crude and by the Global Atmospheric Research Program, Climate Dynamics Research Section, Division of Atmospheric Sciences, National Science Foundation, through Grant ATM77-23111. Their support is gratefully acknowledged.

ABSTRACT

A large number of problems in engineering science involve the solution of differential equations subject to some subsidiary conditions, called constraints (of equality or inequality type). While the derivation of the governing equations is not unduly difficult, it is considerably more difficult to analyze problems with constraints. Most practical methods of analysis are based on unconstrained minimization techniques, such as the Lagrange multiplier method and the penalty function method. These techniques transform a given constrained minimization problem into a set of unconstrained minimization problems. In the practical implementation of these methods, one encounters problems in terms of computer storage, computational time, and more importantly numerical instabilities. The present study is concerned with alternate formulation of two practically important problems which have received great interest of researchers. The novelty of the present work lies in the use of the finite element method in conjunction with variational inequality approach and penalty function method.

The first problem is concerned with elastic-plastic torsion of a bar subjected to terminal twisting couples. Here the yield criterion of plasticity imposes inequality constraints on the gradient of the stress function. The variational inequality approach was used in the

formulation and numerical solution of the problem. The present study concludes that the variational inequality approach is numerically accurate and computationally efficient. Several noncircular and non-rectangular cross section bars were used to show the stress contours and elasto-plastic interface as a function of the twisting couple. Application of the method to two- and three-dimensional elasto-plastic problems is awaiting.

The second problem is concerned with the natural convection of a laminar incompressible Newtonian Fluid in enclosures. Here the divergence-free condition on the velocity field is treated as a constraint. The penalty function method was employed to formulate the problem, and the finite element method was used to solve the problem numerically. A finite element based on the stream function-vorticity formulation was also developed to assess the accuracy and computational simplicity of the penalty-finite element developed herein. The study indicates the penalty-finite element is computationally less expensive, while yielding competitively (or better) accurate solutions for moderately high Rayleigh numbers ($\leq 10^6$). Extension of the present work to time dependent and three dimensional flows is of great interest to industry.

TABLE OF CONTENTS

| | Page |
|---|------|
| ACKNOWLEDGMENTS | iii |
| ABSTRACT | iv |
| LIST OF FIGURES | viii |
| LIST OF TABLES | xi |
| LIST OF SYMBOLS | xii |
| Chapter | |
| I. INTRODUCTION | 1 |
| 1.1 Opening Comment | 1 |
| 1.2 Brief Review on Pertinent Literatures | 3 |
| 1.3 Thesis Objectives | 6 |
| II. GOVERNING EQUATIONS | 7 |
| 2.1 Elastic-plastic Torsion of Bar | 7 |
| 2.2 Natural Convection in Enclosure | 10 |
| III. GENERAL FORMULATIONS OF CONSTRAINED OPTIMIZATION PROBLEMS | 15 |
| 3.1 Introductory Comment | 15 |
| 3.2 Weak Formulation | 16 |
| 3.3 Lagrange Multiplier Formulation | 18 |
| 3.4 Penalty Formulation | 20 |
| 3.5 Variational Inequality Formulation | 24 |

| Chapter | Page |
|---|------|
| IV. NUMERICAL METHOD FOR ELASTIC-PLASTIC TORSION BY VARIATIONAL INEQUALITY | 30 |
| 4.1 Variational Formulations | 30 |
| 4.2 Numerical Procedures | 37 |
| 4.3 Numerical Results | 39 |
| V. A COMPARISON OF PENALTY FINITE ELEMENT MODEL WITH THE STREAM FUNCTION-VORTICITY MODEL OF NATURAL CONVECTION. | 55 |
| 5.1 Penalty Formulation and Stream Function-Vorticity Formulation | 55 |
| 5.1.1 Penalty Formulation | 55 |
| 5.1.2 Stream Function-Vorticity Formulation | 57 |
| 5.2 Finite Element Formulation | 59 |
| 5.2.1 Penalty-Finite Element Model | 59 |
| 5.2.2 Stream Function-Vorticity Finite Element Model | 60 |
| 5.2.3 Computational Procedure | 61 |
| 5.3 Numerical Results and Discussions | 63 |
| 5.4 Concluding Remarks | 71 |
| VI. CONCLUSIONS AND RECOMMENDATIONS FOR FUTURE RESEARCH. | 101 |
| BIBLIOGRAPHY | 104 |
| APPENDIX. Numerical Solution of $ \nabla\phi ^2 = \tau_p^2$ in $\Omega \subset \mathbb{R}^2$ | 111 |

LIST OF FIGURES

| Figure | | Page |
|--------|---|------|
| 3.1 | Minimum point x_0 of function $f(x)$ | 26 |
| 3.2 | Geometrical interpretation of projection | 26 |
| 3.3 | Deflection of continuous beam | 29 |
| 4.1 | Mesh for circular cross section with $r=1$ | 43 |
| 4.2 | Comparison of elastic-plastic solution for circular cross section | 44 |
| 4.3 | Influence of the acceleration parameter on the convergence of ϕ_{\max} | 47 |
| 4.4a | Convergence of λ | 48 |
| 4.4b | Convergence of p | 48 |
| 4.4c | The number of total iterations at the m -th step | 49 |
| 4.5 | Equi-stress function lines and yielded portion for square cross section. + shows yielded nodes | 50 |
| 4.6a | Equi-stress function lines and yielded portion for L-shaped cross section. | 51 |
| 4.6b | The Shear stress distribution for L-shaped cross section | 52 |
| 4.7 | Equi-stress function lines, shear stress distribution, and yielded nodes for square cross section with slit. | 53 |
| 4.8 | Plastic regions for various cross sections | 54 |
| 5.1 | Comparison of isotherms and stream lines obtained by the penalty-finite element models ($\epsilon_2 \neq 0, \epsilon_2 = 0$) for $R_a = 1,000$ and $P_r = 10$ | 73 |
| 5.2 | Velocity and temperature distribution along the center lines of the enclosure | 74 |
| 5.3 | Isotherms and stream lines obtained by the penalty-finite element model for $R_a = 10,000$ and $100,000$ ($P_r = 1$) | 76 |

| Figure | Page |
|--|------|
| 5.4 Vertical velocity at $x=0.5$ by penalty finite element model | 77 |
| 5.5 Temperature at $x=0.5$ by penalty finite element model . | 78 |
| 5.6 (a) Scaled vertical velocity in boundary layer ($x=0.5$) (b) Temperature in boundary layer ($x=0.5$) | 79 |
| 5.7 Core temperature distribution along vertical cross section | 80 |
| 5.8 Isotherms and isostreams for $R_a = 10^6$, $P_r = 1$ by penalty formulation (mesh:12x12) (a) isotherms and (b) isostreams | 80 |
| 5.9 Vorticity distribution along vertical cross section, $R_a = 10^4$, (mesh:10x10) (a) stream function-vorticity model (SVFEM) (b) penalty FEM (PFEM) | 81 |
| 5.10 Effect of penalty parameter ϵ on the stream function ψ . | 85 |
| 5.11 Effect of penalty parameter ϵ on the temperature θ . . | 86 |
| 5.12 Heat flux at cold wall. | 87 |
| 5.13 Isotherms, isostreams, and equivorticity lines for various Prandtl numbers by stream function-vorticity formulation ($R_a = 10,000$) (a) isotherms, (b) isostreams, and (c) equivorticity lines | 88 |
| 5.14 Relative pressure distribution along vertical cross section ($y=0.5$) by penalty finite element model . . | 89 |
| 5.15 Isotherms and stream lines for $R_a = 14,660$, $P_r = 0.733$. | 90 |
| 5.16 Isotherms and stream lines for $R_a = 8,200$, $P_r = 2,450$. | 90 |
| 5.17 Isotherms and isostreams for the vertical slot problem, (Elder (1965a)), ($R_a = 100,000$, $P_r = 1$, $\gamma = 16$, 24x12 nonuniform mesh). | 91 |
| 5.18 Finite element mesh for nonrectangular cavity (14x13 nonuniform mesh) | 92 |
| 5.19 Temperature and stream function for nonsquare enclosure by penalty method (a) temperature and (b) stream function | 93 |

| Figure | Page |
|---|------|
| 5.20 Finite elements and boundary conditions for circular annulus (375 meshes and 336 nodes) | 94 |
| 5.21 Isotherms and isostreams for (a) $R_a = 10^3$ and (b) $R_a = 4.7 \times 10^4$ | 95 |
| 5.22 Vertical velocity distribution along horizontal cross section | 96 |
| 5.23 (a) Stream function along horizontal cross section (b) Temperature distribution along horizontal cross section | 97 |
| 5.24 (a) Temperature distribution along half circle (b) Vertical velocity distribution | 98 |
| 5.25 Heat transfer along inner and outer walls | 99 |
| 5.26 Isotherms and isostreams for half annulus placed horizontally: (a) $R_a = 1000$ and (b) $R_a = 100,000$. . | 100 |

LIST OF TABLES

| Table | Page |
|--|------|
| 3.1 Equality and inequality constraints | 17 |
| 4.1 Comparison of ϕ by various formulations for circular cross section | 45 |
| 4.2 Comparison of $ \nabla\phi ^2$ by various formulations for circular cross section | 45 |
| 4.3 Comparison of percentage errors in various formulations for circular cross section bar | 46 |
| 4.4 Comparison of ϕ for circular cross section with fine mesh ($f=4$) | 46 |
| 5.1 Comparison of the stream function and temperature values obtained by the penalty-finite element model (PFEM) and stream function-vorticity finite element models (SVFEM) ($P_r=1$, mesh: 10×10) | 75 |
| 5.2 Stream function and vorticity values at the center of the enclosure (10×10 mesh) | 82 |
| 5.3 Comparison of the Nusselt number obtained by various investigators ($R_a=14,700$, $P_r=0.733$) | 83 |
| 5.4 Comparison of the Nusselt number, computational time, and number of iterations required for convergence (n) for the penalty-finite element model (PFEM) and stream function-vorticity finite element model (SVFEM) | 84 |

LIST OF SYMBOLS

| | |
|------------------------|---|
| $A(\cdot)$ | differential operator |
| $B(\dots), B_p(\dots)$ | bilinear forms |
| EI | flexural rigidity |
| F, L, G, Q | functionals |
| f, \underline{f} | external force |
| \hat{f}_x, \hat{f}_y | components of external force vector in x and y directions |
| G | shear modulus |
| G_r | Grashof number |
| g | gravitational acceleration |
| $H^k(\Omega)$ | Sobolev space of order k |
| $J(\dots)$ | Jacobian operator |
| K | restricted function space (closed convex set) |
| k | thermal conductivity |
| $L_2(\Omega)$ | set of square integrable functions |
| N | set of Lagrange multipliers with restriction |
| n_i | interpolation |
| n_x, n_y | components of unit normal vector in x and y directions |
| P | pressure |
| $P_k\{u\}$ | projection of u on the set K |
| P_r | Prandtl number |
| \hat{q} | specified head flux on the boundary |
| R_a | Rayleigh number |
| R^n | n-dimensional Euclidean space |
| T | temperature, torque |

| | |
|---|--|
| \hat{T} | specified temperature |
| T_0 | reference temperature |
| T_u, T_c | temperature at hot and cold walls |
| $T(\cdot)$ | mapping operator |
| t_x, t_y | components of traction vector in x and y directions |
| \hat{t}_x, \hat{t}_y | specified traction vector components on the boundary |
| u, v | velocities in x and y directions |
| \underline{u} | unknown vector function |
| x, y | Cartesian coordinates in two dimensions |
| \underline{x} | n-dimensional Cartesian coordinates |
| α | thermal diffusivity |
| β | coefficient of thermal expansion |
| Γ | interface between elastic and plastic torsion |
| $\delta(\cdot)$ | the first variation |
| $\varepsilon, \varepsilon_1, \varepsilon_2$ | penalty parameters |
| ζ | vorticity |
| θ | normalized temperature; twisting angle per unit length |
| λ_i, p_i | Lagrange multipliers |
| ν | kinematic viscosity |
| ρ_0, ρ | reference density and density |
| $\rho_1, \rho_2, \rho_\theta, \rho_\lambda$ | acceleration parameters |
| τ_p | maximum shear stress |
| ϕ | stress function |
| ψ | stream function |
| Ω | global domain of problem |

| | |
|--|---|
| $\partial\Omega$ | boundary of Ω |
| Ω_e, Ω_p | elastic and plastic portion of Ω |
| $\partial\Omega_e, \partial\Omega_p$ | boundary of Ω_e and Ω_p |
| $\partial\Omega_1, \partial\Omega_2$ | disjoint portions of the boundary where natural and essential boundary conditions are specified |
| $\frac{\partial}{\partial n_e}, \frac{\partial}{\partial n_p}$ | normal derivatives on $\partial\Omega_e$ and $\partial\Omega_p$ |
| ∇ | gradient operator in two dimensions |
| ∇^2 | Laplacian operator |
| $\ \cdot\ $ | norm |
| $\langle \cdot, \cdot \rangle$ | inner product |
| $[\cdot]$ | matrix |
| $\{\cdot\}$ | vector |
| \forall | for every |
| \in | is an element of or belongs to |

CHAPTER I

INTRODUCTION

1.1 Opening Comments

A large number of problems in engineering science involve the solution of differential equations subject to some subsidiary conditions, called constraints (of equality or inequality type). While the derivation of the governing equations is not unduly difficult, it is considerably more difficult to analyze problems with constraints. Most practical methods of analysis are based on unconstrained minimization techniques, such as the Lagrange multiplier method and the penalty function method. These techniques transform a given constrained minimization problem into a set of unconstrained minimization problems. In the practical implementation of these methods, one encounters problems in terms of storage, computational time, and more importantly numerical instabilities. The present study is concerned with alternate formulation of two practically important problems, which have received great attention of researchers. The novelty of the present work lies in the use of the finite element method in conjunction with the variational inequality approach and the penalty function method. Two years ago, when the author began this study, these two methods were just beginning to attract the attention of engineers and mathematicians

alike. At the present time there are many papers devoted to the analysis and applications of these techniques (although old in concept, their use in finite element analysis is new) to many important problems that have defied satisfactory solutions heretofore. The problems considered herein are described below.

1. The first problem is the elastic-plastic torsion of a bar, in which the yield criteria of plasticity impose inequality constraints on the gradient of the solution. In addition, the relation between the stress function and total torque is treated as an equality constraint when the torque is given. The location of the elastic-plastic interface is an unknown. Mathematically, this problem is described by an elliptic boundary-value problem and the main difficulty in its numerical analysis is the construction of a scheme to incorporate the inequality constraint. The problem is solved using a modern tool of function analysis, namely the variational inequality approach.

2. The second problem is the steady laminar natural convection of an incompressible Newtonian fluid in enclosures. The Boussinesq approximation is invoked. The incompressibility condition (i.e., divergence free condition) on the velocity field can be viewed as a constraint. Incorporation of this constraint into the numerical scheme is of prime concern, while keeping computational costs to a minimum. Further, when convection dominates the flow, momentum and thermal boundary layers are formed along the enclosure walls, where the velocity and temperature have a large gradient. This rapid change of velocity and temperature near the wall further complicates the construction of a convergent iterative numerical scheme for the

nonlinear terms. The elliptical nature of the governing equation is weakened by the dominance of the convective term. The primary numerical difficulty in such a (first-order derivative dominated) problem lies in severe numerical oscillations in the solution, causing the iteration process to diverge. The penalty function method is employed to solve the problem.

1.2 Brief Review of Pertinent Literature

The type of constraint, whether it is an equality or inequality, varies from problem to problem. Examples of equality constraints are provided by the condition that the first strain invariant is equal to zero in the stress analysis of rubber-like materials, and the divergence-free condition on the velocity field in the incompressible fluid flow analysis. Conservation of (mean) total mass, (mean) total energy and (mean) squared vorticity in certain meteorological schemes provide other types of equality constraints in integram form. Examples of inequality constraints are provided by the yield criteria in plasticity, Coulomb's law of friction at a boundary, and a free-surface condition in seepage flow.

In order to incorporate these constraints, the Lagrange multiplier formulation appears to be the most general and widely used one. However, in certain problems, for example, in incompressible flow analysis, the penalty function method of Courant (1943, 1956) is computationally more advantageous because it does not introduce new variables (i.e., Lagrange multipliers) into the formulations. Applications of the penalty function method in conjunction with the finite element method

can be found in the works of Zienkiewicz and his colleagues (1974, 1975, 1976), Hughes et al. (1976), and Reddy and his colleagues (1977, 1978, 1979a, 1979b, 1980a, 1980b). Part of the present work was conducted during this time (1980a). A specific form of the penalty function method, called 'variational adjustment', was proposed by Sasaki (1976) for the construction of stable numerical schemes; the method is also used in the variational objective analysis in meteorological problems.

Inequality constraints in the past were treated by Pontryagin's (1962) maximum principle, and the inverse penalty method of Carroll (1961) in mathematical programming (also see Bellman (1957)).

In the last decade the variational inequality methods have received greater attention by French and Italian applied mathematicians (e.g., Lions and Stampacchia (1967), Stampacchia (1968), and Fichera (1972)). Direct applications of the variational inequality approach to mechanics were suggested by Duvaut and Lions (1976). The variational inequality approach provides an elegant general theory that, as a special case, includes the classical variational formulation. However, the construction and implementation of efficient numerical schemes in specific problems is extremely complex, and forms a topic of current research (Kikuchi and Oden (1979), and Oden and Kikuchi (1979)).

Besides the difficulties associated with the numerical solution of problems with constraints, nonlinear problems require additional consideration in constructing efficient numerical schemes. In

nonlinear problems, iterative solution methods generally are used; they usually consume considerable computing time. Several general iterative methods were given by Zienkiewicz (1977). Numerical oscillations are often encountered in nonlinear problems involving the first-order derivatives (e.g., convective term); for example, large Reynolds number or Rayleigh number flows are known to present numerical difficulties (see Hughes (1979a)).

Use of refined mesh in the finite element method to avoid numerical oscillations seems to be the first thing numerical analysts try to do (see Gresho et al., (1979)). However, this results in a large system of algebraic equations. Upwind FEM is proposed as an alternative scheme to suppress the numerical oscillations in the solution (see Zienkiewicz (1977) and Hughes (1979a)). There is a great deal of research currently underway in devising proper upwind schemes. The upwind technique is essentially equivalent to the artificial viscosity method which strengthens the elliptic nature of the equation (Roache, 1972).

1.3 Thesis Objectives

The objectives of the present study are:

- (1) to develop general iterative numerical schemes for elastic-plastic torsion problems based on the variational inequality formulation; and,
- (2) to construct numerical schemes for natural convection problems using penalty function method.

Following the introduction, Chapter II defines the governing

equations of the following problems: (i) elastic-plastic torsion of a bar; and (ii) natural convection in enclosures.

In Chapter III, Lagrange multiplier formulation, penalty formulation and variational inequality formulation are summarized.

Chapter IV is devoted to the detailed formulation and numerical analysis (based on variational inequality) of the elastic-plastic torsion of a bar. von Mises yielding criterion is applied.

Chapter V solves natural convection in enclosures assuming steady, Newtonian incompressible fluid under Boussinesq approximation. The penalty and stream function-vorticity formulations are compared in accuracy and efficiency.

Finally, primary results are summarized and future research directions are recommended.

CHAPTER II

GOVERNING EQUATIONS

2.1 Elastic-plastic Torsion of Bar

The problem of elastic-plastic torsion of a bar twisted by terminal couples can be formulated in terms of a stress function ϕ . The elastic-plastic torsion problem involves finding ϕ such that

$$\nabla^2 \phi = -f \quad \text{in } \Omega_e \quad (2.1)$$

$$|\nabla \phi|^2 - \tau_p^2 = 0 \quad \text{in } \Omega_p \quad (2.2)$$

$$|\nabla \phi|^2 - \tau_p^2 < 0 \quad \text{in } \Omega_e \quad (2.3)$$

$$\phi = 0 \quad \text{on } \partial\Omega \quad (2.4)$$

$$\frac{\partial \phi}{\partial n_e} = \frac{\partial \phi}{\partial n_p} \quad \text{on } \Gamma \quad (2.5)$$

$$T = \int_{\Omega} 2\phi \, dx dy \quad (2.6)$$

where Ω_e and Ω_p denote the elastic and plastic portion of the domain (i.e., cross section of the bar), $\Omega = \Omega_e \cup \Omega_p$, $\partial\Omega$ denotes piecewise smooth boundary, Γ is the interface of elastic and plastic portions, $\frac{\partial}{\partial n_e}$ and $\frac{\partial}{\partial n_p}$ are outer normal derivatives on Γ with respect to Ω_e and Ω_p , τ_p is a given plastic (shear) stress, and $f = 2G\theta$; here G is the shear modulus, θ is the angular twist per unit length, and T is the applied torque on the bar. Note that equation (2.3) is an inequality constraint on the gradient of ϕ . It should be pointed out that either

θ or T is known and the other is computed in any given problem.

The first complete description of the elastic-plastic torsion problem is apparently due to von Mises (1949). Existence and uniqueness of solution to elastic-plastic torsion of a square cross-section bar was established by Ting (1966) using a direct approach on equations (2.1)-(2.6). A different approach, based on the theory of variational inequalities, was taken by stampacchia (1968), Lions (1971), and Duvaut and Lions (1976). In the theory of variational inequalities the problem in (2.1)-(2.6) is formulated as a constrained (which is an inequality constraint) minimization problem on a restricted function space. Duvaut and Lions (1976) considered existence, uniqueness, and regularity of solutions to the elastic-plastic torsion.

A vast majority of papers on variational inequalities dwell on theoretical aspects such as existence and uniqueness of solutions, and very little can be found on computational and numerical results. Numerical solutions to the elastic-plastic torsion problem have been obtained using finite difference methods, relaxation methods, non-linear programming methods and finite element methods. Many of the previous works have used direct formulations based on (2.1)-(2.6). While the theory of variational inequalities is a natural (and perhaps the most correct) means of formulating the elastic-plastic torsion problem, its numerical implementation is by no means easy. This fact is reflected by the very few publications on the application of variational inequality to engineering problems. Numerical solution of the elastic-plastic torsion by the variational inequality

is a recent occurrence. Glowinski and his colleagues (1973, 1976) presented numerical results for various twist angles for simply and multi-connected domains using Uzawa's method (Arrow et al., 1958). Recently, Tabata (1976) presented a numerical method for the variational inequality associated with the elastic-plastic torsion problem. There the finite element method was used to reduce the problem to a minimization problem, which was then solved by the interior point unconstrained minimization technique with the steepest descent method and the generalized Newton method (Fiacco and McCormick, 1968). Fiacco and McCormick (1968) pointed out that the gradient method, which is the basis of Uzawa's method, has slow convergence compared to the interior-point unconstrained-minimization technique.

The present investigation is concerned with a new numerical procedure to solve the variational inequality associated with the elastic-plastic torsion problem (2.1)-(2.6). The main difficulty with the problem is to locate the elastic-plastic interface. Lanchon (1970) treated equations (2.2) and (2.3) as constraints by means of a Lagrange multiplier, and it was assumed that the angle of twist is given instead of the terminal torque. In the present investigation, equation (2.2) is solved by means of the method of characteristics, and then an iterative procedure is used to solve for the elastic-plastic interface. We also reformulate the problem in Lanchon (1970, 1974) for the case in which the torque is given. The present investigation is primarily concerned with a new and effective computational scheme to solve the elastic-plastic torsion problem; nevertheless, theoretical aspects, such as the existence and uniqueness of solution

and error estimates, are discussed for the sake of completeness. A number of numerical examples are presented assuming that von Mises' yield criterion holds.

2.2 Natural Convection in Enclosures

Convection phenomena induced by body forces have been the subjects of many theoretical and numerical investigations. As pointed out by Ostrach (1972) convection problems can be classified into two major types: external problems, such as the flow around a heated rod or plate caused by existence of a temperature difference between the body and the fluid; and internal (or confined) problems, such as the flow in a fluid-filled cavity caused by the temperature differences between the walls of the cavity. Due to their important role in many engineering problems of practical interest, internal problems have received greater attention. These problems include: thermal insulation of buildings, Batchelor (1954); heat transfer through double-glazed window, Elder (1965a,b) and Gill (1966); cooling of electronic equipment, Pedersen (1971); general circulation of planetary atmospheres, Hart (1972); crystal growth from the melt, Carruthers (1975); sterilization of canned foods, Hiddink et al. (1976); cooling fluids in channels surrounding a nuclear reactor core, Petuklov (1976); convectively cooled underground electric cable systems, Chato and Abdulhadi (1978) and many others.

For internal high Rayleigh number (i.e. $R_a > 10^3$) flows, the region exterior (i.e. core) to the boundary layer is influenced by the behavior of the surrounding boundary layer. This coupling of

the boundary layer and the core region constitutes the main source of difficulty for obtaining analytical solutions to internal problems, forcing one to seek numerical solutions. In order to capture the boundary layer effects, one must use a small mesh near the walls. This requires the use of a nonuniform mesh in the interest of accuracy and computational efficiency (use of a nonuniform mesh is also necessitated by irregular configurations of enclosures). The inability of the finite difference methods to accurately describe irregular domains and permit the use of nonuniform, non-rectangular meshes, and the complexity involved in developing higher-order finite difference approximations have led the researchers to consider the finite element method, which is known to have overcome the above mentioned shortcomings of the finite difference method. The feasibility of applying the finite element method to convection heat transfer in rectangular enclosures has been studied by Tabarrok and Lin (1977) using the stream function-vorticity-temperature formulation, Gartling (1977) using the pressure-velocity-temperature formulation, Heinrich et al. (1978), and Reddy and Mamidi (1978) using penalty function methods.

Under the standard assumption of convective heat transfer (i.e. Boussinesq approximation holds), the two-dimensional equations governing a Newtonian fluid in the presence of a temperature gradient (but in the absence of other body forces) can be written as,

conservation of mass:

$$\frac{\partial u}{\partial x} + \frac{\partial v}{\partial y} = 0 \quad (2.7)$$

conservation of linear momentum:

$$A(u) = -\frac{1}{\rho_0} \frac{\partial P}{\partial x} + \nu \left[2 \frac{\partial^2 u}{\partial x^2} + \frac{\partial}{\partial y} \left(\frac{\partial u}{\partial y} + \frac{\partial v}{\partial x} \right) \right] - g\beta(T-T_0) \quad (2.8)$$

$$A(v) = -\frac{1}{\rho_0} \frac{\partial P}{\partial y} + \nu \left[2 \frac{\partial^2 v}{\partial y^2} + \frac{\partial}{\partial x} \left(\frac{\partial u}{\partial y} + \frac{\partial v}{\partial x} \right) \right] \quad (2.9)$$

conservation of energy:

$$A(T) = \alpha \left(\frac{\partial^2 T}{\partial x^2} + \frac{\partial^2 T}{\partial y^2} \right) \quad (2.10)$$

where

$$\alpha = k/\rho_0 C_p, \quad A = u \frac{\partial}{\partial x} + v \frac{\partial}{\partial y} \quad (2.11)$$

and x is taken positive downward (i.e. along the acceleration due to gravity). Here (u,v) are the components of velocity along (x,y) - directions, P is the pressure, T is the temperature (T_0 is the reference temperature), ρ_0 is the reference value of the density of the fluid, ν is the kinematic viscosity, β is the coefficient of thermal expansion, k is the thermal conductivity, C_p is the specific heat at constant pressure, and g is the acceleration due to gravity. To complete the description of the equations, equations (2.7)-(2.10) must be adjoined by appropriate boundary conditions of the problem. We assume that the following general boundary conditions (of mixed type) are specified:

$$\alpha \left(\frac{\partial T}{\partial x} n_x + \frac{\partial T}{\partial y} n_y \right) = \hat{q} \text{ on } \partial\Omega_{1T}, \quad T = \hat{T} \text{ on } \partial\Omega_{2T} \quad (2.12)$$

$$\left. \begin{aligned} t_x &\equiv \left(2\nu \frac{\partial u}{\partial x} - \bar{P} \right) n_x + \nu \left(\frac{\partial u}{\partial y} + \frac{\partial v}{\partial x} \right) n_y = \hat{t}_x \text{ on } \partial\Omega_{1u} \\ t_y &\equiv \nu \left(\frac{\partial u}{\partial y} + \frac{\partial v}{\partial x} \right) n_x + \left(2\nu \frac{\partial v}{\partial y} - \bar{P} \right) n_y = \hat{t}_y \text{ on } \partial\Omega_{1v} \end{aligned} \right\} \quad (2.13)$$

$$u = \hat{u} \text{ on } \partial\Omega_{2u}, \quad v = \hat{v} \text{ on } \partial\Omega_{2v}, \quad \bar{P} = P/\rho_0 \quad (2.14)$$

Here $n = (n_x, n_y)$ denotes the unit normal to the boundary $\partial\Omega$, and $\partial\Omega_1$ and $\partial\Omega_2$ denote disjoint (i.e. $\partial\Omega_1 \neq \partial\Omega_2$) portions of the total boundary $\partial\Omega$ of the bounded region Ω . That is,

$$\partial\Omega_{1u} + \partial\Omega_{2u} = \partial\Omega_{1v} + \partial\Omega_{2v} = \partial\Omega = \partial\Omega_{1T} + \partial\Omega_{2T} \quad (2.15)$$

That is, $\partial\Omega_{1u}$ and $\partial\Omega_{1v}$ denote the portions of the boundary on which the tractions t_x and t_y , respectively, are specified, and $\partial\Omega_{2u}$ and $\partial\Omega_{2v}$ denote the portions on which the velocities are specified.

Quantities with a hat '^' denote specified quantities on the appropriate boundary. Further, we use the following variables for the nondimensionalization. Let d denote the length of the enclosure (along y), ℓ the height (along x), and T_h and T_c denote the temperatures of the hot and cold walls, respectively.

The above equations in the primitive variables (u, v, p, T) are often replaced by equations in terms of the descriptive variables (ψ, ζ, T) for numerical approximations. The stream function ψ is introduced to satisfy the incompressibility condition (2.7). Define the stream function by

$$u = \frac{\partial\psi}{\partial y}, \quad v = -\frac{\partial\psi}{\partial x}, \quad (2.16)$$

and the vorticity, ζ , by

$$\zeta = \frac{\partial v}{\partial x} - \frac{\partial u}{\partial y} = -\nabla^2\psi. \quad (2.17)$$

Consequently, equations (2.7)-(2.10) reduce to

$$-\nabla^2\zeta = J(\psi, \zeta) + g\beta \frac{\partial T}{\partial y} \quad (2.18)$$

$$-\nabla^2\psi = \zeta, \quad (2.19)$$

$$-\nabla^2 T = \frac{1}{\alpha} J(\psi, T). \quad (2.20)$$

where $J(.,.)$ is the Jacobian,

$$J(p,q) = \frac{\partial p}{\partial x} \frac{\partial q}{\partial y} - \frac{\partial p}{\partial y} \frac{\partial q}{\partial x}. \quad (2.21)$$

In order to derive the finite element equations, the mixed formulation in terms of variables (u,v,p,T) may be the most direct one. However, it is well known that FEM, based on the mixed formulation, comprises a non-positive definite matrix and zeros appear in the diagonal in the coefficient matrix. Furthermore, iteration to obtain nonlinear solutions often diverges in the analysis of the flow which has a boundary layer. The penalty formulation is an alternative formulation which has the following advantages: (i) in enabling one to obtain solution for larger Rayleigh number (which is proportional to the temperature difference of side walls); and, (ii) in reducing unknown variables (u,v,p,T) to (u,v,T) . Stream function-vorticity and penalty formulations have the same number of unknowns. Comparison of penalty and stream function-vorticity formulations is discussed in Chapter V. Since the exact solution is not available, accuracy of numerical approximations is compared with other results available in the literature. Alternatively, accuracy of solutions is also tested by convergence.

CHAPTER III

GENERAL FORMULATION OF CONSTRAINED OPTIMIZATION PROBLEMS

3.1 Introductory Comment

The objective of the present chapter is to give general formulations of constrained optimization problems for various future uses. Lagrange multiplier formulation, penalty formulation, and variational inequality formulation are applied to satisfy given equality or inequality constraints.

The problems defined in Chapter II have the general form of:

$$\text{either} \quad A(\underline{u}) = \underline{f} \quad \text{in } \Omega \quad (3.1)$$

$$\text{or} \quad u_t + A(\underline{u}) = \underline{f} \quad \text{in } \Omega \times [0, T]$$

where \underline{u} is an unknown vector, \underline{f} is the given vector function and $A(\cdot)$ is a differential operator with respect to $\underline{x} \in R^n$ (n -dimension Euclidean space), and Ω is an open bounded domain in R^n with piecewise smooth boundary $\partial\Omega$ and T is a given time.

Constraint conditions have forms of

$$E_i(\underline{u}) = 0 \quad i = 1, \dots, I \quad (3.2)$$

$$\text{or} \quad I_j(\underline{u}) \geq 0 \quad j = 1, \dots, J \quad (3.3)$$

where I and J show the number of constraints. We assume that (3.2) and (3.3) are independent of time. Eq. (3.2) or (3.3) can be given

either at every point \underline{x} in the domain or by integral form over the domain. Concrete forms of variables and constraints corresponding to the problems in Chapter II are summarized in Table 3.1. Boundary and initial conditions are given by

$$B(\underline{u}) = \underline{g} \quad \text{on} \quad \partial\Omega \quad \text{or} \quad \partial\Omega \times [0, T] \quad (3.4)$$

and
$$\underline{u}|_{t=0} = \underline{u}_0 \quad \text{at} \quad t=0 \quad (3.5)$$

where B is a trace operator on the boundary which represents essential and natural boundary conditions. If operator A contains only the first-order derivative terms, B is the identity, that is, (3.4) is simply

$$\underline{u}|_{\partial\Omega} = \underline{g} \quad (3.6)$$

where \underline{g} and \underline{u}_0 are given vector functions. In the following discussion, we concentrate on the formulation of eq. (3.1) with (3.2) or (3.3) by assuming essential boundary conditions.

3.2 Weak Formulation

From an approximation point of view, it is advantageous to cast the given differential equation (3.1) into an integral equation, called the weak form, in order to satisfy (3.1) in an integral sense. Then the problem of finding \underline{u} satisfying eq. (3.1) becomes to find \underline{u} such that

$$\langle \underline{u}_t + A(\underline{u}) - \underline{f}, \delta \underline{u} \rangle = 0 \quad (3.7)$$

for arbitrary function $\delta \underline{u}$ subject to (3.2), (3.4) and (3.5), where

$$\langle \underline{a}, \underline{b} \rangle = \int_{\Omega} \underline{a} \cdot \underline{b} \, d\Omega.$$

Table 3.1 Equality and inequality constraints

| | variable u | equality $E_i(\underline{u}) = 0$ | inequality $I_j(\underline{u}) \geq 0$ |
|-----------------------------------|---|--|--|
| elastic-plastic torsion of bar | ϕ | $T = \int_{\Omega} 2\phi \, d\Omega$ | $ \nabla\phi ^2 - \tau_p^2 \leq 0$ |
| natural convection | (i) penalty u, v, T (ii) stream function- vorticity ζ, ψ, T | $\frac{\partial u}{\partial x} + \frac{\partial v}{\partial y} = 0$ $u = \frac{\partial \psi}{\partial y}$ $v = -\frac{\partial \psi}{\partial x}$ | |

When \underline{u} and $\delta\underline{u}$ are subject to inequality (3.3), (3.7) is replaced by inequality as is discussed in section 3.5. Since integration in (3.7) is taken in space, (3.7) gives an ordinary differential equation with respect to time. It is possible to integrate (3.7) over time taking $\delta\underline{u} \in \Omega \times [0, T]$. However, it is known that numerical schemes based on the latter integral have no advantages (Oden and Reddy, 1976). Here we note that equations (3.1) and (3.7) offer the same solution only when $\underline{u}_t + A(\underline{u}) - \underline{f}$ and $\delta\underline{u}$ are continuous. If these contain a finite number of discontinuities, two solutions are said to be the same almost everywhere. This implies that a shock type of solution of (3.1) cannot be obtained uniquely by (3.7)

3.3 Lagrange Multiplier Formulation

Equality constraint (3.2) can be taken into the weak formulation by introducing Lagrange multipliers. As is seen in Table 3.1, there are two types of constraints. One is defined pointwise and the other has an integral form over domain.

(i) pointwise constraint If constraint (3.2) is given pointwise, the weak form of (3.1) subject to (3.2) can be given by

$$\langle \underline{u}_t + A(\underline{u}) - \underline{f}, \delta\underline{u} \rangle + \sum_{i=1}^N \delta \langle E_i(\underline{u}), p_i \rangle = 0 \quad (3.8)$$

where p_i 's are Lagrange multipliers and the function of x , δ denotes the first variation.

(ii) constraint in integral form When constraint (3.2) is given by an integral form over the domain, the weak form corresponding to (3.1) subject to (3.2) can be expressed by

$$\langle \underline{u}_t + A(\underline{u}) - \underline{f}, \delta \underline{u} \rangle + \sum_{i=1}^N \delta(\lambda_i E_i(\underline{u})) = 0 \quad (3.9)$$

where the Lagrange multiplier is an unknown number.

Inequality constraint (3.3) can be formulated using a Lagrange multiplier. Formulation of inequality constraint is given in section 3.5. In order to clarify the use of a Lagrange multiplier, an example is given.

Example: Steady incompressible creeping flow in two dimensions is expressed by Stokes' equation,

$$\begin{aligned} \mu \nabla^2 u - \frac{\partial p}{\partial x} &= \rho f_x \\ \mu \nabla^2 v - \frac{\partial p}{\partial y} &= \rho f_y \end{aligned} \quad (3.10)$$

$$\frac{\partial u}{\partial x} + \frac{\partial v}{\partial y} = 0 \quad (3.11)$$

where ∇^2 is Laplace's operator, f_x and f_y , components of body force per unit volume, ρ is the density of body. Then, the weak form associated with (3.10) and (3.11) is given by

$$\begin{aligned} \langle \mu \nabla^2 u - \frac{\partial p}{\partial x} - \rho f_x, \delta u \rangle + \langle \mu \nabla^2 v - \frac{\partial p}{\partial y} + \rho f_y, \delta v \rangle \\ + \langle \frac{\partial u}{\partial x} + \frac{\partial v}{\partial y}, \delta p \rangle = 0 \end{aligned} \quad (3.12)$$

Eq. (3.12) can be written as

$$\begin{aligned} \langle \mu \nabla^2 u + \rho f_x, \delta u \rangle + \langle \mu \nabla^2 v + \rho f_y, \delta v \rangle \\ + \delta \langle p, \frac{\partial u}{\partial x} + \frac{\partial v}{\partial y} \rangle = 0 \end{aligned} \quad (3.13)$$

when homogeneous boundary condition is used. Eq. (3.13) implies that eqns. (3.10) and (3.11) are equivalent to finding u and v which minimize the functional

$$F(u,v) = \int \left[\frac{\mu}{2} \left\{ \left(\frac{\partial u}{\partial x} \right)^2 + \left(\frac{\partial v}{\partial y} \right)^2 \right\} + \rho (f_x u + f_y v) \right] dx dy \quad (3.14)$$

subject to equality constraint (3.11). It is noted that pressure p plays the role of a Lagrange multiplier.

3.4 Penalty Formulation

In 1941, R. Courant (1943, 1956) suggested a novel method of obtaining better convergence (of the derivatives of the solution) in the Rayleigh-Ritz method. The method, as applied to the equilibrium problem for a membrane ($\nabla^2 u = f$ in Ω and $u = 0$ on the boundary $\partial\Omega$ of Ω) under external pressure f , can be described as follows: Instead of considering the usual variational problem of minimizing the functional

$$I(u) = \frac{1}{2} \int_{\Omega} \left[\left(\frac{\partial u}{\partial x} \right)^2 + \left(\frac{\partial u}{\partial y} \right)^2 + 2u f \right] dx dy, \quad u = 0 \text{ on } \partial\Omega, \quad (3.15)$$

the method seeks the minimum of a modified functional obtained from the original functional by adding terms of higher order which vanish for the actual solution u :

$$I_p(u, \epsilon) = I(u) + \frac{1}{2} \int_{\Omega} \epsilon (\nabla^2 u - f)^2 dx dy \quad (3.16)$$

where ϵ is an arbitrary (preselected) positive constant or function. Courant termed the functional in (3.16) a "sensitized" functional since it is more sensitive to variations of u without changing the solution. Another example of the use of this idea is provided by the inclusion of the essential boundary condition in the Dirichlet problem. The modified functional is given by

$$I_p(u, \epsilon) = I(u) + \frac{\epsilon}{2} \int_{\partial\Omega} u^2 ds. \quad (3.17)$$

For sufficiently large values of ϵ , the boundary value problem corresponding to the functional in (3.17) is almost equivalent to that associated with the functional in (3.15).

Although the idea was motivated by physical considerations, its value as a technique for transforming a given constrained minimization problem into a (sequence of) unconstrained minimization problem(s) was not recognized immediately. The idea was apparently not rigorously pursued for over a decade. In 1954 there was renewed interest in the penalty function⁺ method (Leitmann, 1962) as a computational device in mathematical programming (see, for example, the 'logarithmic potential method' of Frisch (1954), and the 'inverse penalty function technique' of Carroll (1961)). In 1956 Moser proved convergence of the solution of the penalty problem to the solution of the original problem. In 1957 a very significant contribution was made by Rubin and Unger (1957) which took the original technique of Courant out of the realm of conjecture for a much wider class of problems. They generalized Courant's technique to multiple variables and multiple equality constraints, and provided a convergence proof and a proof of the existence of Lagrange multipliers. Apart from these results, there was no significant theoretical development of the technique for a long time. However, the penalty function technique was often used as a computational device to approximate solutions of variational problems. There have been numerous papers devoted to various modifications of the method and their applications to

⁺The word 'penalty function' was first used by T. N. Edelbaum in Chapter 1 of the book on optimization techniques edited by Leitmann (1962).

particular problems; see Fiacco and McCormick (1968) and Hestenes (1975) for applications in mathematical programming and optimization, Babuska (1975) for finite-element applications, and Sasaki (1976) for an application in meteorology.

Despite its wide use in mathematical programming and optimization, the penalty function method was not regarded, until recently, as a powerful computational device. This is mainly due to two shortcomings: (i) the technique was used in connection with the approximate solution of variational problems by Rayleigh-Ritz type methods, which were themselves never regarded as competitive when compared to the traditional finite difference methods; (ii) in the practical application of the penalty function method, the penalty terms "misbehave" without proper selection of the approximation functions or integration. These two shortcomings were overcome by the finite element method (and reduced integration techniques). In 1973, the penalty function method was introduced into the finite-element analysis of fluid flow problems by Zienkiewicz (1974). However, the second shortcoming was not overcome until Zienkiewicz, Taylor and Too (1971) devised, rather ingeniously, the so-called reduced integration technique, which was later used by Zienkiewicz and his colleagues (1975, 1976) in the numerical integration of the penalty terms. Thus, over three decades after the original idea was suggested, the penalty function method was brought into the realm of computational mechanics (especially into finite element analysis) where it now serves as a simple yet effective computational technique of handling physical as well as mathematical constraints. Exploitation of further generalizations and extensions

of the technique in the finite-element solution of a variety of engineering problems is the current state of the technique.

Equation (3.1) subject to equality constraint (3.2) given at every point can be formulated by the penalty formulation. The penalty formulation tries to satisfy (3.2) in an approximate sense. Introducing a penalty functional corresponding to constraint (3.2),

$$G_{\underline{\varepsilon}}(\underline{u}) = \sum \frac{\varepsilon_i}{2} \int E_i^2(\underline{u}) \, dx dy \quad , \quad \underline{\varepsilon} = (\varepsilon_1, \dots, \varepsilon_I) \quad (3.18)$$

one can write the weak form of (3.1) subject to (3.2) as

$$\langle \underline{u}_t + A(\underline{u}) + \underline{f}, \delta \underline{u} \rangle + \delta G_{\underline{\varepsilon}}(\underline{u}) = 0 \quad (3.19)$$

Then it is expected that

$$\underline{u}_{\underline{\varepsilon}} \rightarrow \underline{u} \text{ and } E_i(\underline{u}) \rightarrow 0 \text{ as } \underline{\varepsilon} \rightarrow \infty. \quad (3.20)$$

In order to assure the property (3.20), certain properties on operator A and boundary conditions are required. Further mathematical theory of penalty formulation in the Navier-Stokes equation was given by Reddy (1979a).

Example In the example in section 3.3, it was shown that the problem defined by (3.10) and (3.11) is equivalent to minimization of a functional $F(u,v)$ defined by (3.14) subject to eq. (3.11). For the same problem, using the penalty formulation, one defines a new functional $L_{\varepsilon}(u,v)$ using the given parameter ε by

$$L_{\varepsilon}(u,v) = F(u,v) + \frac{\varepsilon}{2} \int \left\{ \left(\frac{\partial u}{\partial x} \right) + \left(\frac{\partial v}{\partial y} \right) \right\}^2 dx dy \quad (3.21)$$

and minimizes $L_{\varepsilon}(u,v)$. Then Euler's equations are given by

$$\begin{aligned}\mu \nabla^2 u_\varepsilon + \varepsilon \frac{\partial \theta}{\partial x} &= \rho f_x \\ \mu \nabla^2 v_\varepsilon + \varepsilon \frac{\partial \theta}{\partial y} &= \rho f_y\end{aligned}\tag{3.22}$$

where

$$\theta = \frac{\partial u_\varepsilon}{\partial x} + \frac{\partial v_\varepsilon}{\partial y}$$

Comparing eq. (3.10) and (3.22) we expect that

$$\varepsilon \theta \rightarrow -p, \quad \theta \rightarrow 0 \quad \text{and} \quad (u_\varepsilon, v_\varepsilon) \rightarrow (u, v) \quad \text{as} \quad \varepsilon \rightarrow \infty.$$

3.5 Variational Inequality

Variational inequality is a formulation of minimization problems subject to inequality constraints. Discussion herein is given for the steady case and evolutionary variational inequality can be referred to Lions (1971).

The idea of variational inequality may be illustrated best by the minimization of a quadratic function $f(x)$ on the closed interval $K = [a, b]$ shown in Figure 3.1. Let c be the point such that $f'(c) = 0$. Then according to the location of interval K , point x_0 which minimizes $f'(x)$ can be

$$\begin{aligned}\text{(i)} \quad & \text{if } b < c, \quad x_0 = b \text{ and } f'(x_0) < 0 \\ \text{(ii)} \quad & \text{if } a \leq c \leq b, \quad x_0 = c \text{ and } f'(x_0) = 0 \\ \text{(iii)} \quad & \text{if } c < a, \quad x_0 = a \text{ and } f'(x_0) > 0\end{aligned}\tag{3.23}$$

These three cases can be stated as a single inequality by finding $x_0 \in K$ such that

$$f'(x_0)(x - x_0) \geq 0 \quad \text{for any } x \in K\tag{3.24}$$

This idea can be extended to a functional rather than a function.

Minimization of a functional $F(\underline{u})$ subject to an inequality constraint of the type $I(\underline{u}) \geq 0$ given in (3.3) can be stated by finding $\underline{u} \in K$ such that

$$(P1) \quad F(\underline{u}) \leq F(\underline{v}) \quad \text{for any } \underline{v} \in K \quad (3.25)$$

where $K = \{\underline{v}: I(\underline{v}) \geq 0\}$. Then the problem (P1) is characterized by finding $\underline{u} \in K$ such that

$$(P2) \quad \delta F(\underline{u}; \underline{v}-\underline{u}) \geq 0 \quad \text{for any } \underline{v} \in K \quad (3.26)$$

$$\text{where} \quad \delta F(\underline{u}; \underline{v}-\underline{u}) = \lim_{t \rightarrow 0} \frac{1}{t} [F(\underline{u} + t(\underline{v}-\underline{u})) - F(\underline{u})] \quad (3.27)$$

If there exists a functional F associated with a differential operator A defined in (3.1) such that for homogenous boundary conditions

$$\delta F(\underline{u}; \underline{v}-\underline{u}) = \langle A\underline{u} - \underline{f}, \underline{v}-\underline{u} \rangle,$$

$$\text{then (3.26) becomes} \quad \langle A\underline{u} - \underline{f}, \underline{v}-\underline{u} \rangle \geq 0 \quad (3.28)$$

Inequality (3.26) or (3.28) is called a variational inequality. The implication of (3.28) can be illustrated geometrically in terms of a projection. Suppose that for given function \underline{h} , $\underline{u} \in K$ satisfies

$$\langle \underline{u}-\underline{h}, \underline{v}-\underline{u} \rangle \geq 0 \quad \text{for any } \underline{v} \in K$$

Then \underline{u} is said to be a projection of \underline{h} on K and denoted by

$$\underline{u} = P_K \{ \underline{h} \}$$

As is shown in Figure 3.2, \underline{u} is the point which gives minimum distance between \underline{h} and a set K . If we identify \underline{h} in (3.28) by

$$\underline{h} = \underline{u} - \rho(A\underline{u} - \underline{f}) \quad \text{for } \rho > 0,$$

inequality (3.28) is equivalent to a projection form

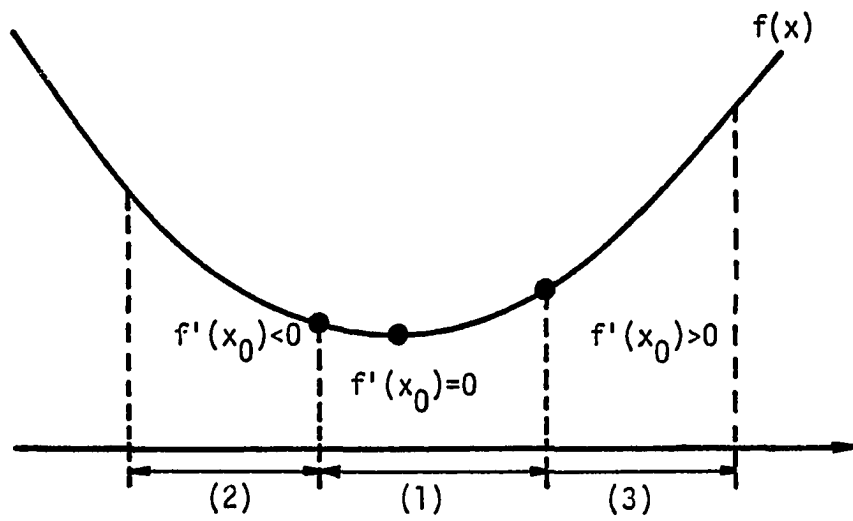


Figure 3.1 Minimum point x_0 of function $f(x)$.

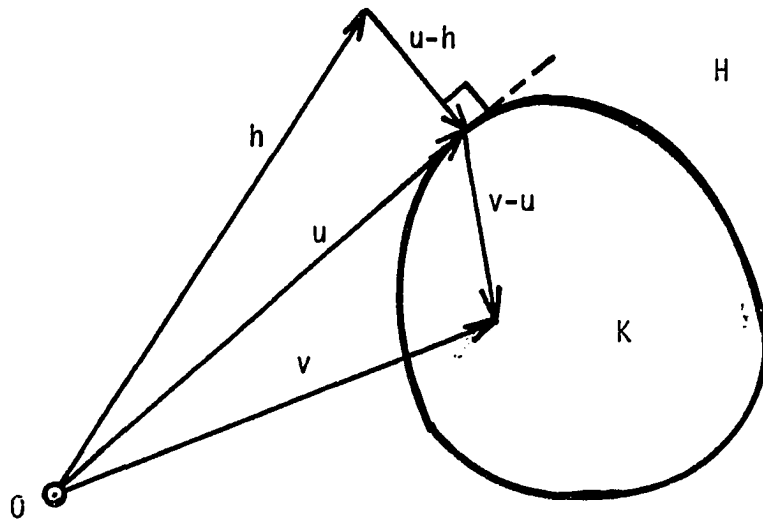


Figure 3.2 Geometrical Interpretation of Projection.

$$\underline{u} = P_K \{ \underline{u} - \rho(A(\underline{u}) - \underline{f}) \} \equiv T(\underline{u}) \quad (3.29)$$

Therefore, the solution of (3.28) is to find the fixed point of equation (3.29). It has been proved that a unique fixed point exists if mapping T is a contraction (Lions and Stampacchia, 1967).

It is noted that an inequality constraint is considered in the definition of the set K . Then set K is explicitly defined in terms of a variable itself (e.g., $|u| \leq 1$), projection of u on K can be easily taken into account as is shown later in an example. However, if K is defined implicitly (e.g., $|\text{grad } u| \leq 1$), finding the solution which belongs to K can be a difficult problem. The following formulation introducing a Lagrange multiplier can convert the variational equality on K to the one on a new set of Lagrange multiplier.

Introducing a set N such that $N = \{p: p \geq 0\}$, problem (P1) is equivalent to finding $(\underline{u}, p) \in H \times N$ such that

$$(P3) \quad L(\underline{u}, q) \leq L(\underline{u}, p) \leq L(\underline{v}, p) \quad \text{for any } (\underline{v}, q) \in H \times N \quad (3.30)$$

where $L(\underline{u}, p) = F(\underline{u}) - \int p I(\underline{u}) d\Omega$, H is a set of function \underline{u} with no constraint. Here, the constraint $I(\underline{u}) \geq 0$ is extended to the condition

$$p I(\underline{u}) \geq 0 \quad \text{and} \quad p \geq 0 \quad (3.31)$$

Inequality (3.31) implies that inequality constraint on \underline{u} is released. Problem (P3) is a minimization problem with respect to \underline{u} and maximization with respect to p , called a saddle-point problem. An example of (P1) is given in the following. Here, we introduce the variational inequality formulation without specifying properties of a function space H , K and N , functional F , and the operation $\langle \cdot, \cdot \rangle$.

In fact, in order to investigate the mathematical properties such as the existence, uniqueness, and regularity of the solution, the mathematical notion of functional analysis is required and can be referred to Duvaut and Lions (1976), Kikuchi and Oden (1979), and Oden and Kikuchi (1979).

Example Consider a continuous beam on discrete supports when a beam is not fixed with the support. Therefore, according to a load condition, some supports do no work. This problem can be solved by classical continuous-beam theory by considering all possible cases in which the actual situation happens. However, variational inequality offers a much easier formulation. Suppose that potential energy in terms of a deflection of a beam w given by

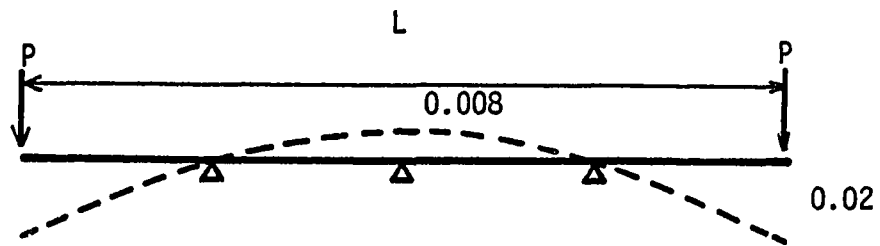
$$F(w) = \int_{\Omega} \left\{ \frac{EI}{2} \left(\frac{d^2w}{dx^2} \right)^2 - fw \right\} dx, \quad f > 0 \quad (3.32)$$

where f is a given force, and EI is the flexural rigidity. The solution should be found in the closed set K such that $K = \{w: w \geq 0\}$. Then the corresponding variational inequality can be stated by finding $w \in K$ such that

$$\int_{\Omega} EI \frac{d^2w}{dx^2} \frac{d^2(v-w)}{dx^2} dx \geq \int_{\Omega} f(v-w) dx \quad \text{for any } v \in K$$

Several numerical results by finite element method are given in Figure 3.3.

$$P=1, EI=1, L=1$$



(a)



(b)



(c)

Figure 3.3 Deflection of Continuous Beam.

CHAPTER IV

A NUMERICAL METHOD FOR ELASTIC-PLASTIC TORSION BY VARIATIONAL INEQUALITY

4.1 VARIATIONAL FORMULATIONS

Associated with the elastic-plastic torsion problem (2.1)-(2.6), we discuss two methods; one due to Lanchon (1970, 1974), called Problem L, and the other is the new method which we will call Problem P. In each method we consider two cases: In case 1, the angle of twist is assumed to be given and in case 2 the torque is assumed to be known. We use the following notation. Let $L_2(\Omega)$ denote the space of square integrable functions in Ω and $H_0^1(\Omega)$ denote the Sobolev space of order 1 with their first derivatives, belong to $L^2(\Omega)$, and vanish on the boundary of Ω).

Problem 1

When $f (= 2G\theta)$ is given, (2.1)-(2.5) are formulated as a minimization problem on the restricted function space K :

(P1). Find $\phi \in K$ such that for given $f \in L^2(\Omega)$

$$F(\phi) \leq F(\bar{\phi}) \quad \text{for } \forall \bar{\phi} \in K \quad (4.1)$$

where $F(\phi) = \int_{\Omega} (|\nabla\phi|^2 - 2f\phi) dx dy$, and K is the closed convex set.

$$K = \left\{ \phi \in H_0^1: |\nabla\phi|^2 - \tau_p^2 \leq 0 \text{ in } \Omega \right\} \quad (4.2)$$

Here torque T can be computed from (2.6) once ϕ is known. It is easy to see that the problem $P1$ is a minimization problem on set K and is equivalent to the problem described by (2.1)-(2.5). To show this, first note that equations (2.2)-(2.4) are included in the definition of K , and it remains to be shown that $P1$ is equivalent to (2.1) and (2.5). Suppose that $\phi_0 \in K$ minimizes $F(\phi)$ on K . Then for $\bar{\phi} \in K$,

$$\delta F(\phi_0, \bar{\phi} - \phi_0) \geq 0$$

or, equivalently, with $\eta = \bar{\phi} - \phi_0$,

$$\lim_{\varepsilon \rightarrow 0} \frac{1}{\varepsilon} (F(\phi_0 + \varepsilon\eta) - F(\phi_0)) = \left. \frac{\partial}{\partial \varepsilon} F(\phi_0 + \varepsilon\eta) \right|_{\varepsilon=0} \geq 0$$

That is,

$$\begin{aligned} \left. \frac{\partial}{\partial \varepsilon} \int_{\Omega} \left\{ |\nabla(\phi_0 + \varepsilon\eta)|^2 - 2f(\phi_0 + \varepsilon\eta) \right\} dx dy \right|_{\varepsilon=0} &\geq 0 \\ \int_{\Omega} \{2\nabla\phi_0 \cdot \nabla\eta - 2f\eta\} dx dy &\geq 0 \\ - \int_{\Omega_e} (\nabla^2\phi_0 + f)\eta dx dy - \int_{\Omega_p} (\nabla^2\phi_0 + f)\eta dx dy &+ \int_{\partial\Omega_e} \frac{\partial\phi_0}{\partial n} \eta ds \\ &+ \int_{\partial\Omega_p} \frac{\partial\phi_0}{\partial n} \eta ds \geq 0 \end{aligned}$$

$$\begin{aligned}
& - \int_{\Omega_e} (\nabla^2 \phi_o + f) \eta \, dx dy - \int_{\Omega_p} (\nabla^2 \phi_o + f) \eta \, dx dy + \int_{\partial\Omega_e/\Gamma} \frac{\partial \phi_o}{\partial n} \eta \, ds \\
& + \int_{\partial\Omega_p/\Gamma} \frac{\partial \phi_o}{\partial n} \eta \, ds + \int_{\Gamma} \left\{ \left(\frac{\partial \phi_o}{\partial n} \eta \right)_e - \left(\frac{\partial \phi_o}{\partial n} \eta \right)_p \right\} ds \geq 0
\end{aligned}$$

where $\Gamma = \Omega_e \cap \Omega_p$ is the interface of the elastic and plastic regions. Since $\eta = \bar{\phi} - \phi_o = 0$ in Ω_p , and η can be positive or negative in Ω_e and $\eta = 0$ on $\partial\Omega = \partial\Omega_e \cup \partial\Omega_p$, we have

$$\begin{aligned}
\nabla^2 \phi_o + f &= 0 \quad \text{in } \Omega_e, \\
\left(\frac{\partial \phi_o}{\partial n} \right)_e - \left(\frac{\partial \phi_o}{\partial n} \right)_p &= 0 \quad \text{on } \Gamma
\end{aligned}$$

which are the same as (2.1) and (2.5).

It is useful to cast Problem 1 into alternate but equivalent forms:

(P1.1) Find $\phi \in K$ such that for $f \in L^2(\Omega)$,

$$B(\phi, \bar{\phi} - \phi) \geq (f, \bar{\phi} - \phi) \quad , \quad \text{for } \forall \bar{\phi} \in K \quad (4.3)$$

where

$$B(\phi, \bar{\phi}) = \int_{\Omega} \nabla \phi \cdot \nabla \bar{\phi} \, dx dy, \quad (f, \bar{\phi}) = \int_{\Omega} f \bar{\phi} \, dx dy \quad (4.4)$$

Equation (4.3) is the variational inequality associated with Problem 1.

Problem 2

Here we assume that the torque T is given, but f is unknown. Introducing a Lagrange multiplier λ , we can state (2.1)-(2.6) as a saddle-point problem.

(P2) Find $(\phi, \lambda) \in K \times R$ such that, for given $T \in R$,

$$G(\phi, \bar{\lambda}) \leq G(\phi, \lambda) \leq G(\bar{\phi}, \lambda) \quad (4.5)$$

for every $(\bar{\phi}, \bar{\lambda}) \in K \times R$. Here $G(\phi, \lambda)$ is given by

$$G(\phi, \lambda) = \int_{\Omega} |\nabla \phi|^2 \, dx dy + \lambda \left(T - \int_{\Omega} 2\phi \, dx dy \right) \quad (4.6)$$

and R denotes the set of real numbers. It can be verified that P2 is equivalent to (2.1)-(2.6). The left inequality in (4.5) gives equation (2.6) and the right inequality gives (2.1)-(2.5). Alternate formulations of (4.5) are possible, as stated below:

(P2.1) Find $(\phi, \lambda) \in K \times R$ such that, for given $T \in R$,

$$B(\phi, \bar{\phi} - \phi) \geq (\lambda, \bar{\phi} - \phi) \quad \text{and} \quad T = \int_{\Omega} 2\phi \, dx dy \quad (4.7)$$

for every $\bar{\phi} \in K$.

Note that Problems 1 and 2 are formulated on a special set K . From the numerical point of view, it is difficult to construct a finite-dimensional subspace of K . However, by solving the equation (say, by the method of characteristics), the set K can be defined by the condition with respect to ϕ rather than a gradient of ϕ . A general formulation would be to include equation (2.2) and (2.3) as a constraint by means of a Lagrange multiplier (see Lanchon, 1974).

Problem 3

Problem 3 seeks to find a solution to (2.1)-(2.6) over a larger set (instead of K).

(L1) Find $(\phi, P) \in H_0^1(\Omega) \times N$ such that, for given $f \in L^2(\Omega)$,

$$L(\phi, \bar{P}) \leq L(\phi, P) \leq L(\bar{\phi}, P) \quad (4.8)$$

for every $(\bar{\phi}, \bar{P}) \in H_0^1(\Omega) \times N$, where

$$L(\phi, P) = F(\phi) - \int_{\Omega} P(|\nabla\phi|^2 - \tau_p^2) \, dx dy \quad (4.9)$$

$$N = \left\{ q \in L^\infty(\Omega) : q \leq 0 \text{ in } \Omega \right\}$$

It is not difficult to show that Problem 3 is equivalent to Problem 1, and hence to equations (2.1)-(2.5).

Once again, alternate formulations to (4.8) are possible.

(L1.1) Find $(\phi, P) \in H_0^1(\Omega) \times N$ such that for given $f \in L^2(\Omega)$

$$B_p(\phi, \bar{\phi}) = (f, \bar{\phi}) \quad , \quad \forall \bar{\phi} \in H_0^1(\Omega) \quad (4.10)$$

$$\int_{\Omega} \{ |\nabla\phi|^2 - \tau_p^2 \} (\bar{P} - P) \, dx dy \geq 0 \quad , \quad \forall \bar{P} \in N \quad (4.11)$$

where,

$$B_p(\phi, \bar{\phi}) = \int_{\Omega} (1 - P) \nabla\phi \cdot \nabla\bar{\phi} \, dx dy \quad (4.12)$$

Problem 4

Problem 4 is the same as Problem 3, except that instead of given f , T is given.

(L2) Find $(\phi, \lambda, P) \in H_0^1(\Omega) \times R \times N \equiv X$ such that

$$Q(\phi, \lambda, \bar{P}) \leq Q(\phi, \lambda, P) \leq Q(\bar{\phi}, \lambda, P) \quad (4.13)$$

$$Q(\phi, \bar{\lambda}, P) \leq Q(\phi, \lambda, P) \leq Q(\bar{\phi}, \lambda, P) \quad (4.14)$$

for $T \in \mathbb{R}$, and every $(\bar{\phi}, \bar{\lambda}, \bar{P}) \in \mathcal{X}$, where

$$Q(\phi, \lambda, P) = \int_{\Omega} |\nabla \phi|^2 \, dx dy + \lambda \left(T - \int_{\Omega} 2\phi \, dx dy \right) - \int_{\Omega} P (|\nabla \phi|^2 - \tau_p^2) \, dx dy \quad (4.15)$$

Equivalence of Problem 4 to the other formulations given herein can be established. Problem 4 is the most general (and less restrictive) one for the elastic-plastic torsion problem. Equivalent alternate forms of (4.13) and (4.14) are given by

(L2.1) Find $(\phi, \lambda, p) \in \mathcal{X}$ such that

$$B_p(\phi, \bar{\phi}) = (\lambda, \bar{\phi}) \quad , \quad T - \int_{\Omega} 2\phi \, dx dy = 0 \quad , \quad T \in \mathbb{R} \quad (4.16)$$

$$\int_{\Omega} (|\nabla \phi|^2 - \tau_p^2)(\bar{P} - P) \, dx dy \geq 0 \quad (4.17)$$

for every $(\bar{\phi}, \bar{\lambda}, \bar{P}) \in \mathcal{X}$.

Existence and Uniqueness

Existence and uniqueness of solutions to variational inequalities have been established by Lions and Stampacchia (1967) for coercive and nonnegative forms. Since the variational inequalities considered here are special cases of those given by Lions and Stampacchia(1967), existence and uniqueness of solutions follow immediately. Here we state a theorem on the existence and uniqueness of solutions to a general variational inequality. Problem 1 is a special case of it.

Theorem 1 (Existence and Uniqueness). Let $B(u,v)$ be a bilinear form on H (not necessarily symmetric) satisfying the conditions,

$$(i) \quad |B(u,v)| \leq C \|u\| \|v\| \text{ for } u,v \in H \text{ (continuity)} \quad (4.18)$$

$$(ii) \quad |B(u,u)| \geq \mu \|u\|^2 \quad \mu > 0 \quad \text{(coersivity)} \quad (4.19)$$

where H is a Hilbert space with inner product $((\dots))$ and norm $\|\cdot\|$. Let K be a closed convex set of H , and f be an element of the dual H' of H . Then there exists a unique solution to the problem of seeking $u \in K$ such that

$$B(u,v - u) \geq (f,v - u) \quad \text{for } v \in K \quad (4.20)$$

where (\dots) denotes the duality pairing between H' and H .

Proof. Proof of this theorem was given by Lions and Stampacchia (1967) using the fixed point theorem. Here we prove only the uniqueness. Let u_1 and u_2 be the solutions of (4.20) in K . Then

$$B(u_1, v - u_1) \geq (f, v - u_1)$$

$$B(u_2, v - u_2) \geq (f, v - u_2)$$

By setting $v = u_2$ in the first and $v = u_1$ in the second and adding we have

$$-B(u_1 - u_2, u_1 - u_2) \geq 0 \quad \text{or} \quad B(u_1 - u_2, u_1 - u_2) \leq 0$$

In view of the coercivity (4.19), it follows that $\|u_1 - u_2\| = 0$ or $u_1 = u_2$.

4.2 Numerical Procedure

Here we describe the solution procedure for Problems P1 and P2. Solution procedures for Problems L1 and L2 can be found in Lanchon (1970, and 1974) and Glowinski and Lanchon (1973). In Problem 1 and 2, the convex set K is unknown from the numerical approximation point of view. An alternate way to find the elements of K is to seek elements from an equivalent set, \bar{K} defined by

$$\bar{K} = \{\phi \in H_0^1(\Omega) : |\phi| \leq |\phi_p|\} \quad (4.21)$$

wherein ϕ_p is determined by solving the equation

$$|\nabla\phi_p|^2 - \tau_p^2 = 0 \quad (4.22)$$

The modified problem enables the numerical solution of P1 and P2, provided (4.22) can be solved for ϕ_p .

Note that ϕ_p is the solution of the fully-plastic case. Prager and Hodge (1951) and Nadai (1950) have given, in connection with the fully-plastic torsion problem, a physical construction of ϕ_p as a surface of constant slope belonging to a given cross section. Nadai demonstrated, by means of sandhills, the solution to the fully-plastic problem (4.22). It is recognized that (4.22) is a hyperbolic equation (see, for example, Geiringer, 1973), and its solution can be obtained by means of the theory of characteristics. Here, we exploit this idea to construct the numerical scheme to solve Problems 1 and 2. Details of the methodology are given in Appendix. The solution procedure can be summarized as follows:

(i) Solve equation (4.22) using the theory presented in Appendix.

(iia) When f is given (like in Problem P1) solve equation (4.3).

The finite-dimensional form (or numerical analog) of (4.3) is obtained by the use of the finite element method:

$$\{\phi\} = P_K^h [\{\phi\} - \rho([K]\{\phi\} - \{F\})] \quad (4.23)$$

where K_{ij} is the stiffness matrix, and F_j is the load vector,

$$K_{ij} = B(N_i, N_j), \quad F_j = (f, N_j)$$

Here N_i denotes the shape function, and P_K^h is the projection operator from finite-dimensional subspace $S_h \subset H_0^1(\Omega)$ to $S_h \cap K \equiv K_h$. This is equivalent to finding the minimum of the set (the quantity in the square brackets, the solution of (4.22)). Note that equation (4.23) must be solved iteratively: for $f > 0$

$$\{\phi\}_{n+1} = \min\left\{[\{\phi\}_n - \rho([K]\{\phi\}_n - \{F\})], \{\phi_p\}\right\} \quad (4.24)$$

At the beginning of the iterative procedure, one can choose $\{\phi\}_0$ as a zero vector.

(iib) When T is given (like in Problem P2), the same procedure outlined in (iia) must be followed for (4.7)₁;

$$\{\phi\}_{n+1} = \min\left\{[\{\phi\}_n - \rho_\phi([K]\{\phi\}_n - \{\Lambda\}_m)], \{\phi_p\}\right\} \quad (4.25)$$

where $\Lambda_i^m = (\lambda_m, N_i)$, λ_m being the trial value at the m -th iteration on the second equation in (4.7):

$$\lambda_{m+1} = \lambda_m - \rho_\lambda (T - \{\phi_\lambda\}^T \{g\})$$

where $\{\phi_\lambda\}$ is the converged solution of (4.25) for λ_m and $\{g\}$ is the vector

$$g_i = \int_{\Omega} 2N_i \, dx dy$$

At the beginning of the iteration procedure, a value for λ is assumed and equation (4.25) is solved iteratively for $\{\phi_{\lambda_m}\}$ until it converges. Using $\{\phi_m\}$, one solves equation (4.26) for new λ_{m+1} . Using λ_{m+1} in (4.25), one repeats the procedure until the difference between two consecutive iteration values of λ differ by a small preassigned value.

Note that equation (4.22) is solved only once for a given problem. The convergence of the iterative procedure in step (ii) depends on the relaxation parameters ρ , ρ_ϕ , ρ_λ etc. More specific comments will be made later. The approximation error for ϕ , for fixed λ , is given by the usual error estimates (see Oden and Reddy, 1976):

$$\|\phi_0 - \phi\|_{H^1(\Omega)} \leq C h^{k-m+1} \|\phi_0\|_{H^k(\Omega)}$$

where ϕ_0 is the exact solution, and $2m$ is the order of the differential equation.

4.3 Numerical Results

First the circular cross-section problem, for which the exact solution is available, is solved using all four formulations P1.1, P2.1, L1.1, and L2.1. The finite element mesh is shown in Fig. 4.1a (page 46). A modified form of successive over-relaxation (SOR) method is used to obtain the solution and $\tau_p=1$ is used in all problems.

The results are shown in Tables 4.1-4.3. Formulations P1.1 and P2.1 (present) give more accurate results for ϕ compared to those obtained by formulations L1.1 and L2.1. However, the square of the gradient of ϕ is more accurately computed by formulations L1.1 and L2.1. This is expected since in the latter case the gradient condition is included as part of the problem and therefore is satisfied more closely. However, formulations L1.1 and L2.1 took more computational time (almost twice) compared to formulations P1.1 and P2.1. Table 4.4 shows the solution for the refined mesh shown in Fig. 4.1b. The elastic-plastic torsion solution for $f=4$ using mesh (a) gives a torque of $T=0.49146$. The elastic torsion problem is solved using $f=4.0$ and also using $T=0.49146$, and the solutions are plotted along with the elastic-plastic solution in Fig. 4.2. Note that the elastic solution given by the applied torque $T=0.49146$ is redistributed due to the constant slope of ϕ in the plastic region.

The choice of the acceleration parameter ρ is very important for numerical convergence of the solution. It was shown by Young (1971) that the acceleration parameter in the SOR method for positive definite linear equations should be such that $0 < \rho < 2$ for convergence. To find the optimum value of ρ_ϕ in (4.24) on the convergence, we solved the elastic-plastic torsion of a circular shaft for various values of ρ_ϕ . Figure 4.3 shows ϕ_{\max} vs. the number of iterations for various values of ρ_ϕ between zero and two. However, $\rho_\phi = 1$ is the best value for the problem and ρ_ϕ tends to increase as the mesh parameter h decreases. Optimum value appears to be the maximum one which gives monotonic convergence.

In the case of ρ_λ , Young's estimate is not valid. In our tests we found that ρ_λ around 4.0 gives the fastest rate of convergence. Fig. 4.4a shows the log of the difference between values of λ in two consecutive

iterations against the number of iterations. Similarly, it is found that ρ_p around 0.5 gives the faster convergence for P, the Lagrange multiplier. Figure 4.4b shows the log of the difference between values of P in two consecutive iterations against the number of iterations. Finally, Fig. 4.4c shows the total number of iterations required for convergence at m^{th} iteration on λ and P for all four formulations (for circular cross section) using $\rho_\phi = 1.7$, $\rho_\lambda = 4.0$ and $\rho_p = 0.5$.

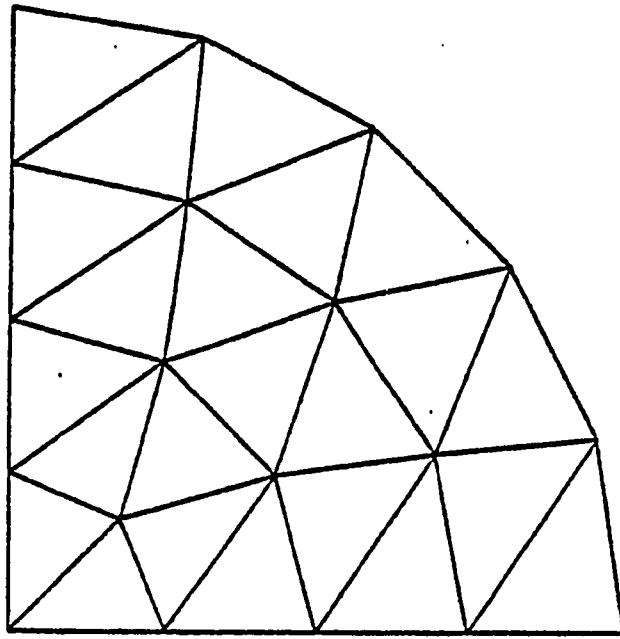
Using formulation P1.1 several other examples are solved. These include: square cross section, L-shaped cross section, and square cross section with a slit. We have used $f = 2G\theta = 2, 4, \text{ and } 6$ to compute the elastic-plastic solution. Biaxial symmetry in the square cross section case, and axial symmetry in the square cross section with a slit case are used in the finite element analysis.

Figure 4.5 shows the finite element mesh, and equi-stress function lines for $f = 2, 4, \text{ and } 6$ for the square cross section problem. Figure 4.6a shows the nonuniform finite element mesh for the L-shaped cross section and equi-stress function lines for $f = 2, 4, \text{ and } 6$. The shear stress distribution is shown in Figure 4.6b. Finally, Figure 4.7 shows the nonuniform mesh for half the domain, equi-stress function lines and the shear stresses for $f = 1, 2 \text{ and } 4$. The propagation of plastic region with increasing f can be seen from Figure 4.8.

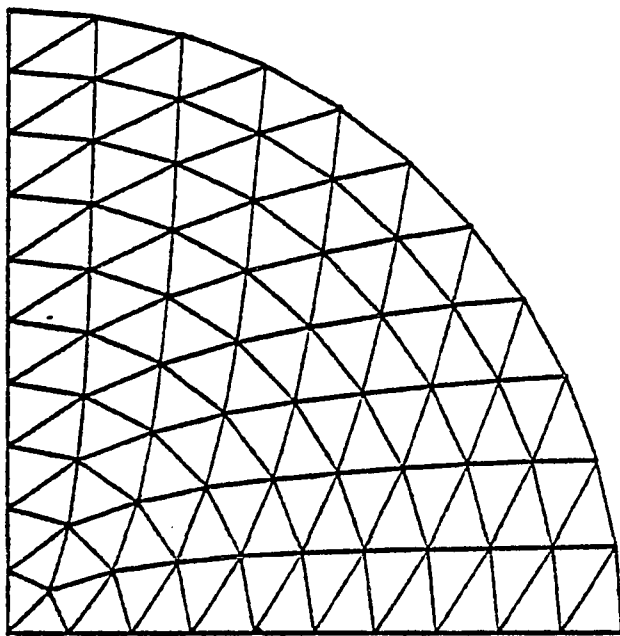
Here we presented various variational formulations of the elastic-plastic torsion problem. We chose for numerical calculation the projectional form of the formulation which is based on the proof of existence and uniqueness of solutions. The fully-plastic equation (4.22) is solved for ϕ_p by means of the theory of characteristics and

then an iterative procedure is employed to solve the finite element analog of equation (4.3) for ρ . A number of numerical examples are presented to show the feasibility and effectiveness of the present method.

As indicated in Section 4.2, the choice of the acceleration parameter ρ is very crucial in obtaining convergent solutions. A working value of ρ is obtained by trial in the present investigation. Lack of theoretical bounds, analogous to those established by Young (1971) for positive definite linear equations, on ρ in the present case necessitated numerical investigation of the influence of ρ on the convergence. Thus, there exists a need to find theoretical bounds on ρ for non-positive definite forms.



(a)



(b)

Figure 4.1 Mesh for circular cross section with $r=1.0$.

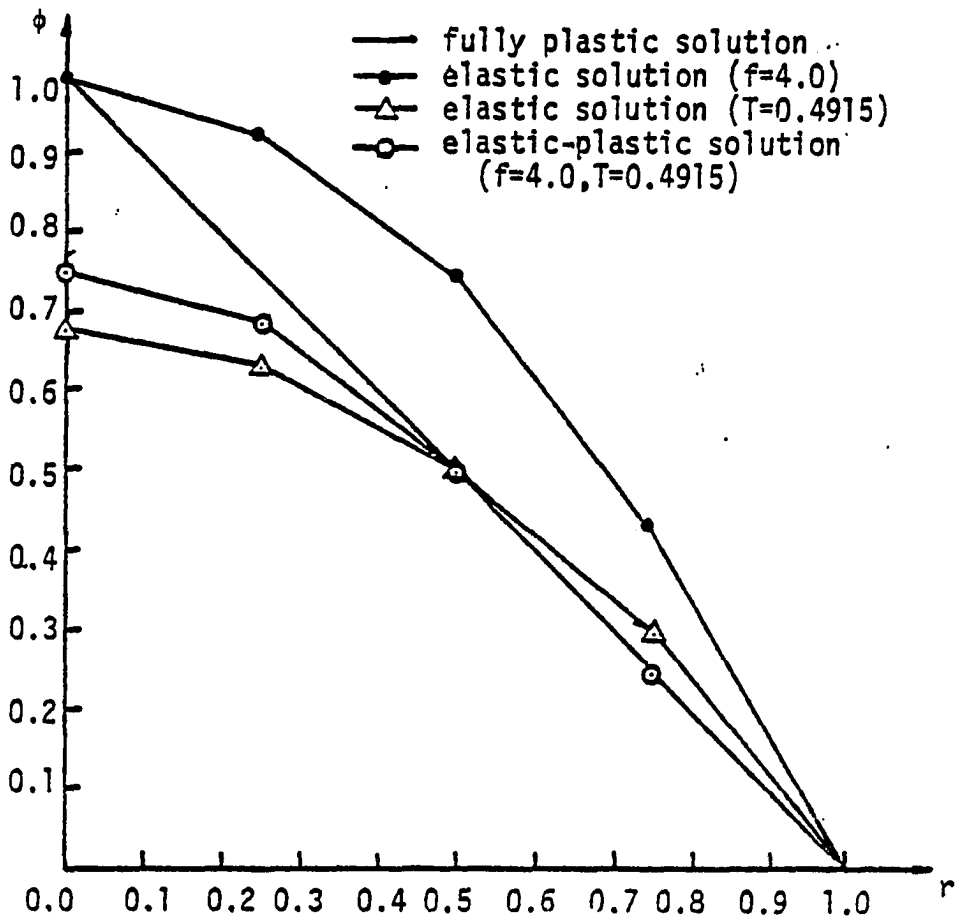


Figure 4.2 Comparison of elastic and elastic-plastic solution for circular cross section.

Table 4.1

Comparison of ϕ by various formulations for circular cross-section

| Method r | Exact | Method P1.1 | Method L1.1 | Method P2.1 | Method L2.1 |
|---|--------|----------------|----------------|----------------|----------------|
| 0.0 | 0.75 | 0.7564 | 0.7374 | 0.7564 | 0.7362 |
| 0.25 | 0.6875 | 0.6884 | 0.6703 | 0.6884 | 0.6695 |
| 0.5 | 0.5 | 0.5 | 0.4909 | 0.5 | 0.4911 |
| 0.75 | 0.25 | 0.25 | 0.2469 | 0.25 | 0.2470 |
| 1.0 | 0.0 | 0.0 | 0.0 | 0.0 | 0.0 |
| Comparison of torque and the lagrange multiplier* | | | | | |
| T. | 0.5072 | 0.4915 | 0.4748 | (0.4915) | (0.4748) |
| λ | 4.0 | (4.0) | (4.0) | 4.0003 | 3.9784 |

* values in parenthesis indicate specified values

Table 4.2

Comparison of v_{ϕ}^2 by various formulations for circular cross-section

| r | Exact | Method P1.1 | Method L1.1 | Method P2.1 | Method L2.1 |
|-------|--------|----------------|----------------|----------------|----------------|
| 0.125 | 0.0625 | 0.3099 | 0.3112 | 0.3097 | 0.3094 |
| 0.375 | 0.5625 | 0.7801 | 0.7610 | 0.7802 | 0.7568 |
| 0.625 | 1.0 | 1.0195 | 0.9999 | 1.0195 | 1.0005 |
| 0.875 | 1.0 | 1.0125 | 1.0001 | 1.0125 | 1.0003 |

Table 4.3

Comparison of percentage errors in various formulations for circular cross-section bar

| Quantity | Method P1.1 | Method L1.1 | Method P2.1 | Method L2.1 |
|---------------|-------------|-------------|-------------|-------------|
| ϕ_{\max} | 0.0086 | 0.0168 | 0.0086 | 0.0184 |
| λ | — | — | 0.0 | 0.0054 |
| T | 0.031 | 0.0639 | 0.031 | 0.0639 |

Table 4.4

Comparison of solution ϕ for circular cross-section with fine mesh ($f = 4$)

| r | Method P1.1 | | Exact Solution | |
|-----|-------------|--------|----------------|--------|
| | ϕ | τ | ϕ | τ |
| 0.0 | 0.7498 | 0.1082 | 0.75 | 0.1 |
| 0.1 | 0.7390 | 0.2962 | 0.74 | 0.3 |
| 0.2 | 0.7094 | 0.4960 | 0.71 | 0.5 |
| 0.3 | 0.6598 | 0.6975 | 0.66 | 0.7 |
| 0.4 | 0.5900 | 0.9002 | 0.59 | 0.9 |
| 0.5 | 0.5 | 1.0 | 0.5 | 1.0 |
| 0.6 | 0.4 | 1.0 | 0.4 | 1.0 |
| 0.7 | 0.3 | 1.0 | 0.3 | 1.0 |
| 0.8 | 0.2 | 1.0 | 0.2 | 1.0 |
| 0.9 | 0.1 | 1.0 | 0.1 | 1.0 |
| 1.0 | 0.0 | 1.0 | 0.0 | 1.0 |

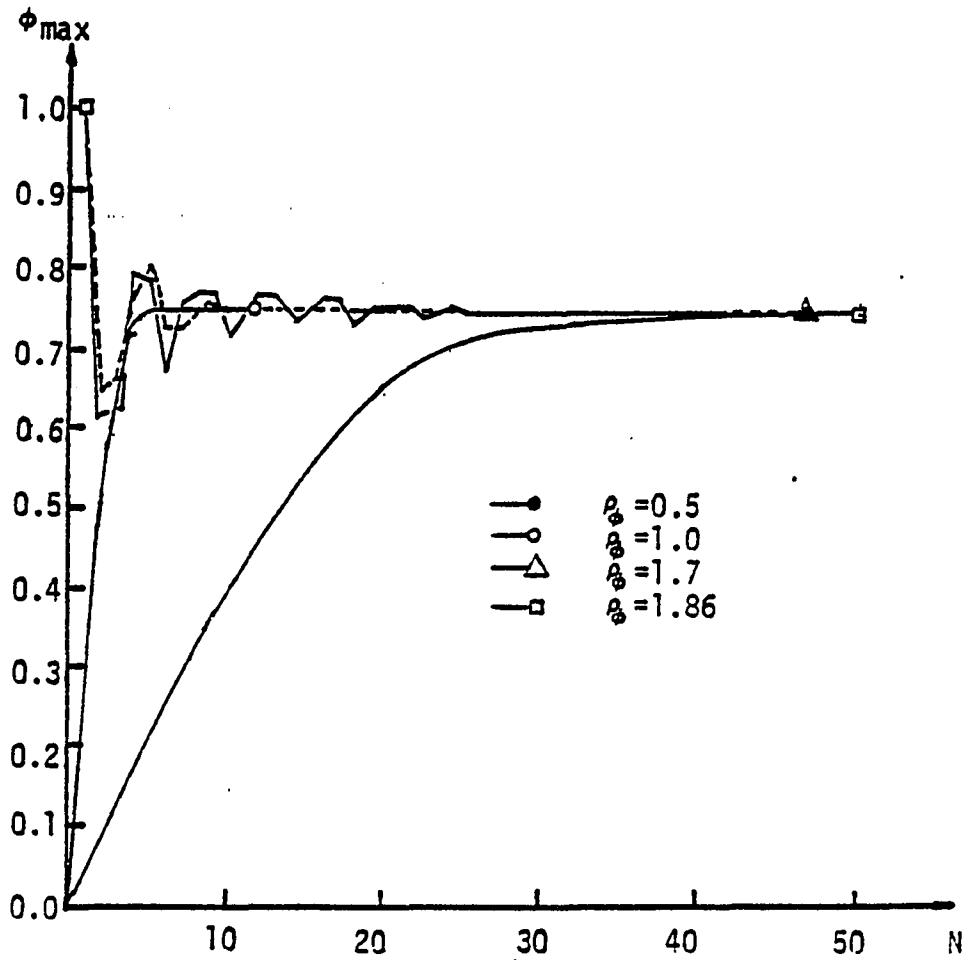


Figure 4.3 Influence of the acceleration parameter on the convergence of ϕ_{\max}

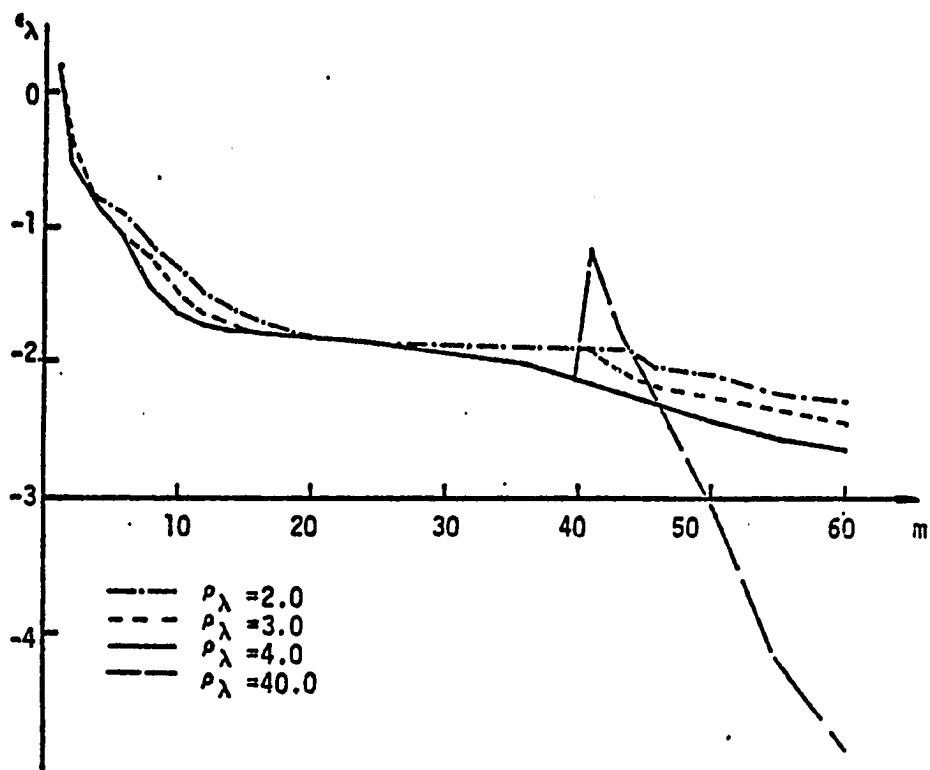


Figure 4.4a Convergence of λ .

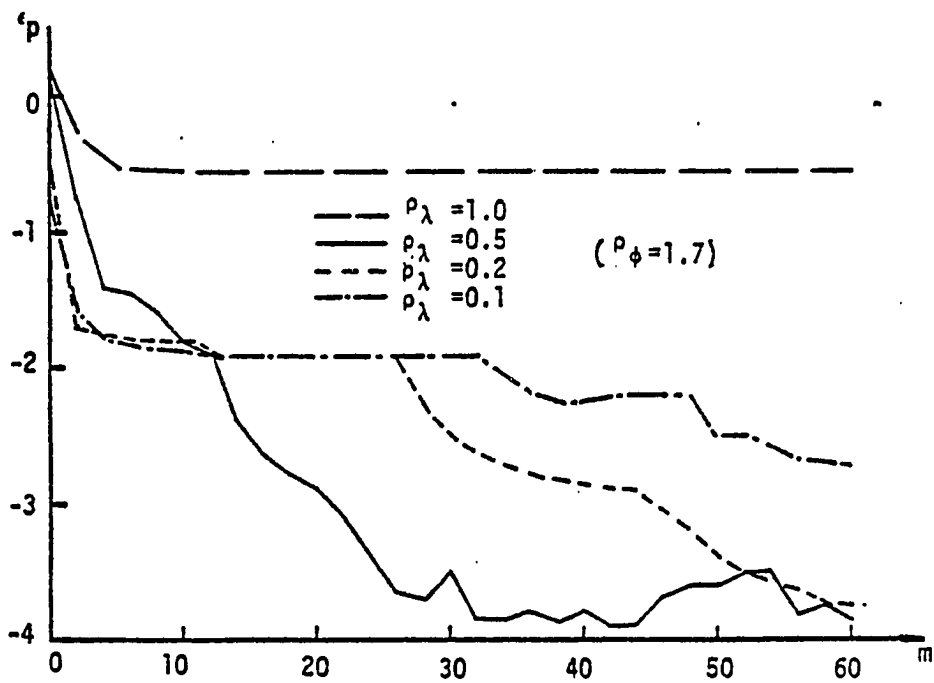


Figure 4.4b Convergence of p .

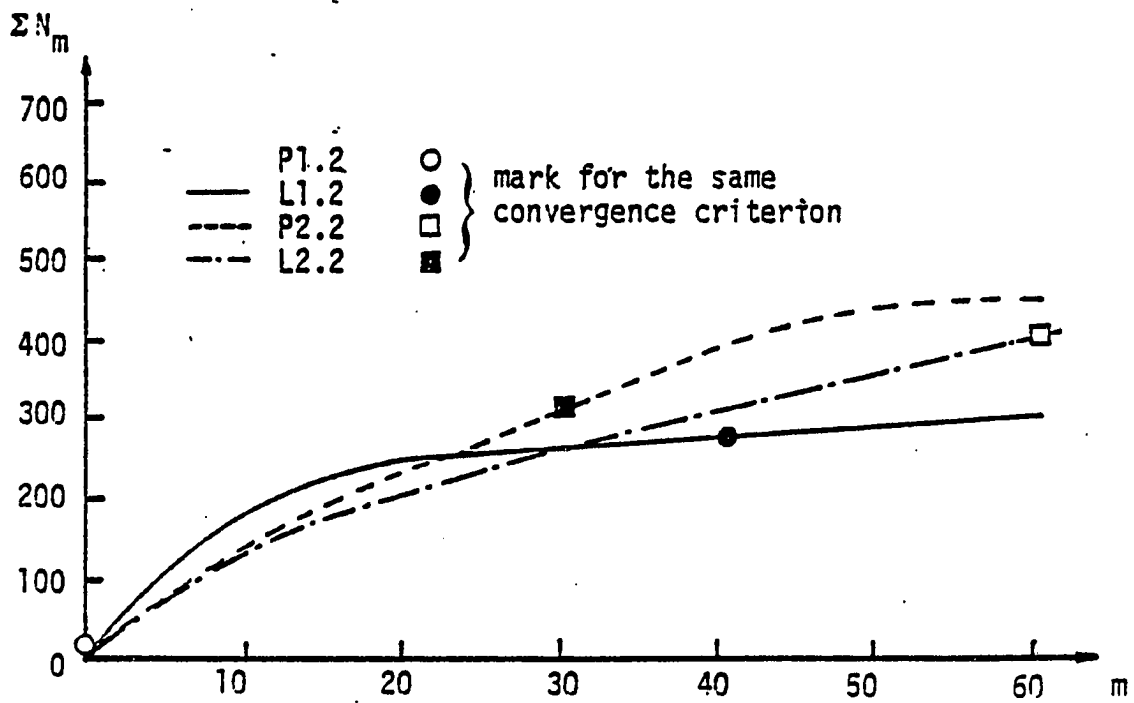


Figure 4.4c The number of total iterations at the m -th step.

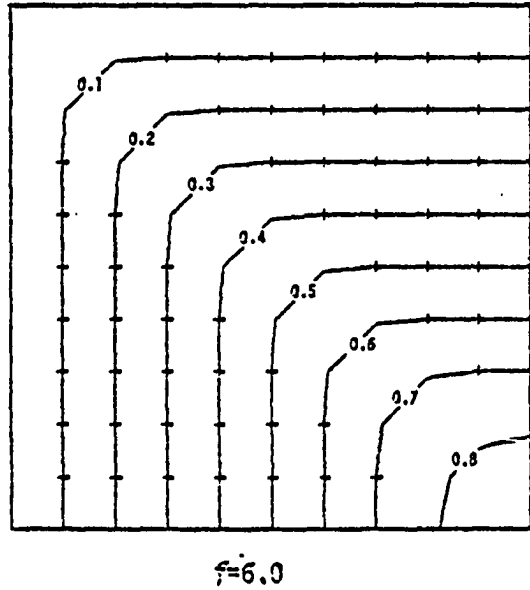
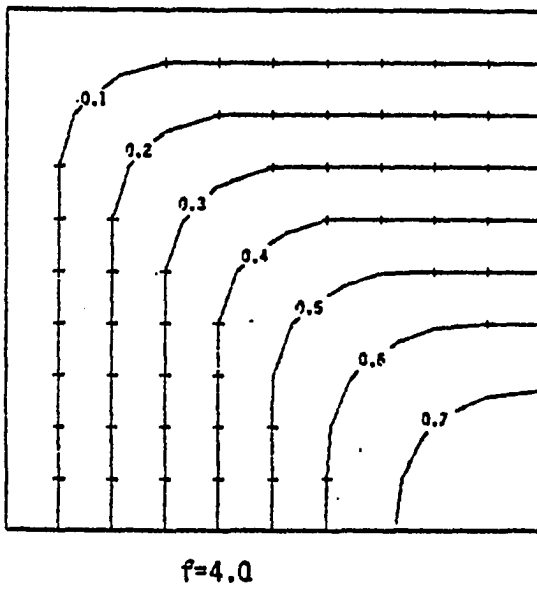
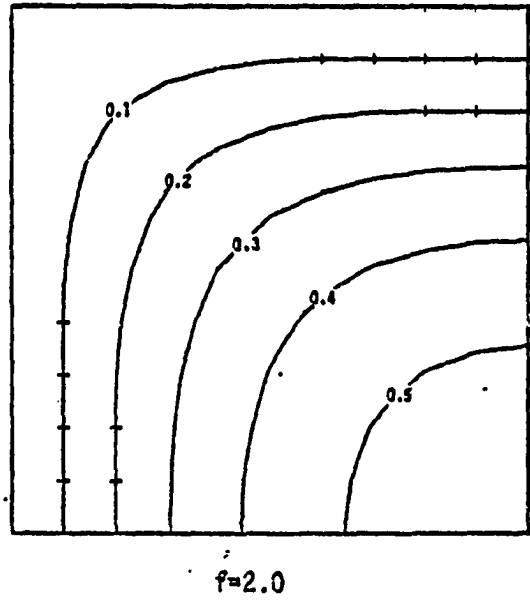
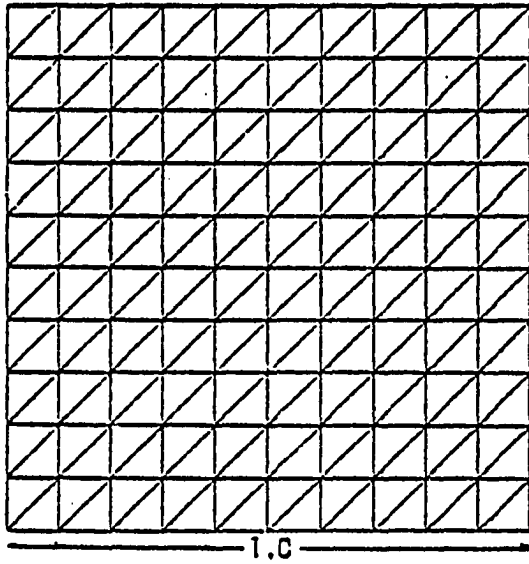
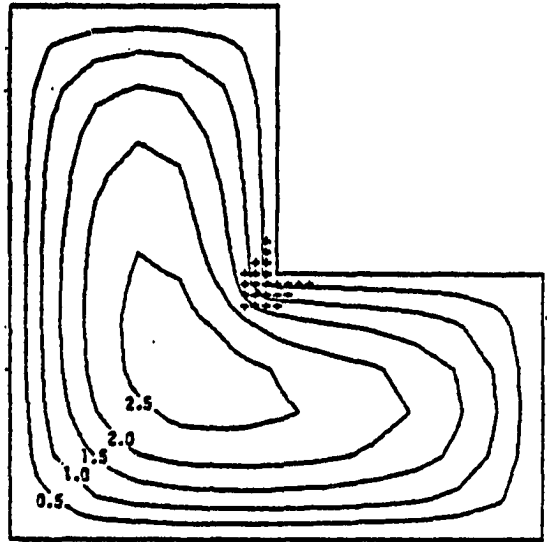
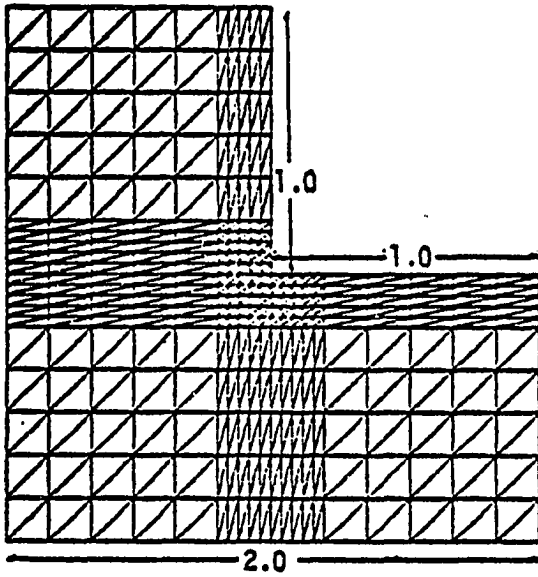
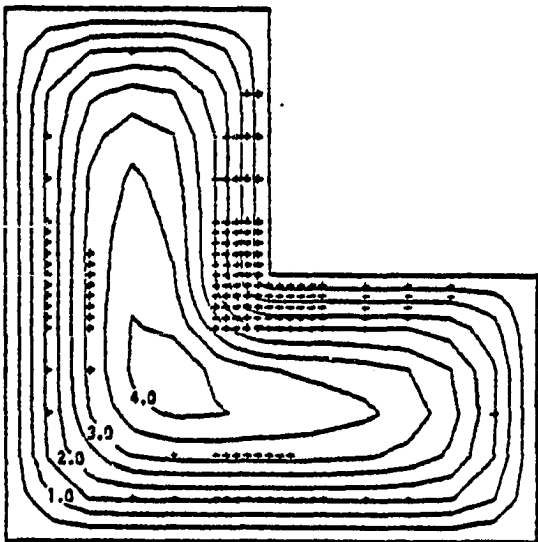


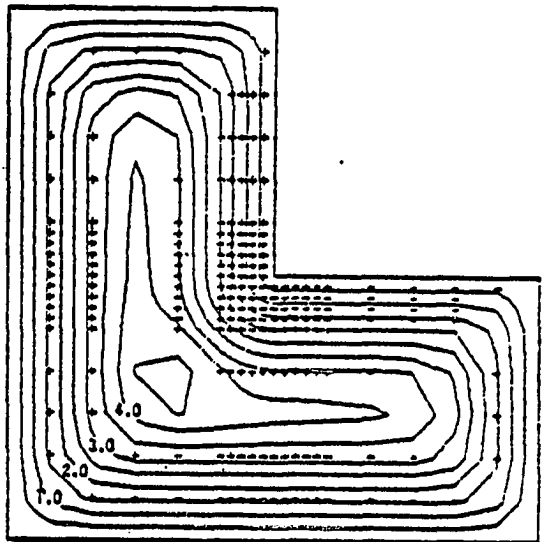
Figure 4.5 Equi-stress function lines and yielded portion for square cross section. + shows yielded nodes.



f=2.0

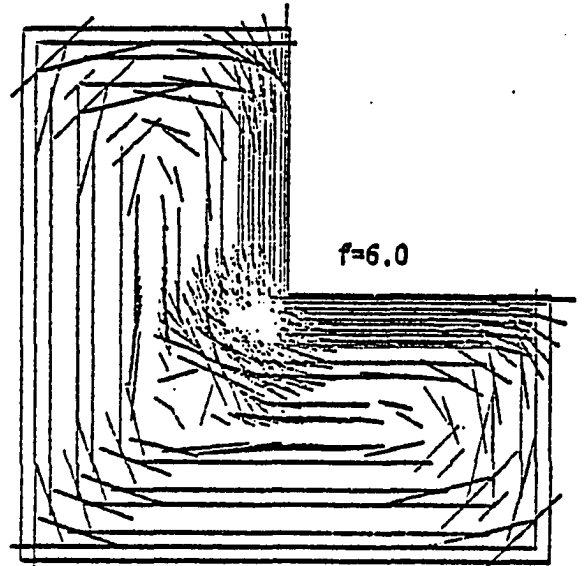
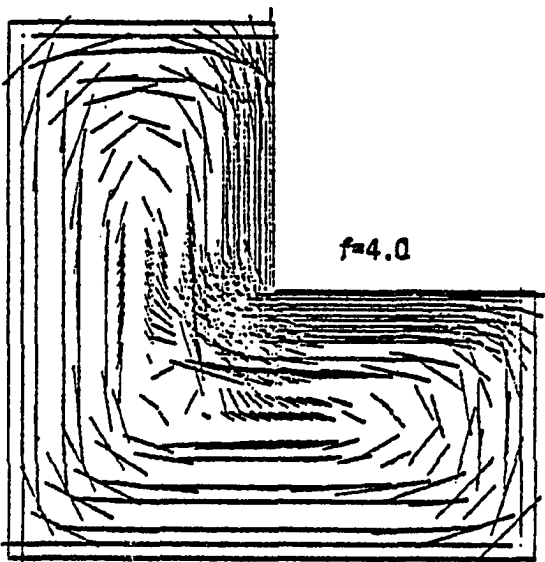
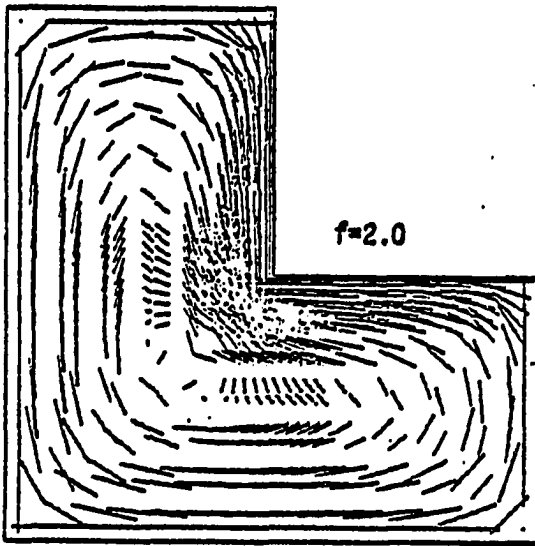


f=4.0

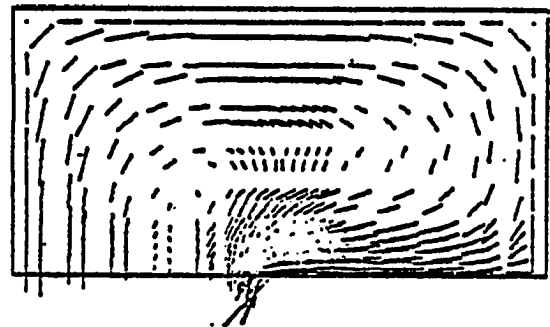
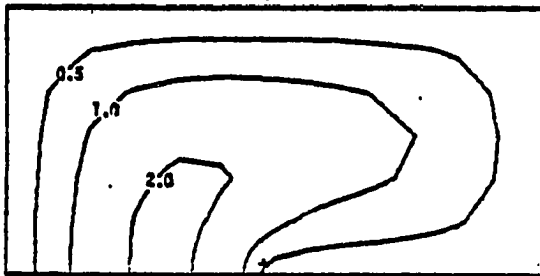
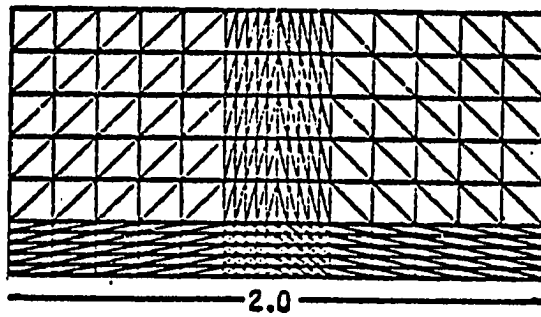


f=6.0

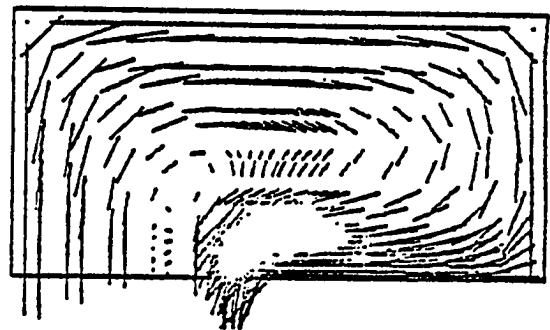
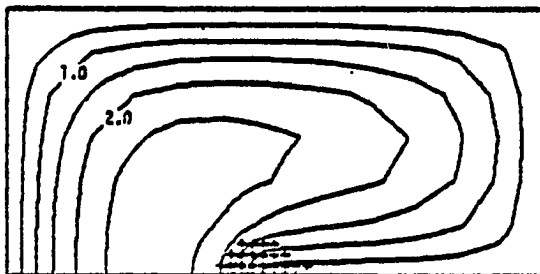
4.6a Equi-stress function lines and yielded portion for L-shaped cross section .



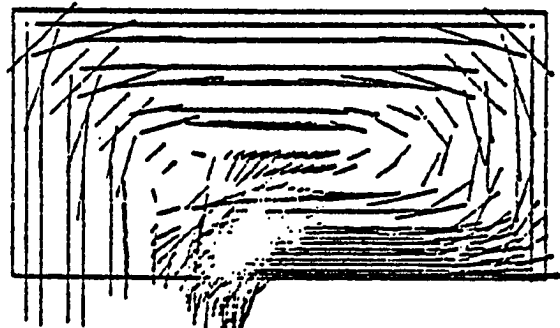
4.6b The shear stress distribution for L-shaped cross section .



f=1.0

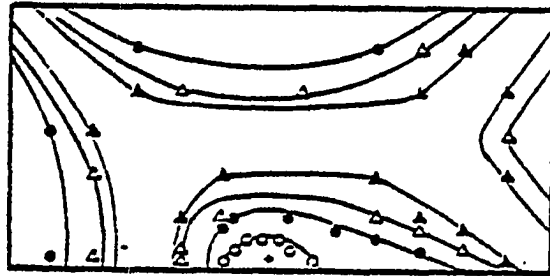
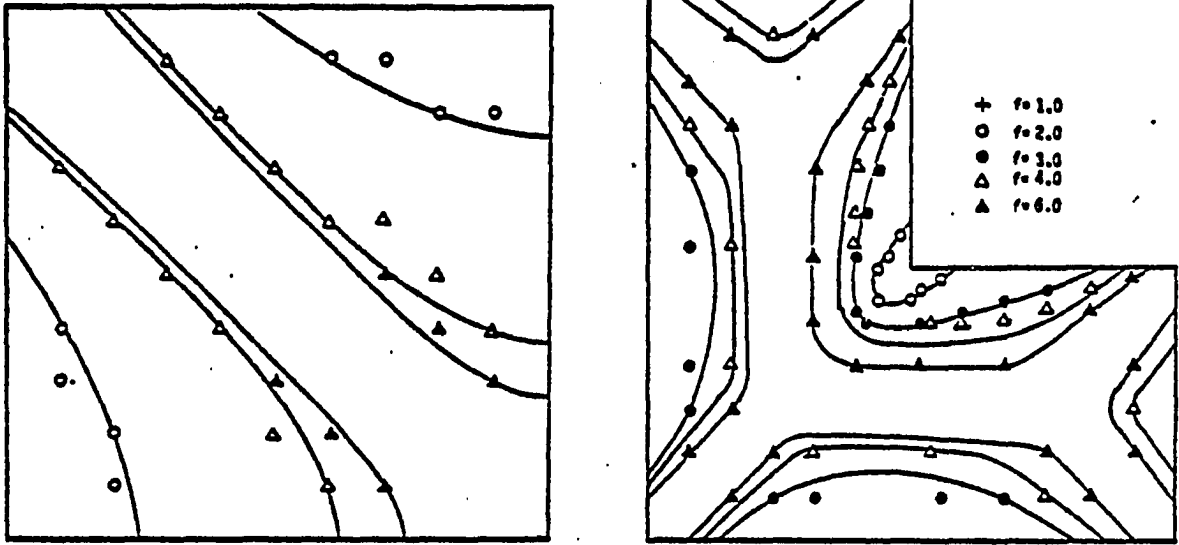


f=2.0



f=4.0

4.7: Equi-stress function lines, shear stress distribution and yielded nodes for square cross section with slit .



4.8 Plastic regions for various cross sections

CHAPTER V

A COMPARISON OF A PENALTY FINITE ELEMENT MODEL WITH THE STREAM FUNCTION-VORTICITY MODEL OF NATURAL CONVECTION IN ENCLOSURES

5.1 Penalty and Stream Function-Vorticity Formulation

For the governing equations of natural convection in enclosures defined in Chapter II, we now give two formulations, one based on the primitive variables equations (2.7)-(2.10), and the other based on the stream function and vorticity equations (2.18)-(2.20). It is convenient to recast these equations in terms of the normalized (i.e., non-dimensionalized) variables. We use here two different normalizations ($i = 1, 2$):

$$x = x'd, \quad y = y'd, \quad u = u'U_i, \quad v = v'U_i, \quad \theta = (T - T_c)/(T_h - T_c)$$

$$P = P'U_i^2, \quad \rho U_i = \alpha_i/d,$$

where $\alpha_1 = \alpha$, and $\alpha_2 = \nu$, and the quantities with primes denote the non-dimensional variables. For the sake of brevity, we shall omit the primes in the following.

5.1.1 Penalty Formulation

The penalty function concept of Courant (1956) involves the reduction of variational problems which are posed as conditional extremum

problems to variational problems without the constraints by the introduction of a penalty functional associated with the constraints. The concept has been known for a long time, and at present, many investigations are devoted to the exploitation of the concept to other situations and applications to particular problems. Zienkiewicz (1974), guided by the analogy between nearly incompressible elasticity and Stokes' problem, suggested the application of the penalty method to viscous incompressible flow problems; the incompressibility condition was treated as the constraint (e.g., Heinrich et al., 1978, Marshall et al., 1978 and Reddy, 1978). Another modification was suggested recently by Reddy (1979b,c), who treated, in order to introduce the stream function into the primary calculations, the stream function-velocity relations along with the incompressibility condition as constraints. The formulation presented by Reddy (1979b,c) appears to be the best way to describe the penalty formulation of natural convection in enclosures.

The penalty method seeks to satisfy the constraint conditions in a least-square sense. Applied to the problem at hand, i.e. find the solution (u,v,P,T) to equation (2.7)-(2.10) subject to the constraint conditions in (2.7) and (2.16), the penalty method seeks solutions to the variational problem,

$$\delta I(u,v,\psi,\theta) \equiv \delta I_0(u,v,\theta) + \delta G(u,v,\psi) = 0 \quad (5.2)$$

where u,v,ψ , and θ are the nondimensional variables, and

$$\begin{aligned} \delta I_p(u,v,\psi,\theta) = & \int_{\Omega} \left\{ [A(u) - P_r R_a \theta] \delta u + P_r \left[2 \frac{\partial u}{\partial x} \frac{\partial \delta u}{\partial x} + \right. \right. \\ & + 2 \frac{\partial v}{\partial y} \frac{\partial \delta v}{\partial y} + \left. \left. \left(\frac{\partial u}{\partial y} + \frac{\partial v}{\partial x} \right) \left(\frac{\partial \delta u}{\partial y} + \frac{\partial \delta v}{\partial x} \right) \right] + \right. \\ & + A(v) \delta v + A(\theta) \delta \theta + \left. \frac{\partial \theta}{\partial x} \frac{\partial \delta \theta}{\partial x} + \frac{\partial \theta}{\partial y} \frac{\partial \delta \theta}{\partial y} \right\} dx dy \\ & - \int_{\partial \Omega | u} \hat{t}_x \delta u ds - \int_{\partial \Omega | v} \hat{t}_y \delta v ds - \int_{\partial \Omega | T} \hat{q} \delta \theta ds \end{aligned} \quad (5.3)$$

$$G(u,v,\psi) = \frac{\varepsilon_1}{2} \int_{\Omega} \left(\frac{\partial u}{\partial x} + \frac{\partial v}{\partial y} \right)^2 dx dy + \frac{\varepsilon_2}{2} \int_{\Omega} \left\{ \left(u - \frac{\partial \psi}{\partial y} \right)^2 + \left(v + \frac{\partial \psi}{\partial x} \right)^2 \right\} dx dy \quad (5.4)$$

Here P_r is the Prandtl number, R_a is the Rayleigh number,

$$P_r = \nu/\alpha, \quad R_a = g\beta d^3(T_h - t_c)/\nu\alpha, \quad (5.5)$$

and ε_1 and ε_2 are the penalty parameters (for normalization $i = 1$).

Note that in the penalty method, the pressure does not appear. This is because the pressure is the Lagrange multiplier associated with the incompressibility constraint, which is satisfied only in a weak sense in the penalty method. However, the Lagrange multiplier can be computed in the penalty method by (see Polyak, 1971)

$$P_{\varepsilon} = -\varepsilon \left(\frac{\partial u_{\varepsilon}}{\partial x} + \frac{\partial v_{\varepsilon}}{\partial y} \right). \quad (5.6)$$

Convergence of the solution $(u_{\varepsilon}, v_{\varepsilon}, P_{\varepsilon}, \psi_{\varepsilon}, \theta_{\varepsilon})$ of the penalty formulation to the true solution (as $\varepsilon \rightarrow \infty$) can be proved (see Bercovier, 1978 and Reddy, 1979a, 1980b).

5.1.2 Stream Function-Vorticity Formulation

In terms of the nondimensional variables, equations (2.18)-(2.20) can be expressed as

$$\begin{aligned} -\nabla^2 \zeta &= b_i J(\psi, \zeta) + c_i \frac{\partial \theta}{\partial y}, \\ -\nabla^2 \psi &= \zeta, \\ -\nabla^2 \theta &= a_i J(\psi, \theta). \end{aligned} \quad (5.7)$$

where (a_i, b_i, c_i) denote the coefficients for the two types of nondimensionalizations:

$$(a_1, b_1, c_1) = (1, 1/Pr, Ra), \quad (a_2, b_2, c_2) = (Pr, 1, Gr). \quad (5.8)$$

Here Gr denotes the Grashoff number, $Gr = Ra/Pr$. The variational formulation of equations (5.7) indicates that one of θ , ζ , and ψ be specified on portions of boundary. It is now a common practice (see Tabarrok, 1977) to approximate the boundary values of ζ using the second equation in (5.7). The Taylor series expansion is employed to express the stream function inside the domain in terms of its values on the boundary:

$$\psi_i = \psi_w + \left(\frac{\partial \psi}{\partial n} \right) \Big|_w (\Delta n) + \frac{1}{2} \left(\frac{\partial^2 \psi}{\partial n^2} \right) \Big|_w (\Delta n)^2 + \dots, \quad (5.9)$$

where $(.)|_w$ is the value at the wall of the enclosure, and Δn is the normal distance from the wall to a point (or node) i . Using $\zeta_w = -\frac{\partial^2 \psi_w}{\partial n^2}$ and noting that $\psi_w = \text{constant} = 0$ along the solid wall of the enclosure, we obtain (omitting the higher order terms in equation (5.9)),

$$\zeta_w = -\frac{2\psi_i}{(\Delta n)^2}. \quad (5.10)$$

The variational formulation of equations (5.7) is given by

$$\begin{aligned} B(\zeta, \bar{\zeta}) &= b_i J(\psi, \zeta; \bar{\zeta}) + c_i Q(\bar{\zeta}), \\ B(\psi, \bar{\psi}) &= R(\bar{\psi}), \\ B(\theta, \bar{\theta}) &= a_i J(\psi, \theta; \bar{\theta}), \end{aligned} \quad (5.11)$$

where

$$\begin{aligned} B(p, q) &= \int_{\Omega} \left(\frac{\partial p}{\partial x} \frac{\partial q}{\partial x} + \frac{\partial p}{\partial y} \frac{\partial q}{\partial y} \right) dx dy, \\ J(p, q; f) &= \int_{\Omega} J(p, q) f dx dy \\ Q(\zeta) &= \int_{\Omega} \frac{\partial \theta}{\partial y} \zeta dx dy, \quad R(\psi) = \int_{\Omega} \zeta \psi dx dy. \end{aligned} \quad (5.12)$$

Here we assumed that the boundary values of ψ , ζ , and θ are specified.

5.2 Finite-Element Formulations

5.2.1 Penalty-Finite Element Model

In the penalty method, we discretize the region occupied by the fluid into a finite set of subregions, called finite elements. We consider a typical finite element, Ω_e , and develop the finite element equations corresponding to the equations (5.2)-(5.4). We assume the following interpolation of the variables (u, v, ψ, θ) over the element Ω_e :

$$u = \sum u_i N_i(x, y), \quad v = \sum v_i N_i(x, y), \quad \psi = \sum \psi_i N_i(x, y), \quad \theta = \sum \theta_i N_i(x, y), \quad (5.13)$$

wherein $N_i(x, y)$ are the interpolation (or shape) functions, which depend on the type of element chosen, and u_i, v_i, ψ_i , and θ_i are the values of the functions $(u, v, \psi, \text{ and } \theta)$ at the i -th node of the element. In the present paper a bilinear quadrilateral element (with four nodes) is used.

Since the variational formulation (5.2) is valid in Ω , it is valid, in particular, in Ω_e with t_x , t_y and q assumed, for the moment, to be known on the element boundary. Substituting (5.13) into the element equation corresponding to (5.2) we obtain (collecting the coefficients of δu_i , δv_i , $\delta \psi_i$ and $\delta \theta_i$),

$$[K^e] \{\Delta^e\} = \{F^e\}, \quad [C^e] \{\theta^e\} = \{Q^e\}, \quad (5.14)$$

where

$$[K^e] = \left[\begin{array}{cc|cc} [H^x] + \epsilon_1[S^x] + \epsilon_2[S] & P_r [S^{xy}]^T + \epsilon_1[S^{xy}] & -\epsilon_2[S^{oy}] & \\ P_r[S^{xy}] + \epsilon_1[S^{xy}]^T & [H^y] + \epsilon_1[S^y] + \epsilon_2[S] & \epsilon_2[S^{ox}] & \\ -\epsilon_2[S^{oy}]^T & \epsilon_2[S^{ox}]^T & \epsilon_2[S^x + S^y] & \end{array} \right],$$

$$C_{ij}^e = A_{ij} + S_{ij}^x + S_{ij}^y, \quad A_{ij} = \int_{\Omega_e} N_i A(N_j) dx dy, \quad [S] = [S^{00}],$$

$$S_{ij}^{\xi\eta} = \int_{\Omega_e} N_{i,\xi} N_{j,\eta} dx dy, \quad (\xi, \eta = 0, x, y), \quad S_{ij}^{\xi\xi} = S_{ij}^{\xi}, \text{ etc.}$$

$$H_{ij}^x = A_{ij} + P_r (2 S_{ij}^x + S_{ij}^y), \quad H_{ij}^y = A_{ij} + P_r (2 S_{ij}^y + S_{ij}^x),$$

$$\{F^e\} = \{F_i^x, F_i^y\}^T, \quad \{\Delta^e\} = \{u_i, v_i, \psi_i\}^T, \quad \{\theta^e\} = \{\theta_i\}^T,$$

$$F_i^x = P_r R_a \int_{\Omega_e} \theta N_i dx dy + \int_{\partial\Omega_{1u}^e} \hat{t}_x N_i ds, \quad (5.15)$$

$$F_i^y = \int_{\partial\Omega_{1v}^e} \hat{t}_y N_i ds, \quad Q_i^e = \int_{\partial\Omega_{1T}^e} \hat{q} N_i ds.$$

Note that the matrix [A] is computed assuming that u and v are known a-priori, necessitating the use of an iterative procedure for the solution of the assembled equations. By setting ε_2 to zero, one obtains from equation (5.14), the penalty finite-element model presented by Heinrich (1978) and Reddy and Mamidi (1978).

5.2.2 Stream Function-Vorticity Finite Element Model

Using interpolation of the form in equation (5.13) in equations (5.11), we obtain

$$\begin{aligned} [B^e - b_i J^e] \{\zeta^e\} &= \{F^{1e}\}, \\ [B^e] \{\psi^e\} &= \{F^{2e}\}, \\ [B^e - a_i J^e] \{\theta^e\} &= \{0\}, \end{aligned} \quad (5.16)$$

where

$$\begin{aligned} B_{ij}^e &= B(N_i, N_j), \quad J_{ij}^e = J(\psi, N_i; N_j), \\ F_j^{1e} &= c_i Q(N_j), \quad F_j^{2e} = R(N_j), \end{aligned} \quad (5.17)$$

and $B(.,.)$, $J(.,.;.)$, $Q(.)$, and $R(.)$ are given by equation (5.12).

5.2.3 Computational Procedure

The element equations in (5.14) and (5.16) are assembled in the usual manner to obtain the associated global matrices. However, these matrix equations are nonlinear and require iterative procedures. The following iterative procedure is employed in the present study. At the beginning of the first iteration the matrix coefficients are computed assuming that the velocity vector is zero. Then the temperature equation is solved for $\{\theta\}$. Using the computed temperature, the velocity and stream function equations are solved, completing one cycle of iteration. Using the velocity (and/or stream function) field obtained in the previous iteration, matrix coefficients for the next iteration are computed and the procedure is repeated until the Euclidean norm of the difference of the solutions at any two successive iterations becomes sufficiently small (say, $<10^{-4}$). In the present study we used, to accelerate the convergence, a weighted sum of the variables in computing the matrix coefficients for the next iteration. For example, at the end of r -th iteration we have, $0 < \rho_1, \rho_2 < 1$,

$$\{u\}^* = \rho_1 \{u\}_r + (1-\rho_1) \{u\}_{r-1}, \quad (5.18)$$

$$\{\theta\}^* = \rho_2 \{\theta\}_r + (1-\rho_2) \{\theta\}_{r-1}.$$

One can transfer the nonlinear (convective) terms to the right side of the equation and assume that it is known from the previous iteration. This gives a constant coefficient matrix and saves computational time in recomputing the coefficient matrices during each iteration.

However, this procedure is found to result in divergent solutions even

for moderately high Rayleigh numbers.

The algebraic complexity and the nonlinear nature of the matrices in equation (5.14) forces one to use numerical integration to evaluate various matrix coefficients. Another reason which necessitates the use of numerical integration is the "reduced integration" required by the penalty method. To establish the existence and uniqueness of solutions, the penalty-finite element approximations should satisfy the continuity and coercivity conditions of a generalized Lax-Milgram theorem (see Oden and Reddy, 1976). These conditions are satisfied by the penalty finite-element approximations, provided the parameter appearing in the coercivity condition is independent of the mesh size. That is, the finite element chosen for the penalty method must be such that this parameter does not depend on the mesh size. It is found that (see Zienkiewicz, Taylor and Too, 1971) numerical integration of matrix coefficients associated with the penalty functional $G(u,v,\psi)$ with one less number of Gaussian points (in each direction) will ensure that the parameter is independent of the mesh size. Further study in this direction seems to be necessary.

Alternate but more direct explanation of this latter observation is also given here. The penalty-finite element equation (5.14)₁ has the form ($\epsilon_1 = \epsilon_2 = \epsilon$),

$$([K_1] + \epsilon[K_2])\{\Delta\} = \{F\} . \quad (5.19)$$

As ϵ is increased to a large value (in an attempt to satisfy the constraints more closely), the magnitude of $[K_1]$ in comparison to $\epsilon[K_2]$ becomes negligible in the computer, and we have

$$\epsilon[K_2]\{\Delta\} = \{F\} , \text{ or } [K_2]\{\Delta\} = \frac{1}{\epsilon} \{F\} . \quad (5.20)$$

This implies that as ϵ is made larger and larger, only constraint equations are left (which results in a trivial solution since $\epsilon^{-1} \sim 0$); and the contributions of conservation of momentum and energy are lost. To circumvent this difficulty two things must be done. First, the magnitude of ϵ must be such that the matrix $[K_1]$ is not negligibly small compared to $[K_2]$. Second, the matrix $[K_2]$ must be singular so that there are fewer constraint equations than the number of unknowns. This can be achieved by using reduced integration on the elements of $[K_2]$. That is, the standard 2x2 Gauss rule must be used to evaluate the elements of $[K_1]$, whereas only a 1x1 Gauss rule must be used to evaluate the elements of $[K_2]$. A value of $\epsilon_1 = \epsilon_2 = \epsilon = 10^8$ was used in all problems discussed here.

5.3 Numerical Results and Discussion

In any approximate method, physics of the problem plays a crucial role in constructing a reasonable approximation. The finite element method is no exception. For example, one needs to visualize, using physical arguments, possible flow and temperature patterns in an enclosure in order to lay a mesh that can reasonably approximate what is intuitively expected. In the case of high-Rayleigh-number flows in rectangular enclosures, a boundary layer appears (due to the no-slip boundary condition) at the walls. Since the boundary layer influences the behavior of the core region, it must be modeled adequately by employing refined mesh at the walls. Another important consideration, when using an approximate method, is in the specification of physically realistic boundary conditions of the problem at hand. In the penalty formulation, all physical boundary conditions can be handled without difficulty.

Here we compare the numerical results obtained by the penalty-finite element model and the stream function-vorticity finite element model for free convection in rectangular enclosures. The right and left vertical walls of the enclosure are maintained, respectively, at cold and hot ($\theta_c = -.5, \theta_h = .5$) temperatures, and the top and bottom (horizontal) walls are either insulated or have specified temperature variations (see Figure 5.1, page 73). The models are compared for relative accuracy and computational time. Since most of the previous investigators presented results in graphical form, it is not possible to compare the present results quantitatively. However, present results are compared for Nusselt numbers, vorticity and stream function values with those available in the literature.

First, the effect of the two normalizations mentioned earlier on the numerical convergence was studied. Normalization 1 ($i=1$) was used in both models, while Normalization 2 ($i=2$) was used only in the stream function-vorticity model. All of the calculations were carried in double precision on an IBM 370/158 computer. It was found that the use of Normalization 2 presents convergence problems for $Ra > 10^4$ and $Pr < 1$. The numerical procedure used there employed the constant coefficient matrix, treating $\{F^1\}$ in equation (5.16) as known from the previous iteration. The slow convergence (or divergence) is a direct result of this numerical procedure, which yields numerical solution proportional to c_2 (or inversely to the Prandtl number). Thus any error in $\partial\theta/\partial y$ is amplified in this procedure and leads to non-convergent solution. Normalization 1 was found to give faster convergence, even for large Rayleigh numbers, for both formulations.

Next, a penalty-finite element model with stream function included in the model (i.e., $\epsilon_2 \neq 0$) was compared with the penalty-finite element model without stream function (i.e., $\epsilon_2 = 0$). The model problem used was

that of a square cavity with top and bottom walls insulated. A 12x12 mesh of linear elements (see Fig. 5.1) was used in both models. The vorticity was computed at the Gauss points in both models. The stream function in the second model ($\epsilon_2 = 0$) was calculated using equation (2.17), in which the velocities are known from the primary calculations. It is clear from Fig. 5.1 that the results, for isotherms and streamlines (for $Ra = 10^3$, $Pr = 10$), obtained by the two models are identical. However, the computational time required by the first model ($\epsilon_2 \neq 0$) is about fifty percent more than that required by the second model ($\epsilon_2 = 0$). For this reason, the remaining problems were analyzed using the second model ($\epsilon_2 = 0$).

The effect of the Rayleigh number (for fixed Prandtl number) on the velocity and temperature fields was investigated using the two formulations. Figure 5.2 shows the vertical velocity component and the temperature along the (horizontal) center of the cavity. The results were obtained by the penalty-finite element model with a 10x10 uniform mesh for $Ra = 10^3$, 10^4 , and 12x12 nonuniform mesh for $Ra = 10^5$, of linear elements. Figure 5.3 shows the isotherms and stream lines obtained by the penalty-finite element model for $Ra = 10^4$, and 10^5 , and $Pr = 1$. The numerical results obtained by the stream function-vorticity finite element model, for $Ra = 10^3$ and 10^4 , were found to be very close to those obtained by the penalty-finite element model and cannot be plotted distinctly on the present scale. Therefore, the results are compared in Table 5.1 for $Ra = 10^3$, 10^4 , and $Pr = 1$. As can be seen from the table, the penalty-finite element model (PFEM) predicts values of the stream function lower than those predicted by the stream function-vorticity finite element model (SVFEM). However, the stream function-vorticity finite-element model did not give convergent results for these two Rayleigh numbers.

Thus, the penalty formulation could be used to analyze higher Rayleigh number flows than those which could be analyzed by the stream function-vorticity model.

Figure 5.4 and 5.5 are comparisons between the linear element (the present penalty-finite element model) and a quadratic element (Upson et al., 1980) in which 168 isoparametric elements with 745 nodes are used. Those figures show that the results obtained by the linear element using rather coarse mesh agree very well with those by Upson et al. (1980).

In Figures 5.6a and b, vertical velocity and temperature along the horizontal cross section A-B (see Fig. 5.1) are superposed. This shows the similarity of solution for various Rayleigh numbers. Figure 5.7 compares distribution of core temperature along cross section C-D obtained by penalty-finite element model and the experiment given by Elder (1965a). Since the insulated boundary condition in Elder's experiment is not satisfied completely, temperature pattern around $x=0$ and 1 shows significant difference. Figure 5.8 shows isotherms and stream lines obtained using the penalty-finite element model (with 12×12 nonuniform mesh) for $R_a = 10^6$, and $P_r = 1$.

Figures 5.3 and 5.8 show that isotherms tend to be vertical in the (thermal) boundary layer at vertical walls (i.e., vertically stratified) and they are horizontal in the core region. The vorticity and stream function values at the center of the enclosure obtained by both formulations are compared in Table 5.2 for various Rayleigh numbers and Prandtl numbers. Again, the results obtained using the penalty-finite element model (also see Heinrich et al., 1978) are lower than those obtained using the stream function-vorticity model. However, the vorticity values

in the penalty model were computed at the Gaussian points (which do not coincide with the vorticity center) and therefore cannot be the same as those computed at the vorticity center.

The vorticity distribution along vertical cross section C-D of the enclosure is shown in Figure 5.9 for $Ra = 10^4$. In the penalty-finite element model, the vorticity was computed from the velocity field at the Gaussian points. Note that the solutions obtained by both formulations are almost identical for $Pr = 1$; however, for small Prandtl numbers there seem to exist small differences in the solutions.

Figures 5.10 and 5.11 show that the influence of the penalty parameter ϵ on the solution is sensitive to neither mesh size nor Rayleigh number.

Table 5.3 shows a comparison of the Nusselt number computed by various investigators (for square enclosure, $Ra = 1.47 \times 10^4$, $Pr = 0.733$). Note that the Nusselt number obtained by the penalty-finite element model is the lowest of all.

Also Figure 5.12 compared the present linear element to the quadratic element (Upson et al., 1980) for $Ra = 10^3, 10^4, 10^5$ and 10^6 . The present results tend to predict smaller values because of the use of coarse mesh compared to those by Upson et al. (1980).

In Table 5.4 the two finite-element formulations are compared for computational time (in CPU), number of iterations taken for convergence, and the Nusselt number. The penalty-finite element model requires only slightly more (because of the computation of ψ) time than the stream function-vorticity model; however, the number of iterations required is smaller in the former model.

Figure 5.13 shows the effect of Prandtl number on the temperature, stream function, and vorticity (for $Ra = 10^4$). These solutions were obtained using the stream function-vorticity finite element model. Similar plots for the temperature and stream function were obtained by the penalty finite element model, but due to their close agreement with those obtained by the stream function-vorticity finite model, they are not shown here. Different Prandtl numbers, for a fixed Rayleigh number, mean fluids with different (material) properties. For fluids with low Prandtl number (i.e., ratio of viscosity to thermal diffusivity), the stream lines and vorticity lines show symmetry about the center.

Figure 5.14 shows the relative pressure distribution along the vertical cross section C-D. Pressure is relatively high near the walls and low near the center.

Figures 5.15 through 5.17 show the effect of the aspect ratio (height to width of the enclosure, $\gamma = \ell/d$) on the temperature and flow fields. All of the results were obtained by the penalty-finite element model. Figure 5.15 shows the isotherms and stream lines for a rectangular enclosure of aspect ratio 3. The Rayleigh number and Prandtl numbers are the same as those used by Hellums and Churchill (1962): $Ra = 1.466 \times 10^4$, $Pr = 0.733$. The present results agree qualitatively with those of Hellums and Churchill. Figure 5.16 shows similar results for a rectangular enclosure of aspect ratio 1.83, and with linear temperature distribution on the horizontal walls as indicated in the figure ($Ra = 8,200$, $Pr = 2,450$). This example is the same as that considered by Szekely and Todd (1971), who have presented experimental and finite difference solutions. The plotted values of the steady-state isotherms seem to agree well with

those of Szekely and Todd. In general, it was observed that for larger aspect ratios the numerical solutions converged faster. Finally, Figure 5.17 shows similar results for an aspect ratio of 16, $Ra = 10^5$, and $Pr = 1$. This problem was studied experimentally by Elder (1965a) for slightly different Rayleigh number ($Ra = 3 \times 10^5$). A symmetric (about the center) but nonuniform mesh of 24×14 was used. The isotherms and stream lines shown in Figure 5.17a are those obtained at the end of 30 iterations, with the error (in the velocity field) between the last two iterations being less than 10^{-3} . Due to time limitation on the job card, the solution at the end of thirty iterations was stored on a tape using free format. The computation was initiated with the solution on the tape as the starting value for the 31st iteration. After 30 more (i.e. total 60) iterations, the error was found to be only slightly less than that computed at the end of the first thirty iterations, and computation was terminated plotting the isotherms and stream lines (see Fig. 5.17b). While the isotherms remained virtually unaltered, the stream lines in the core region separated into small cells. Also, the stream lines in the boundary layer remained stratified vertically. The results in Fig. 5.17a seem to agree, qualitatively, well with those reported by Elder.

We also present numerical results for a nonrectangular enclosure (see Fig. 5.18). Figure 5.19 shows isotherms and stream lines for $Ra = 10^4$ and 10^5 , $Pr = 1$. The top and bottom walls were assumed to be insulated. Since no results are available in the literature at this writing, comparison is not made. These results could serve as test cases for future numerical investigations.

In closing, natural convection in a cylindrical annulus is solved.

Experimental as well as numerical results using the finite difference method based on the stream-function formulation was given by Kuehn and Goldstein (1976). Assuming symmetry with respect to the vertical center-line, only half of the annulus is considered here. Domain, boundary conditions, and finite element mesh are shown in Figure 5.20.

Figures 5.21a and b show the isotherms and isostreams for two Rayleigh numbers (a) $Ra = 10^3$ and (b) $Ra = 4.7 \times 10^4$ with $Pr = 0.706$. Heat is transferred mainly by conduction for case (a) while convection effect is significant in case (b). Figure 5.22 shows vertical velocity along the horizontal cross section (shown by broken line in the figure). It is observed that the inner boundary layer is thinner than the outer boundary layer. Figures 5.23a and b show the stream function and temperature distribution along the same cross section. In Figures 5.24a and b, temperature and vertical velocity distribution along the half circle (shown by broken line in the figure) are given for two Rayleigh numbers. Position is shown by angle α (degree) measured from the horizontal line passing through the center of annulus. Rapid change of both temperature and velocity around $\alpha = 75$ shows the existence of a plume for $Ra = 4.7 \times 10^4$.

Heat transfer along the inner and outer walls are shown in Figure 5.25. For comparison, analytical solution by Farshchi (1978) and numerical solution by Kuehn and Goldstein (1976) are given along the inner wall for $Ra = 4.7 \times 10^4$. The present results show local effects compared to those given by other investigators. Finally, Figures 5.26a and b show isotherms and isostreams for a problem in which the inner wall is kept cold while the outer wall is hot. The same number of mesh as in the previous problem is used. As the temperature difference between walls is increased, the fluid tends to become stratified.

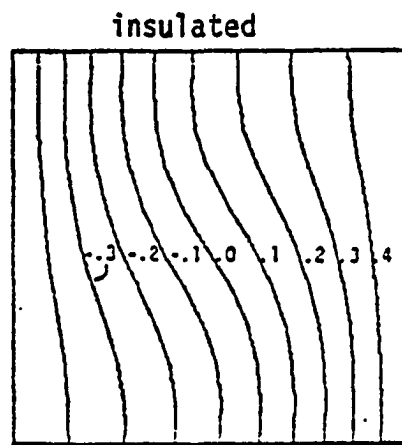
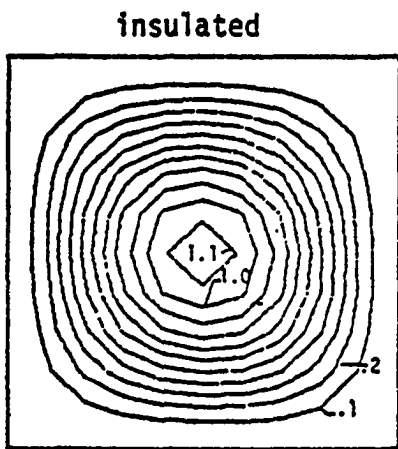
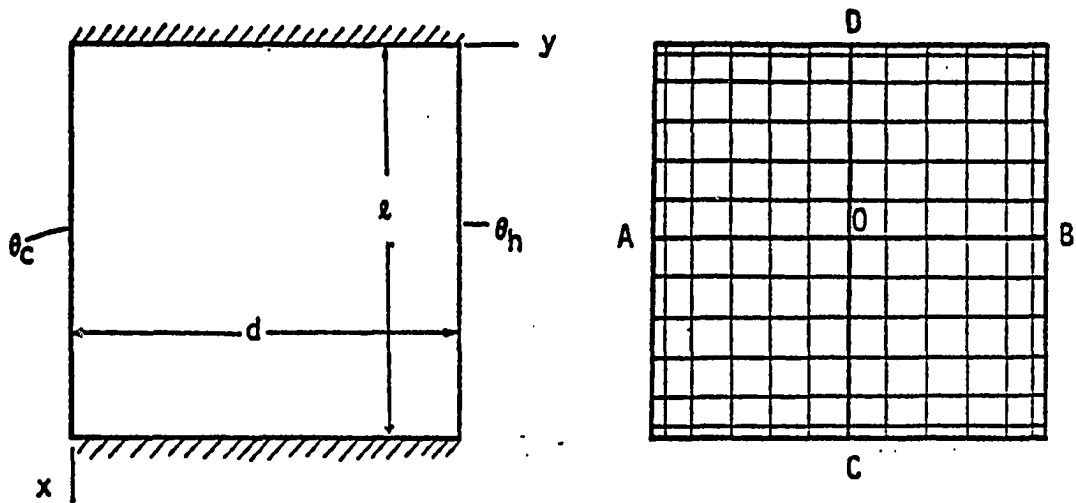
This agrees with our intuition.

5.4 Concluding Remarks

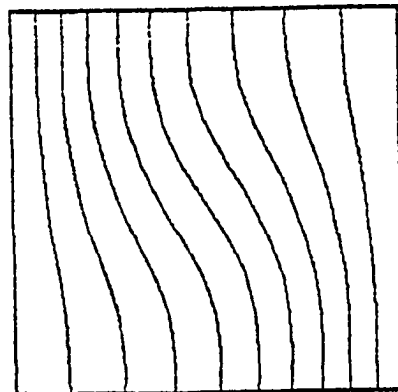
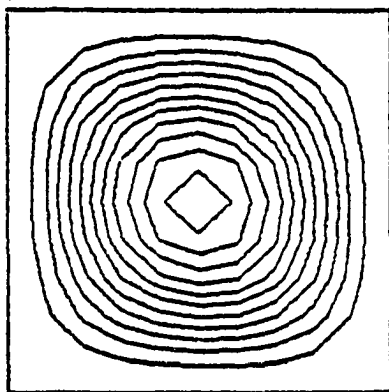
Compared to the mixed finite element model of Gartling (1977), the stream function-vorticity finite element model and the penalty-finite element model seem to be computationally simpler. The mixed model, by formulation, results in a large system of (non-positive definite) equations. Without special consideration, results obtained for the pressure are often erroneous. The stream function-vorticity model suffers from the disadvantage that the boundary conditions on the vorticity must be known a priori. De Vahl (1968) pointed out that computation of the boundary values of the vorticity from the stream function could result in up to 30% error. The results obtained by the penalty method are on the lower side of those obtained by the stream function-vorticity model. It is desirable to have experimental results in order to compare and make an accuracy evaluation of the formulations. The stream function-vorticity model presents convergence problems for Rayleigh numbers higher than 10^4 . In the penalty model, one is required to assess an optimal value of the penalty parameter. For very high Rayleigh numbers, the penalty parameter should be very large, and this in turn (coupled with word length in the computer) could cause the equations to become ill-conditioned.

In the present study, only moderate Rayleigh numbers were studied. For Rayleigh numbers higher than 10^6 , say of the order 10^7 - 10^9 , most traditional numerical schemes have computational difficulties (in terms of convergence and numerical stability). The so-called upwind differ-

encing could prove to be very effective. In order to use the upwind differencing a logical procedure that can be automated on the computer must be thought out for the finite element method. This area seems to be open for additional research. Another area for which sufficient information is lacking is the free convection in non-rectangular (or irregular) and three-dimensional enclosures. In both cases, unsteady analyses need to be performed. Theoretical as well as numerical investigations into instabilities at high Rayleigh numbers (say, in the turbulent region) are definitely far from complete.



cpu = 25 sec/iteration, $\psi_{\max} = 1.1697$



cpu = 15 sec/iteration, $\psi_{\max} = 1.1689$

Figure 5.1. Comparison of isotherms and stream lines obtained by the penalty-finite element models ($\epsilon_2 \neq 0$, $\epsilon_2 = 0$) for $R_a = 1,000$ and $P_r = -10$.

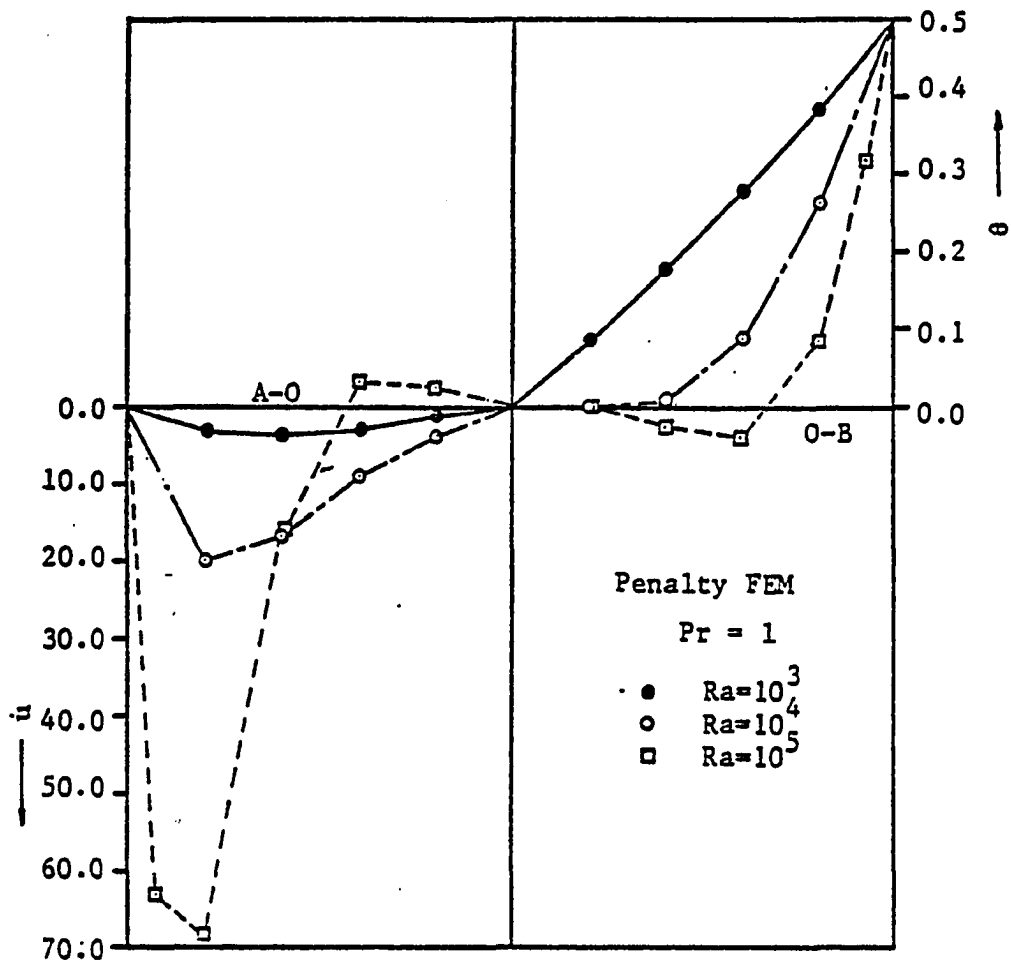


Figure 5.2. Velocity and temperature distribution along the center lines of the enclosure.

Table 5.1. Comparison of the stream function and temperature values obtained by the penalty-finite element model (PFEM) and stream function-vorticity finite element models (SVFEM) (Pr = 1.0, Mesh: 10 x 10)

| Quantity | x/y | Ra = 10 ³ | | Ra = 10 ⁴ | |
|-------------------------------|-----|----------------------|--------|----------------------|--------|
| | | PFEM | SVFEM | PFEM | SVFEM |
| Stream function at y = 0.5 | 0.0 | 0.0 | 0.0 | 0.0 | 0.0 |
| | 0.1 | 0.1566 | 0.2236 | 0.70671 | 0.9811 |
| | 0.2 | 0.5011 | 0.6094 | 2.2585 | 2.7201 |
| | 0.3 | 0.8410 | 0.9746 | 3.7707 | 4.3745 |
| | 0.4 | 1.0755 | 1.2228 | 4.7925 | 5.4913 |
| | 0.5 | 1.1581 | 1.3098 | 5.1474 | 5.8797 |
| Temperature at x = 0.5 | 1.0 | 0.5 | 0.5 | 0.5 | 0.5 |
| | 0.9 | 0.3871 | 0.3851 | 0.2646 | 0.2514 |
| | 0.8 | 0.2777 | 0.2744 | 0.0883 | 0.0733 |
| | 0.7 | 0.1765 | 0.1734 | 0.0011 | 0.0006 |
| | 0.6 | 0.0851 | 0.0832 | -0.0150 | -0.011 |
| | 0.5 | 0. | 0. | 0. | 0. |

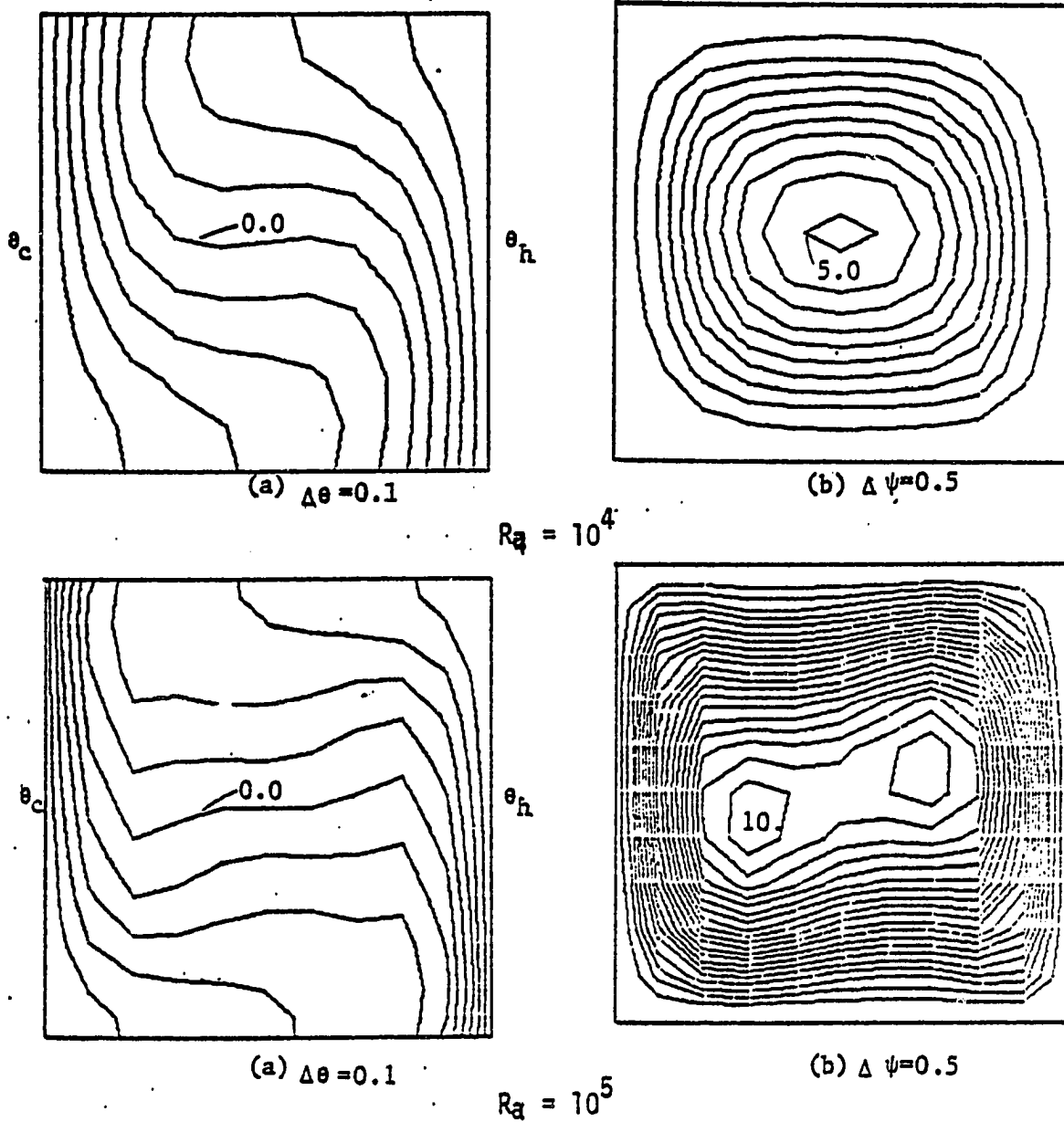
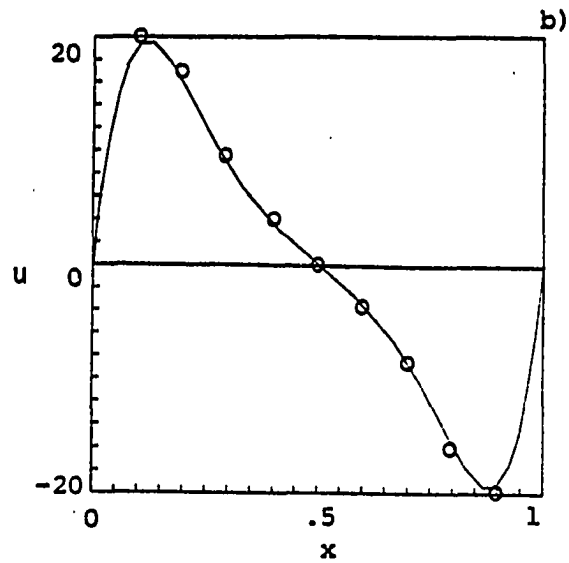
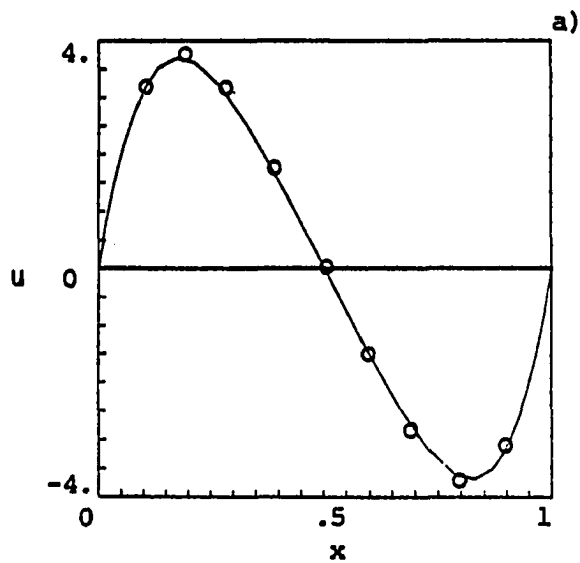


Figure 5.3. Isotherms and stream lines obtained by the penalty-finite element model for $Ra = 10,000$ and $100,000$ ($Pr=1$).



○ Present penalty FEM
 — Upson et al. (1980)

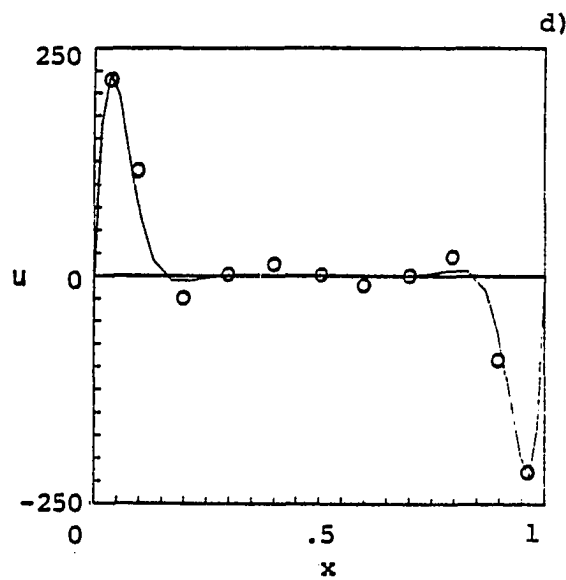
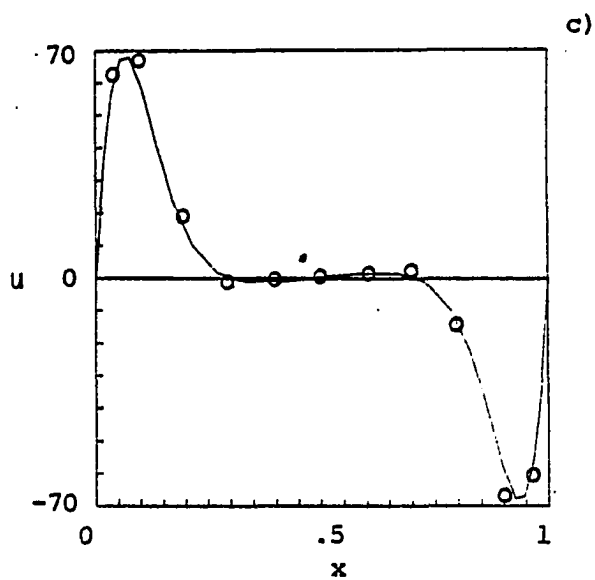
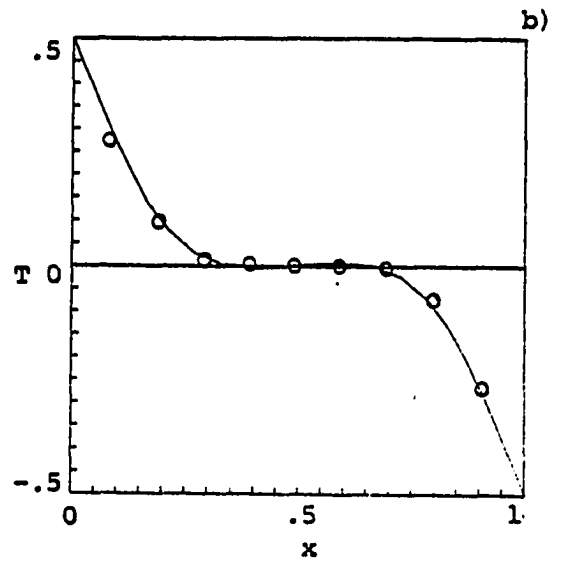
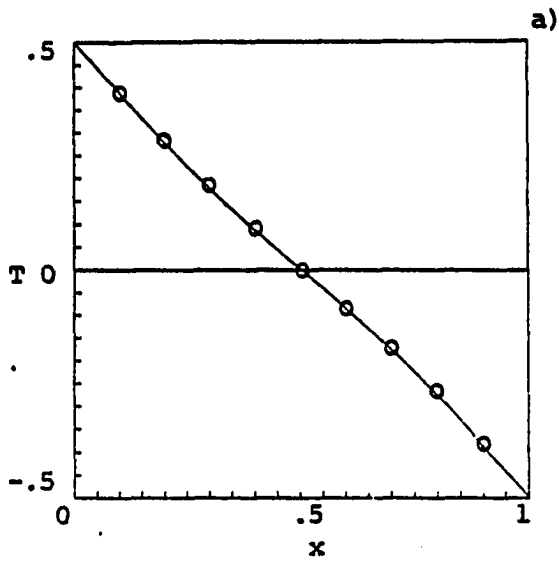


Figure 5.4 Vertical velocity at $x=0.5$ by penalty finite element model .

- a) $Ra = 10^3$
- b) $Ra = 10^4$
- c) $Ra = 10^5$
- d) $Ra = 10^6$



○ Present penalty FEM
 — Upson et al. (1980)

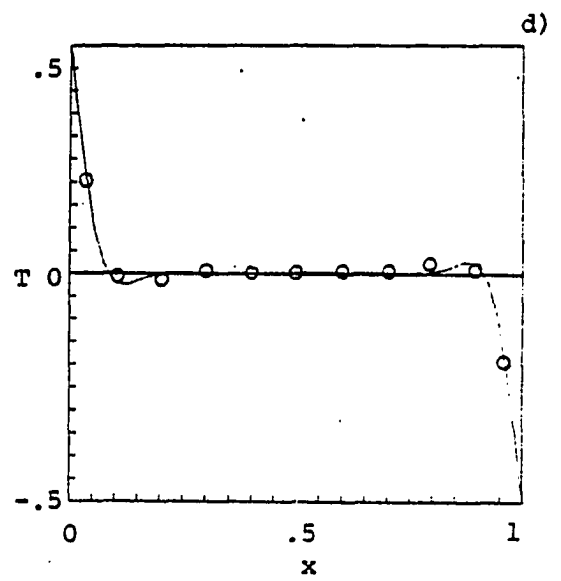
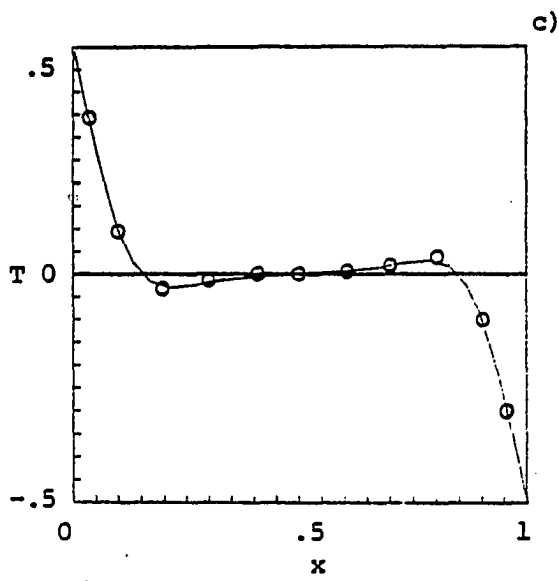


Figure 5.5 Temperature at $x=0.5$ by penalty finite element model .

- a) $Ra = 10^3$
- b) $Ra = 10^4$
- c) $Ra = 10^5$
- d) $Ra = 10^6$

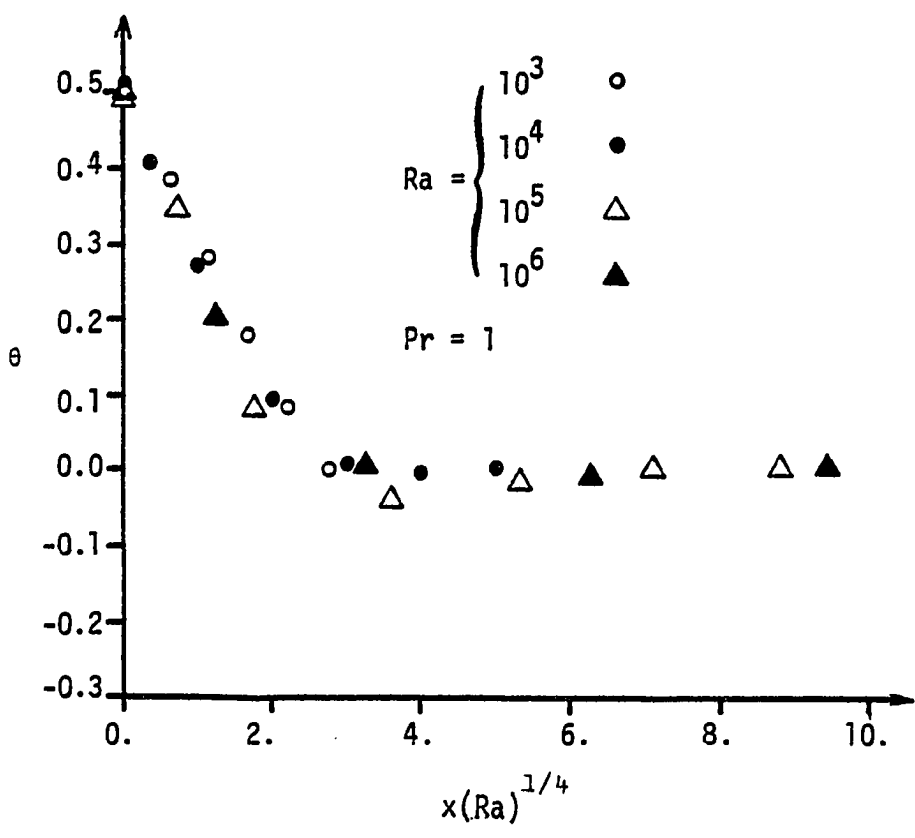
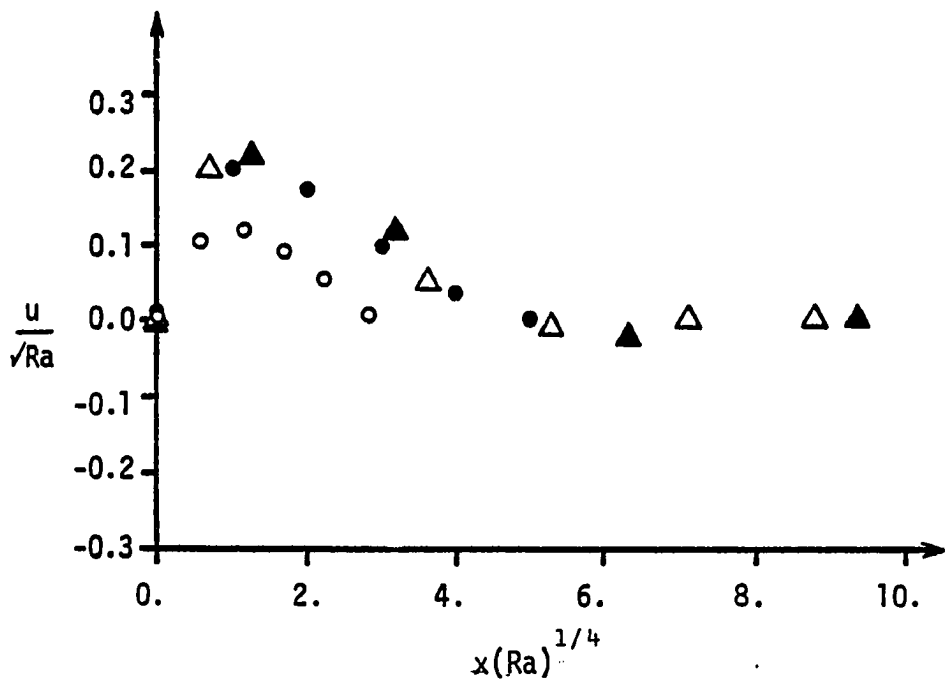


Figure 5.6 (a) Scaled vertical velocity in boundary layer ($x=0.5$)
 (b) Temperature in boundary layer ($x=0.5$).

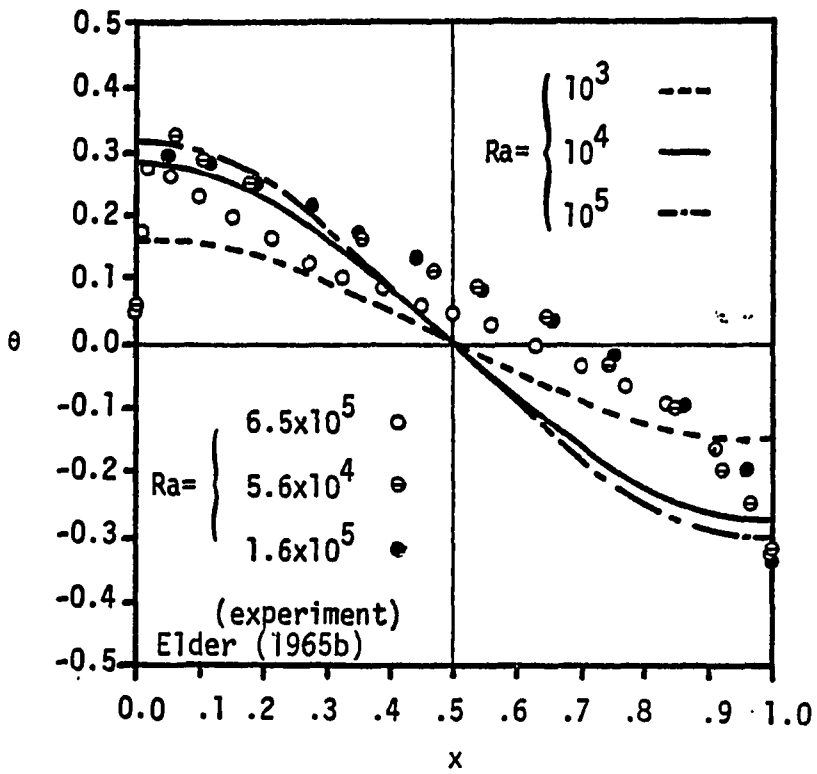


Figure 5.7 Core temperature distribution along vertical cross section .

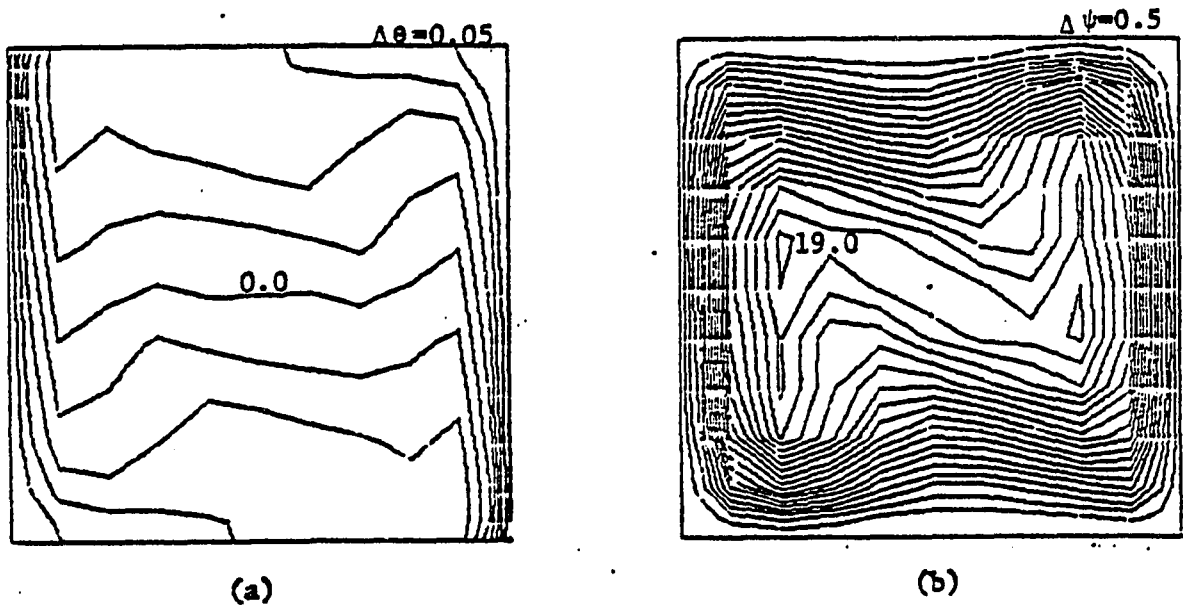


Figure 5.8 Isotherms and isostreams for $Ra = 10^6$, $Pr = 1$ by penalty formulation (mesh: 12×12)
 (a) isotherms and (b) isostreams

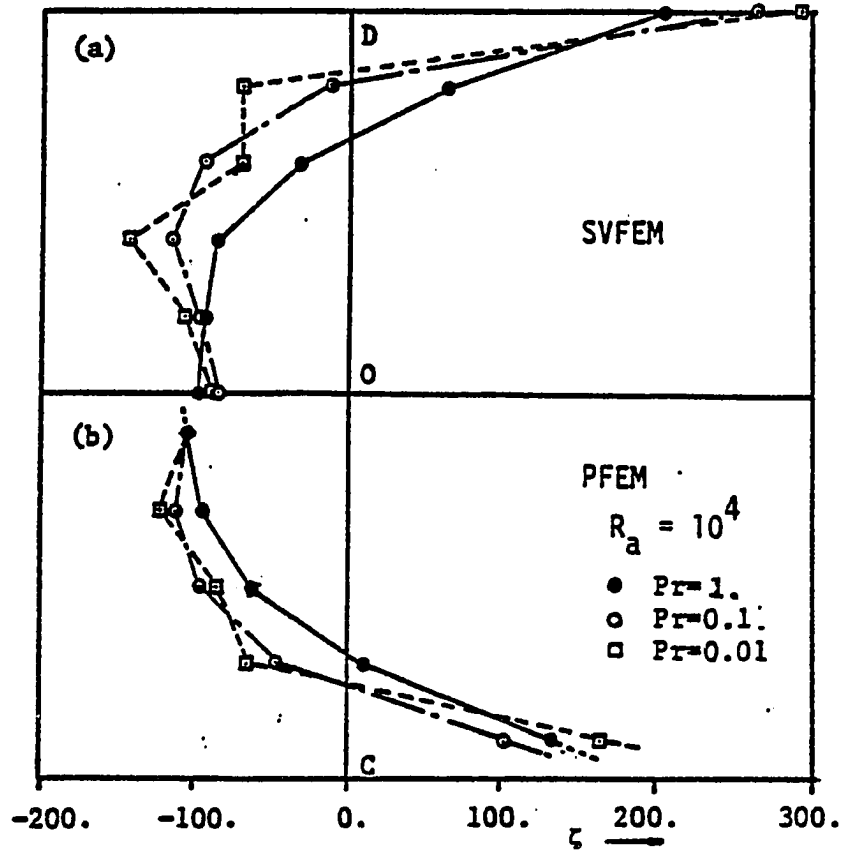


Figure 5.9 Vorticity distribution along vertical cross section ($Ra=10000$, Mesh: 10×10)
 (a) stream function -vorticity model (SVFEM)
 (b) penalty FEM (PFEM)

Table 5.2. Stream function and vorticity values at the center of the enclosure (10x10 mesh).

| Ra | Pr | Stream function (ψ) | | Vorticity (ξ) | |
|--------|-----------|----------------------------|--------|---------------------|--------|
| | | PFEM | SVFEM | PFEM | SVFEM |
| 10^3 | 10^{-2} | 1.1386 | 1.2636 | -31.26 | -33.36 |
| | 10^{-1} | 1.1561 | 1.3041 | -31.41 | -34.44 |
| | 1 | 1.1581 (1.18)* | 1.3096 | -31.31 | -34.52 |
| | 10^1 | 1.1581 | 1.3098 | -31.32 | -34.52 |
| | 10^2 | 1.1581 | 1.3098 | -31.32 | -34.52 |
| 10^4 | 10^{-2} | 5.0128 | 5.4504 | -96.32 | -83.99 |
| | 10^{-1} | 5.0403 | 5.5451 | -101.5 | -88.94 |
| | 1 | 5.1474 (5.13)* | 5.7823 | -103.1 | -99.78 |
| | 10^1 | 5.2016 | 5.8797 | -106.9 | -104.1 |
| | 10^2 | 5.2070 | 5.8892 | -107.3 | -104.5 |

* values from Heinrich et al. (1978), wherein a 4x4 of the 9-node rectangular elements was used.

Table 5.3. Comparison of the Nusselt number obtained by various investigators ($Ra = 1.47 \times 10^4$, $Pr = 0.733$)

| Source | Nusselt number (Nu)* | Remarks | |
|-------------------------|----------------------|-------------------------------------|--------------------------------------|
| Present { | PFEM | 2.360 | 4-node rect. element (10x10 mesh) |
| | SV.FEM | 2.687 | 4-node rect. element (10x10 mesh) |
| Tabarrok and Lin (1977) | 2.695 | 3-node triangular element(10x10) | |
| Catton, et al. (1974) | 2.71 | Galerkin Method | |
| Cormack, et al. (1974) | 2.64 | 21 x 21 FDM | |
| Wilkes, et al. (1966) | 2.874 | 11 x 11 FDM | |
| | 2.516 | 21 x 21 FDM | |
| Ozoe, et al. (1975) | 2.75 | experiment | |

* Nusselt number is defined (in the present coordinates) by,

$$\text{average, Nu} = \int_0^1 \frac{\partial \theta}{\partial y} \Big|_{y=0} dx .$$

Table 5.4. Comparison of the Nusselt number, computational time and number of iterations required for convergence (n) for the penalty finite element model (PFEM) and stream function vorticity finite element model (SVFEM).

| Ra | Pr | Penalty finite element | | | Stream function-vorticity | | |
|-----------------|------------------|------------------------|------|-------------------|---------------------------|------|--------|
| | | n ⁺ | cpu | Nu | n | cpu | Nu |
| 10 ³ | 10 ⁻² | 11 | 3.09 | 1.0992 | 18 | 2.55 | 1.2582 |
| | 10 ⁻¹ | 9 | 2.38 | 1.1558 | 16 | 2.36 | 1.1367 |
| | 1 | 8 | 2.33 | 1.1666 (1.14)* | 16 | 2.39 | 1.1387 |
| | 10 | 8 | 2.29 | 1.1666 | 15 | 2.34 | 1.1387 |
| | 10 ² | 8 | 2.25 | 1.1666 | 15 | 2.31 | 1.1387 |
| 10 ⁴ | 10 ⁻² | 20 | 5.26 | 1.9993 | 22 | 3.35 | 2.2004 |
| | 10 ⁻¹ | 20 | 5.33 | 2.0390 | 28 | 4.28 | 2.2600 |
| | 1 | 16 | 4.26 | 2.1318 (2.49*) | 26 | 4.05 | 2.3962 |
| | 10 | 17 | 4.33 | 2.1440 | 20 | 3.13 | 2.4144 |
| | 10 ² | 17 | 4.37 | 2.1442 | 20 | 3.12 | 2.4146 |

+ convergence tolerance, 10⁻⁴.

* values given by Heinrich et al., (1978), wherein a 4x4 mesh of 9-node rectangular elements was used.

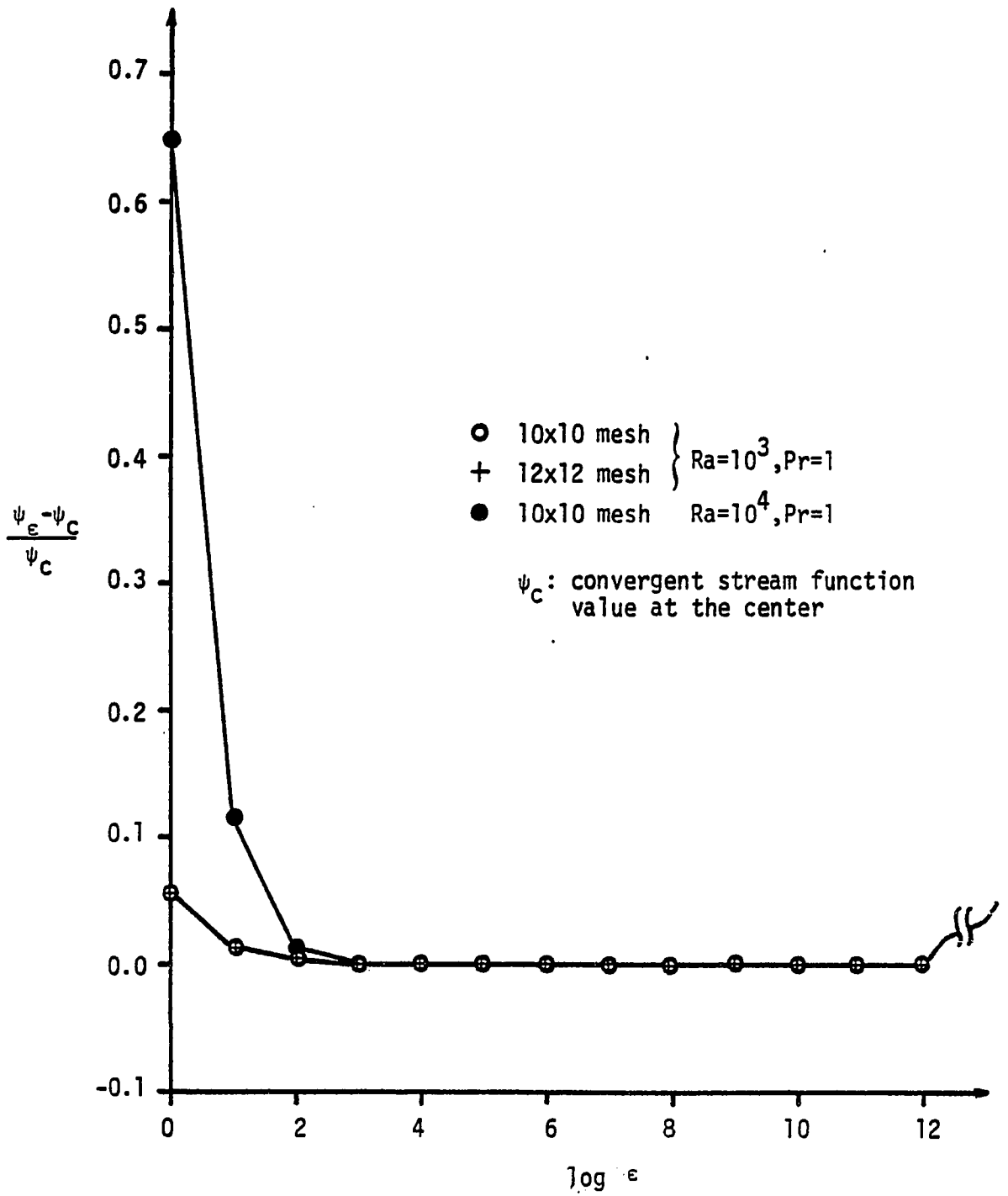


Figure 5.10 Effect of penalty parameter ϵ on the stream function ψ .

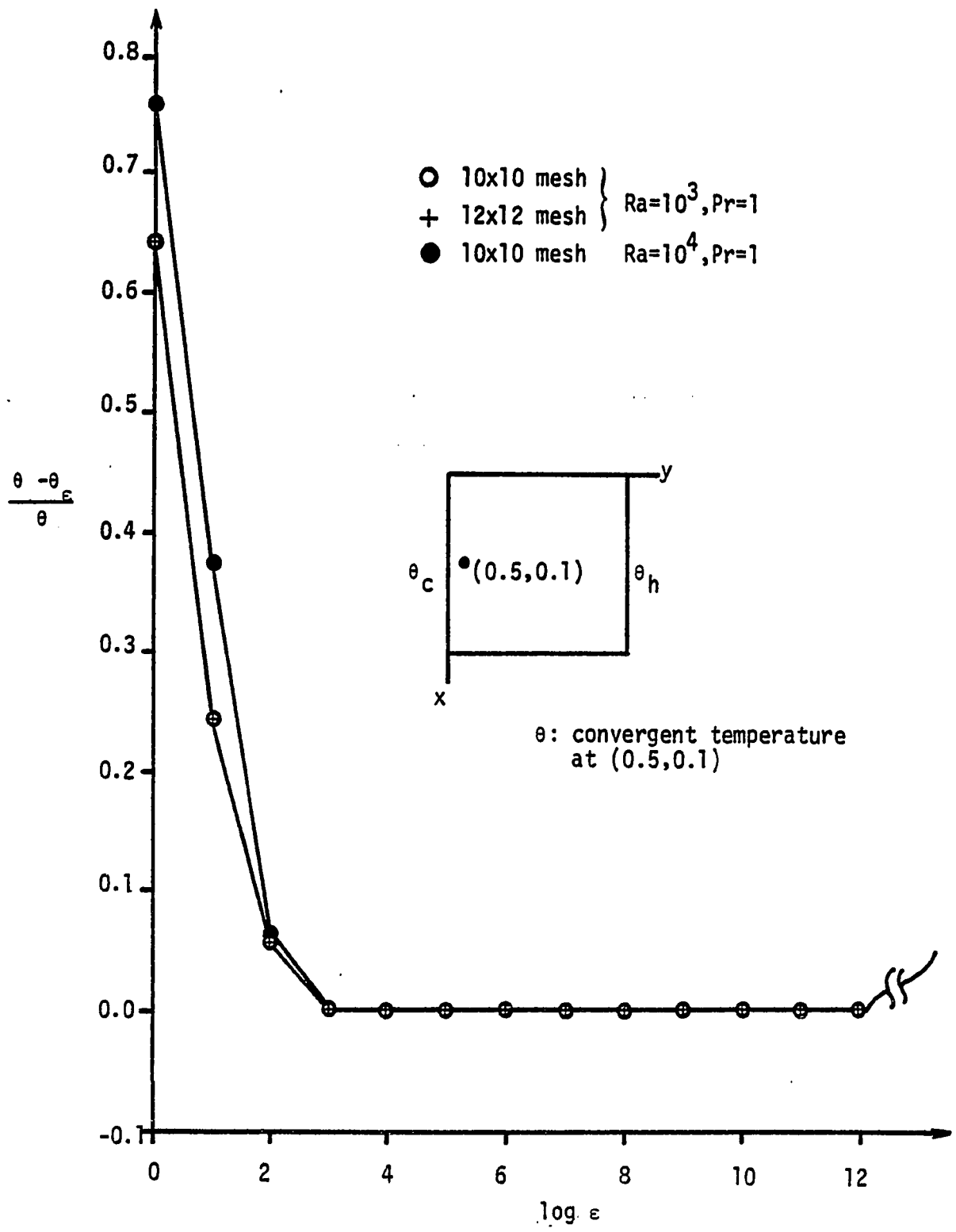
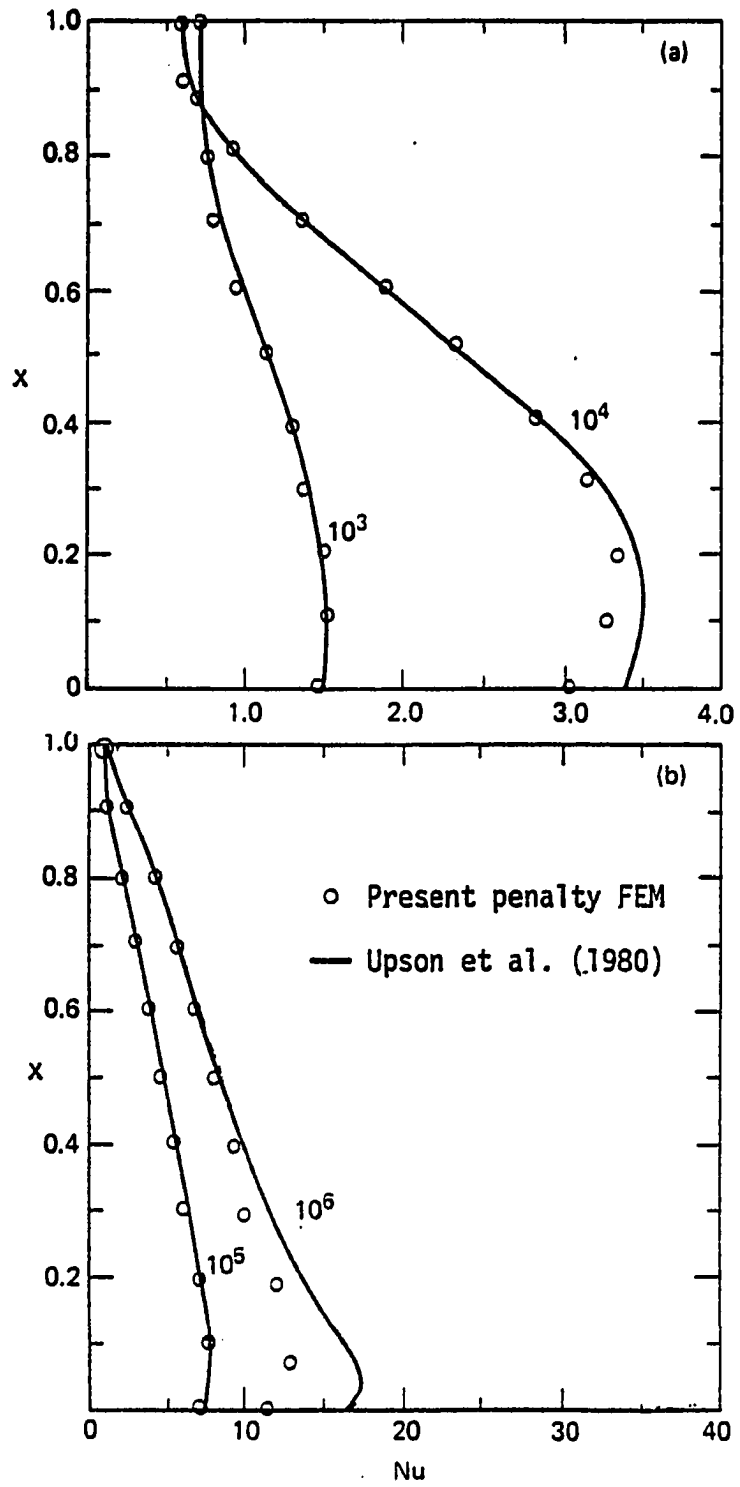


Figure 5.11 Effect of penalty parameter ϵ on the temperature θ .



a) $Ra = 10^3, 10^4$
 b) $Ra = 10^5, 10^6$

Figure 5.12 Heat flux at cold wall .

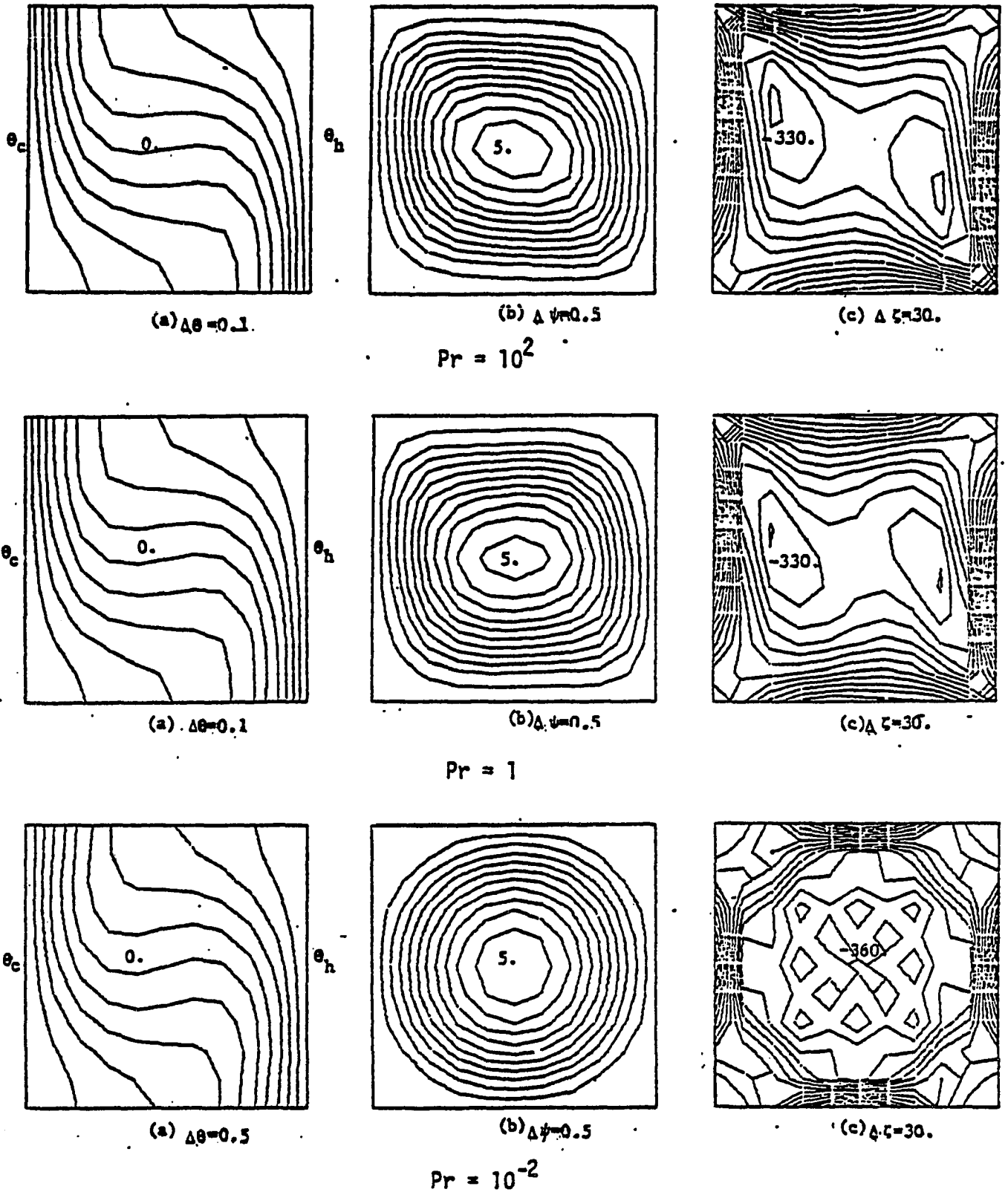


Figure 5.13 Isotherms, isostreams, and equivorticity lines for various Prandtl numbers by stream function-vorticity formulation ($Ra=10^4$). (a) isotherms, (b) isostreams, and (c) equivorticity lines.

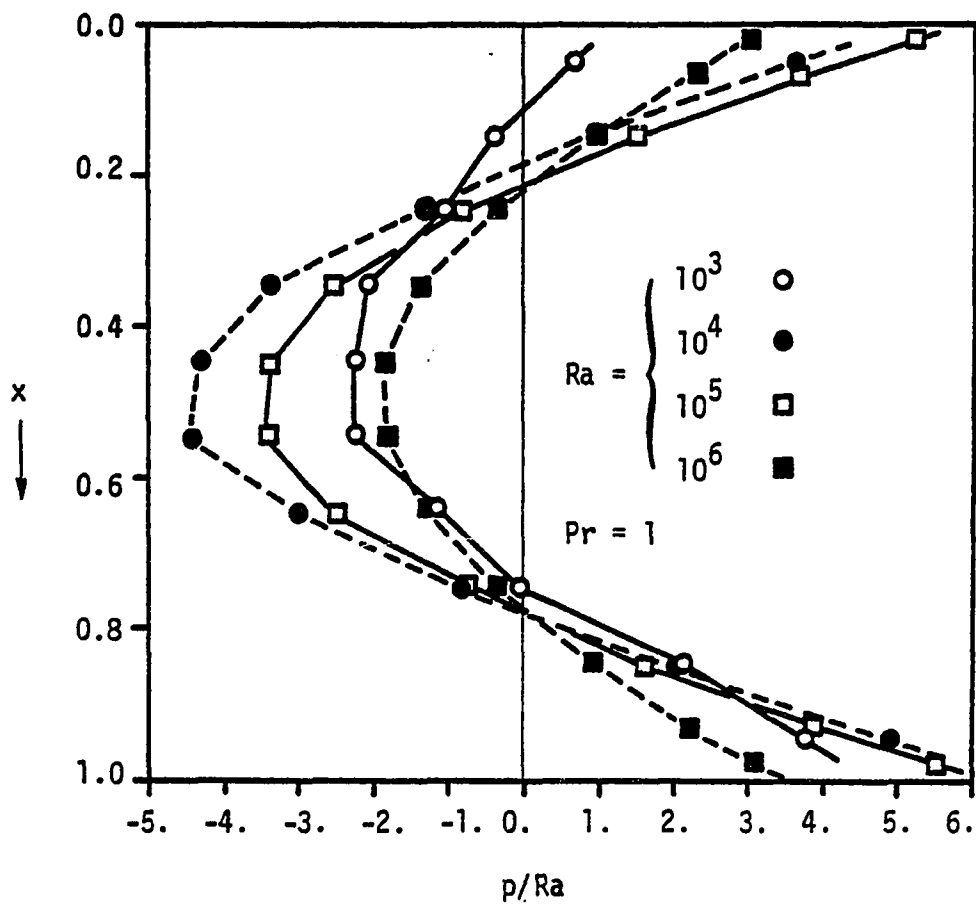


Figure 5.14 Relative pressure distribution along vertical cross section ($y=0.5$) by penalty finite element model .

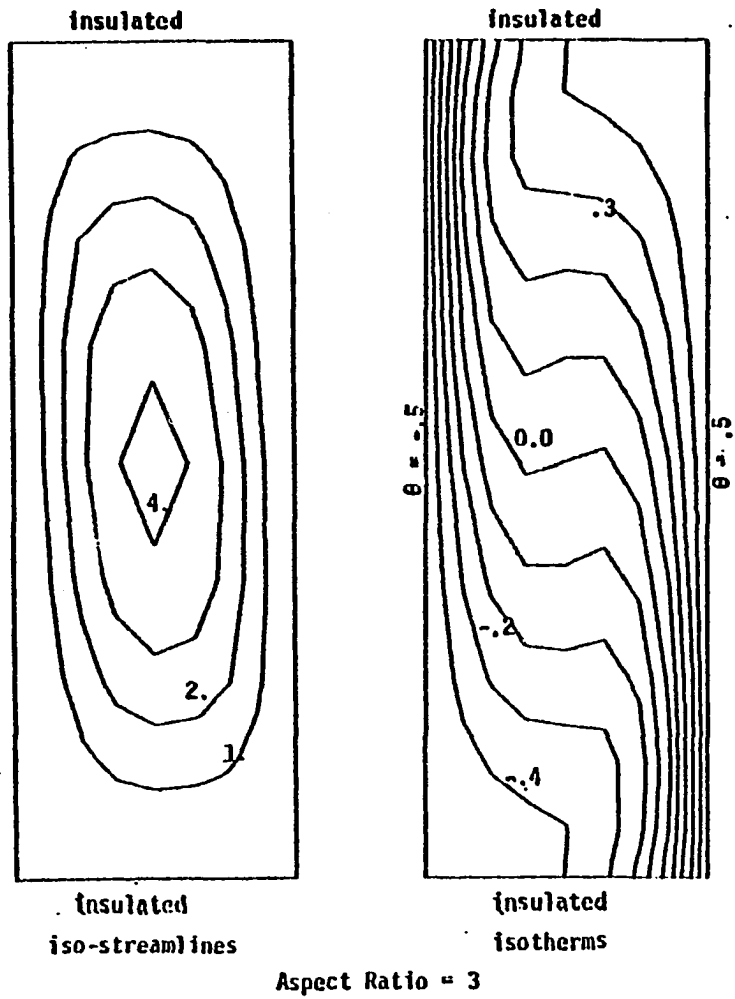


Figure 5.15 Isotherms and stream lines for
 $R_a = 14,660$, $P_r = 0.733$.

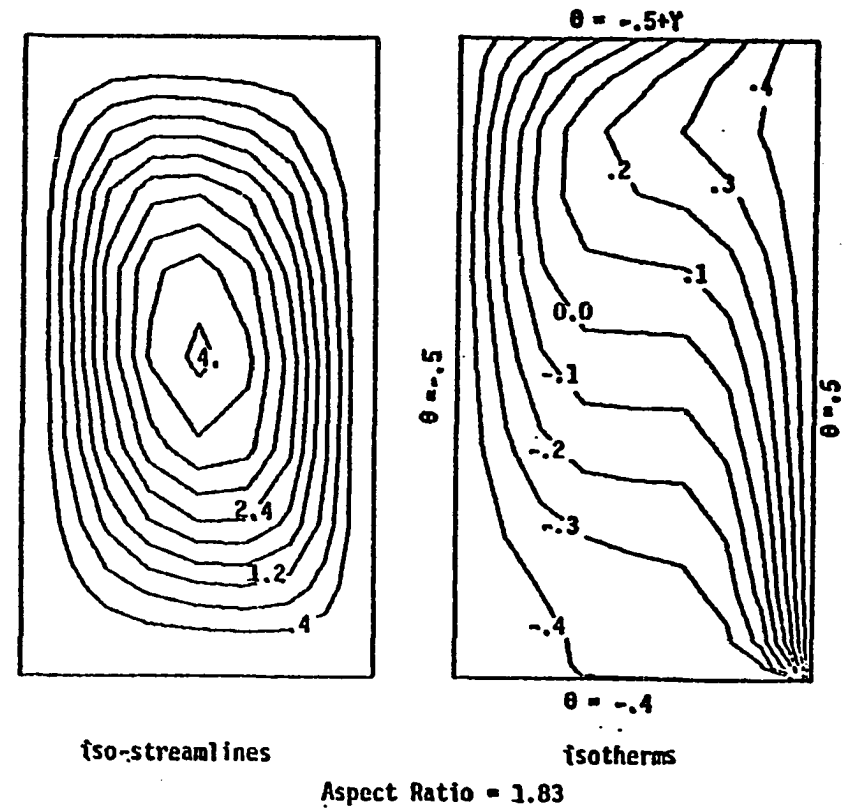
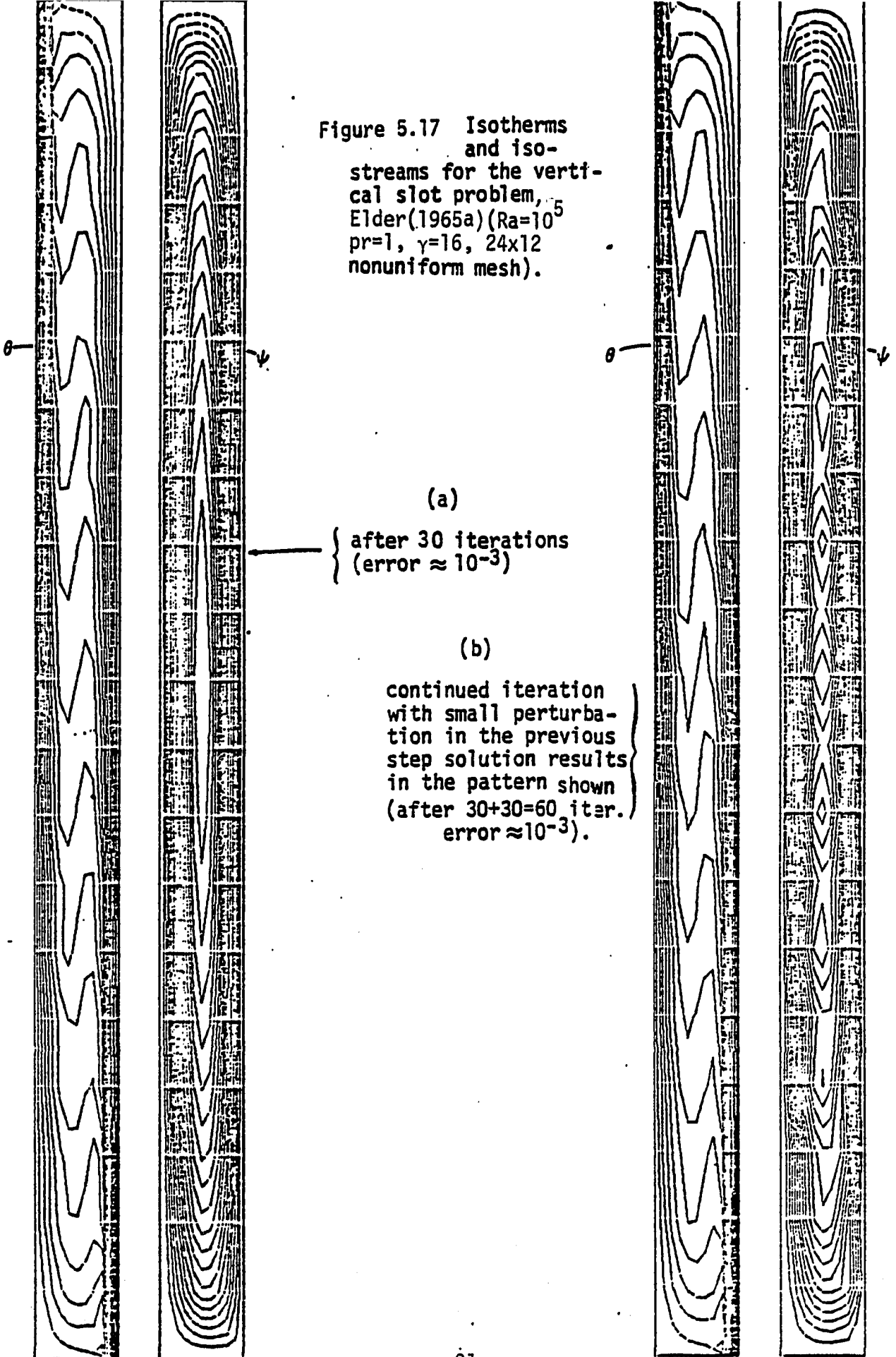


Figure 5.16 Isotherms and stream lines for
 $R_a = 8,200$, $P_r = 2,450$.

Figure 5.17 Isotherms and iso-streams for the vertical slot problem, Elder(1965a) ($Ra=10^5$, $Pr=1$, $\gamma=16$, 24×12 nonuniform mesh).



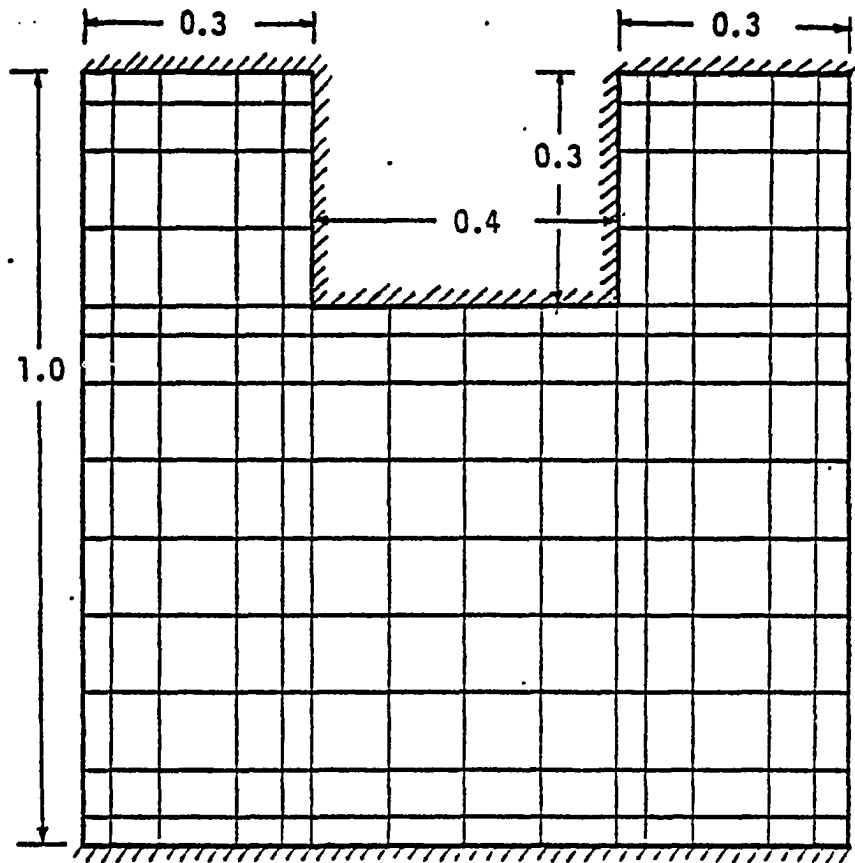


Figure 5.18 Finite element mesh for nonrectangular cavity (14 x 13 nonuniform mesh).

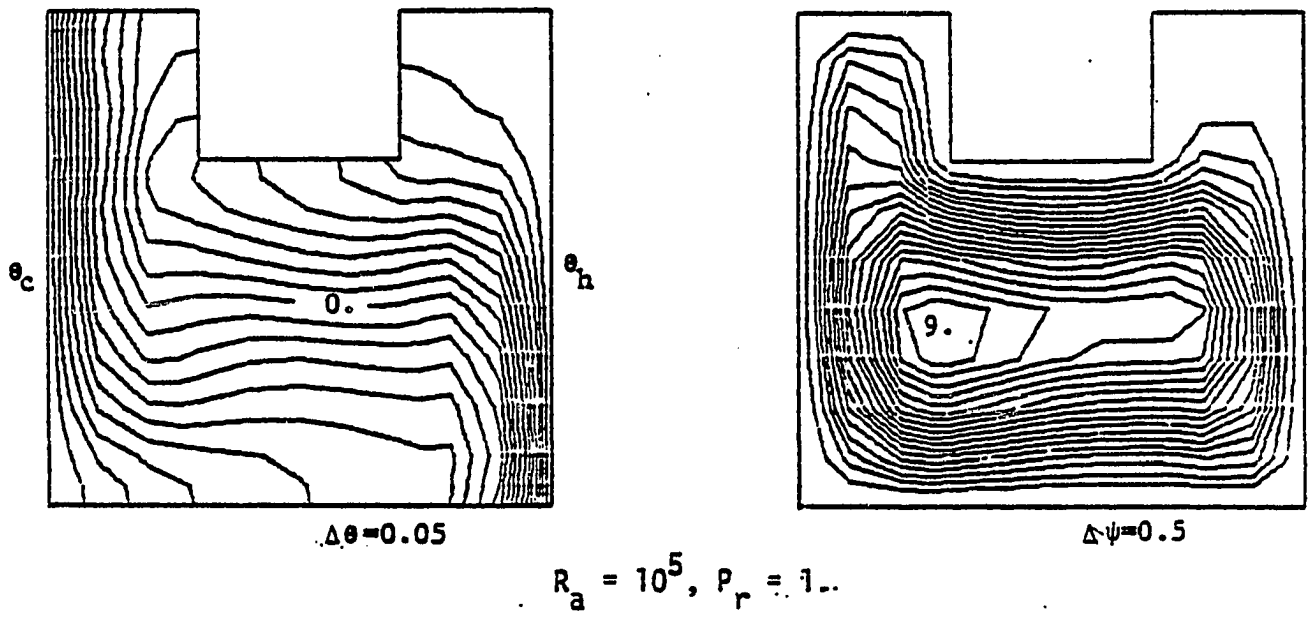
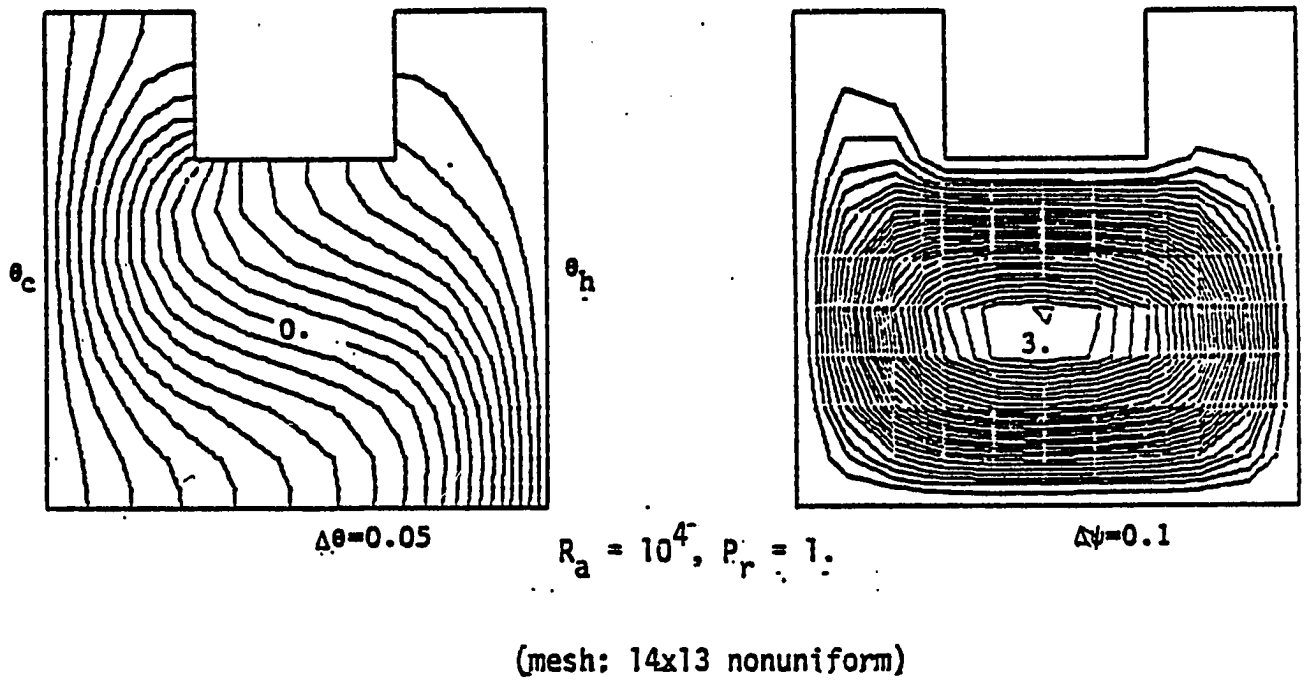


Figure 5.19 Temperature and stream function for non-square enclosure by penalty method. (a) temperature and (b) stream function.

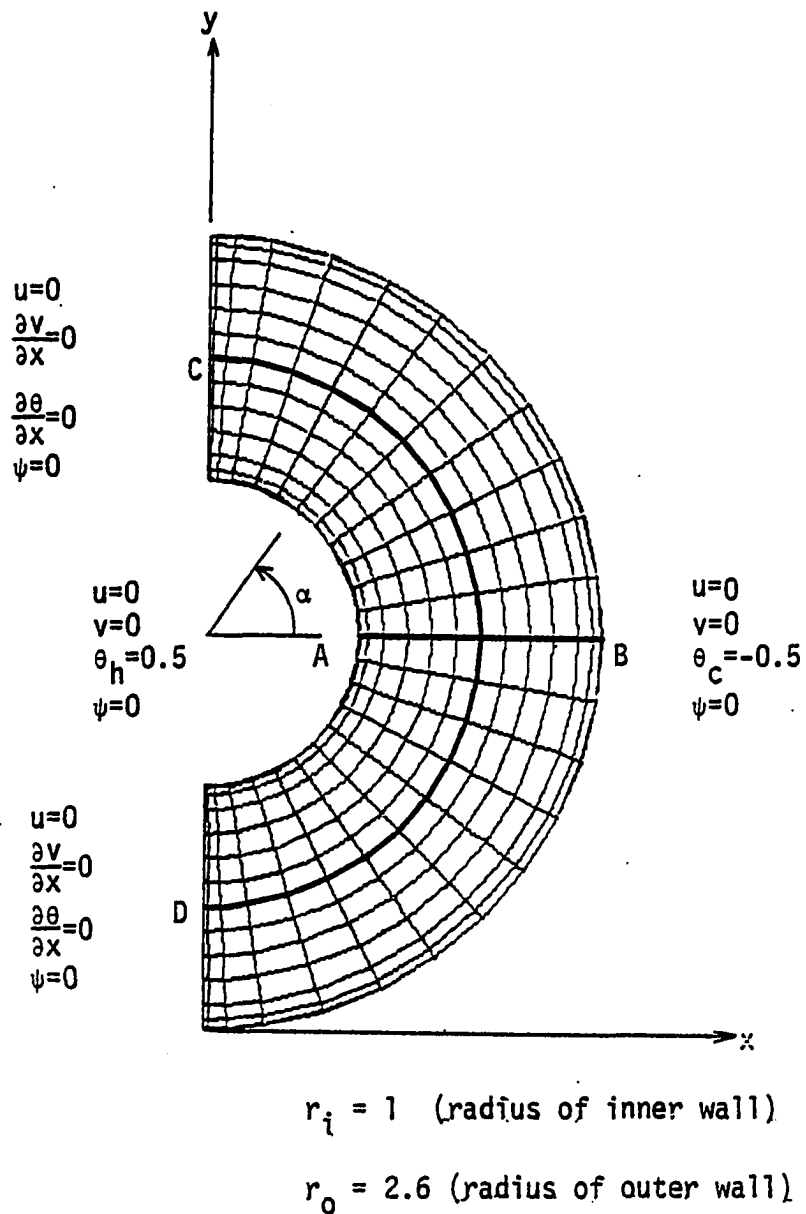


Figure 5.20. Finite elements and boundary conditions for circular annulus (375 meshes and 336 nodes) .

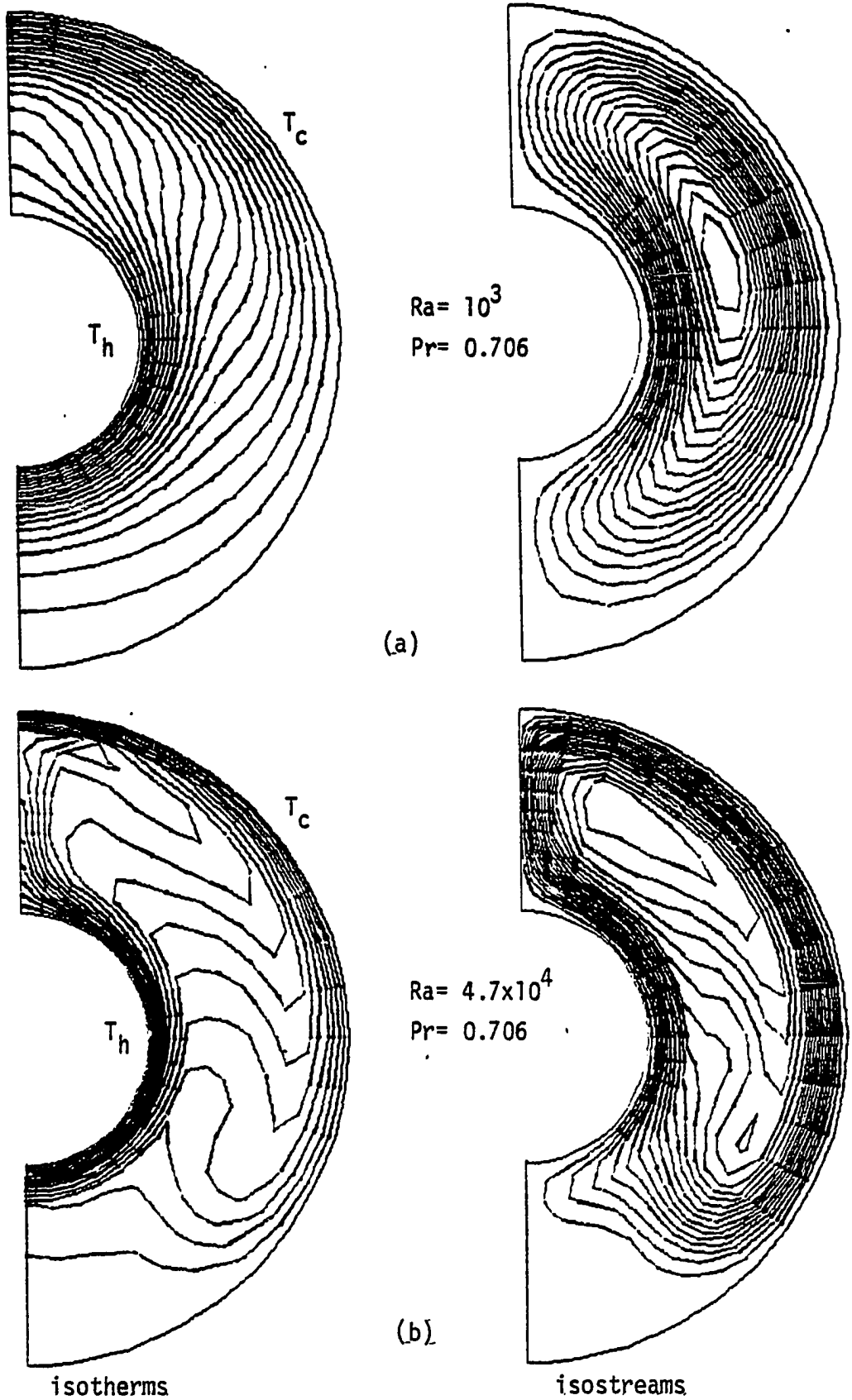


Figure 5.21 Isotherms and isostreams for (a) $Ra=10^3$ and (b) $Ra=4.7 \times 10^4$.

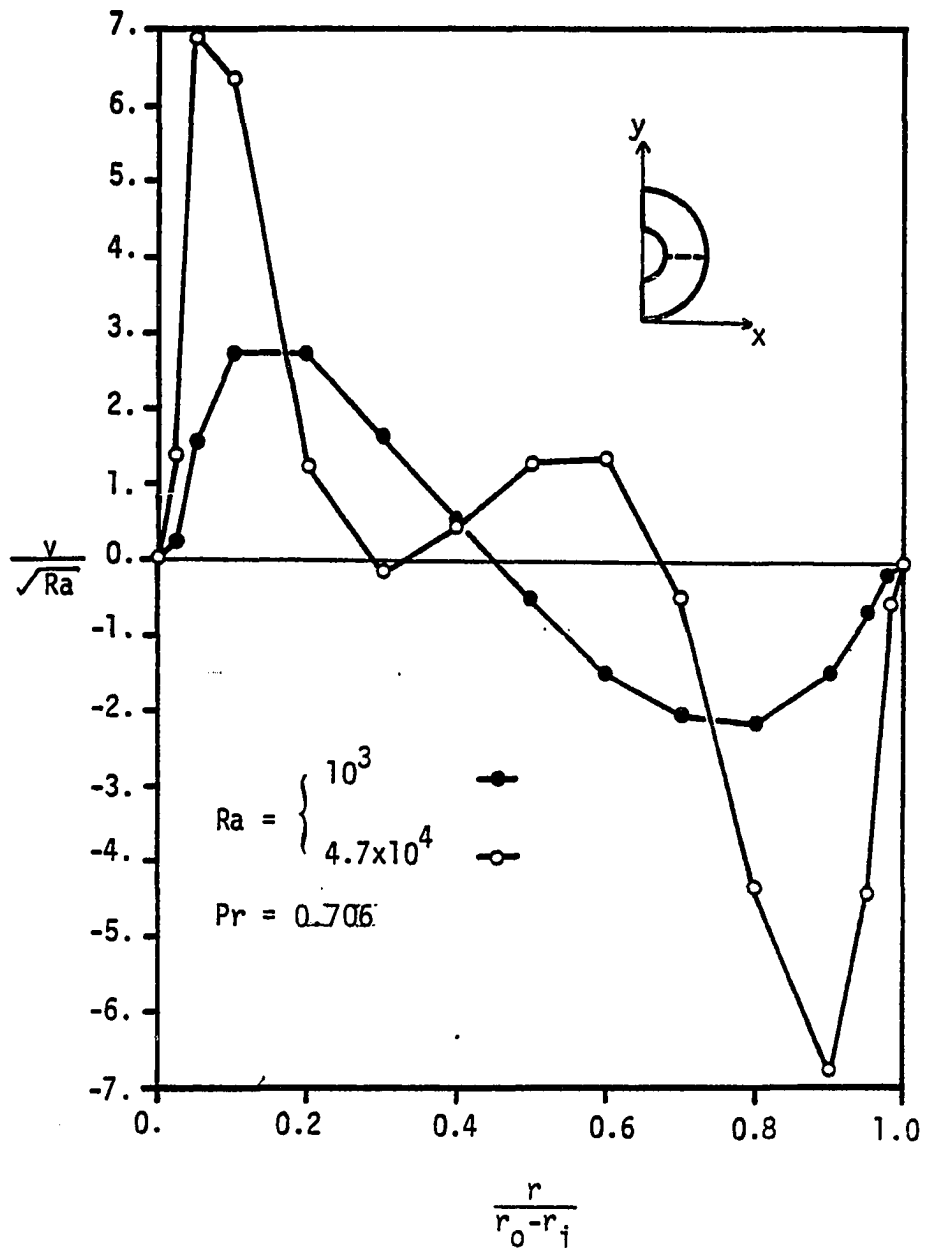


Figure 5.22 Vertical velocity distribution along horizontal cross section .

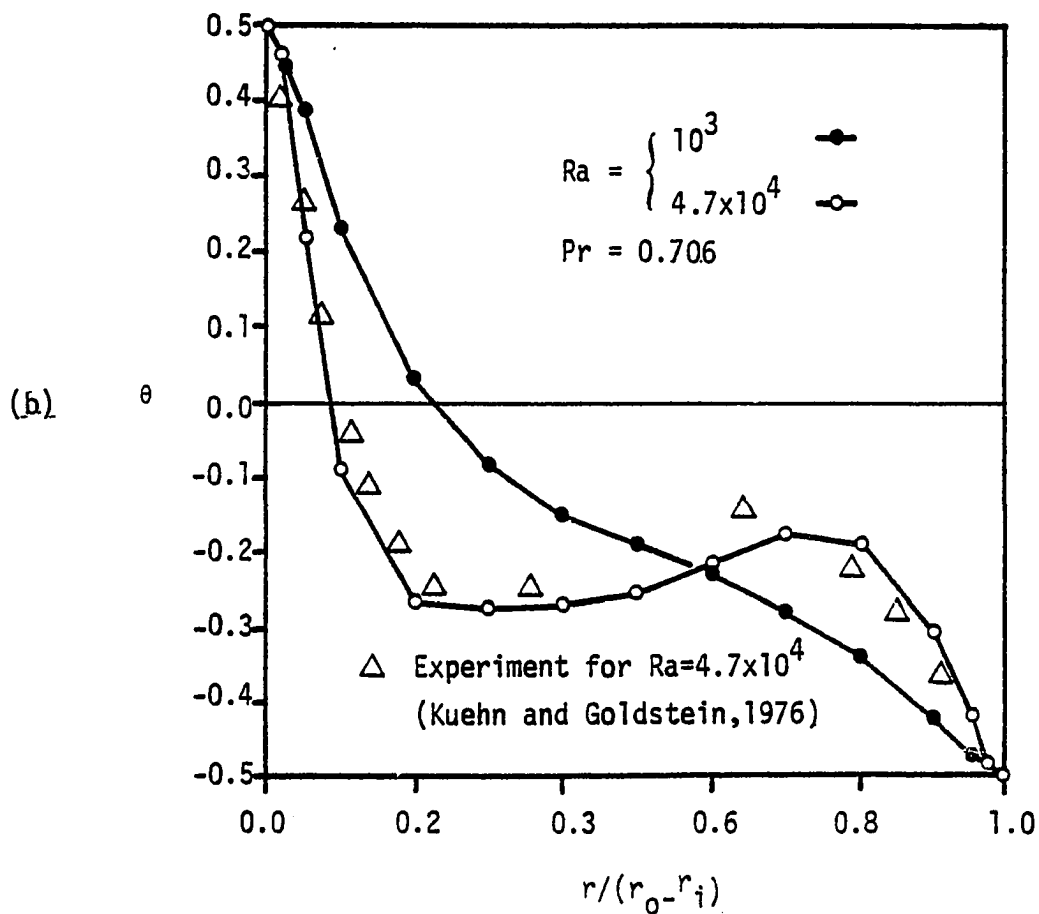
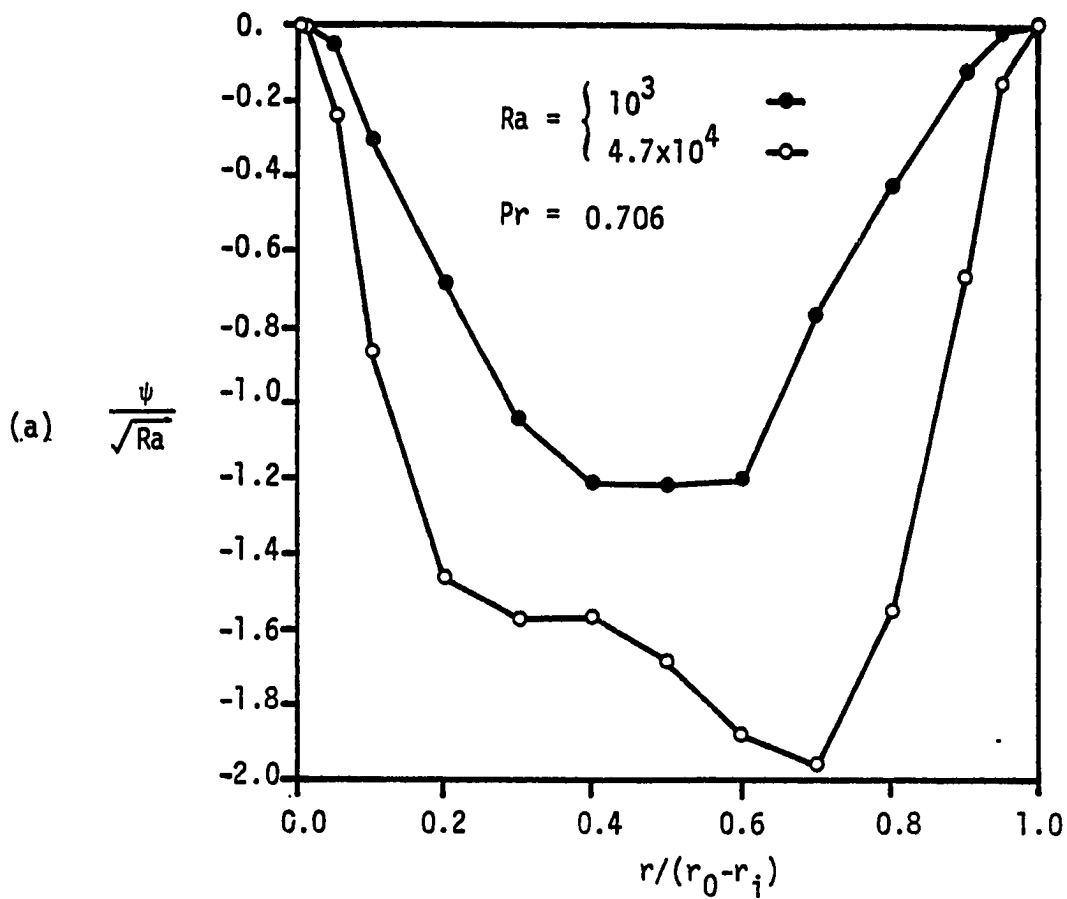


Figure 5.23 (a) Stream function along horizontal cross section
 (b) Temperature distribution along horizontal cross section .

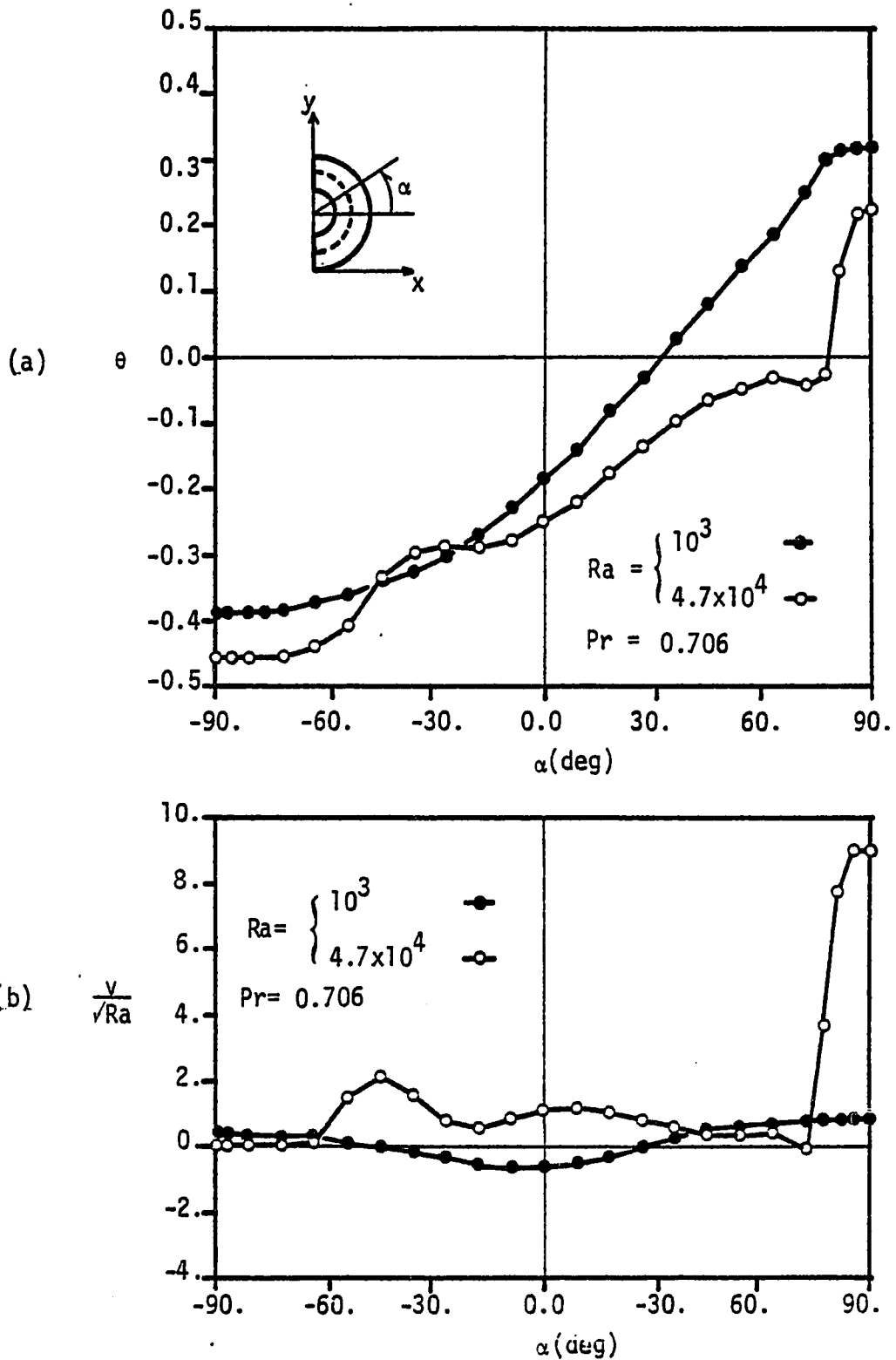
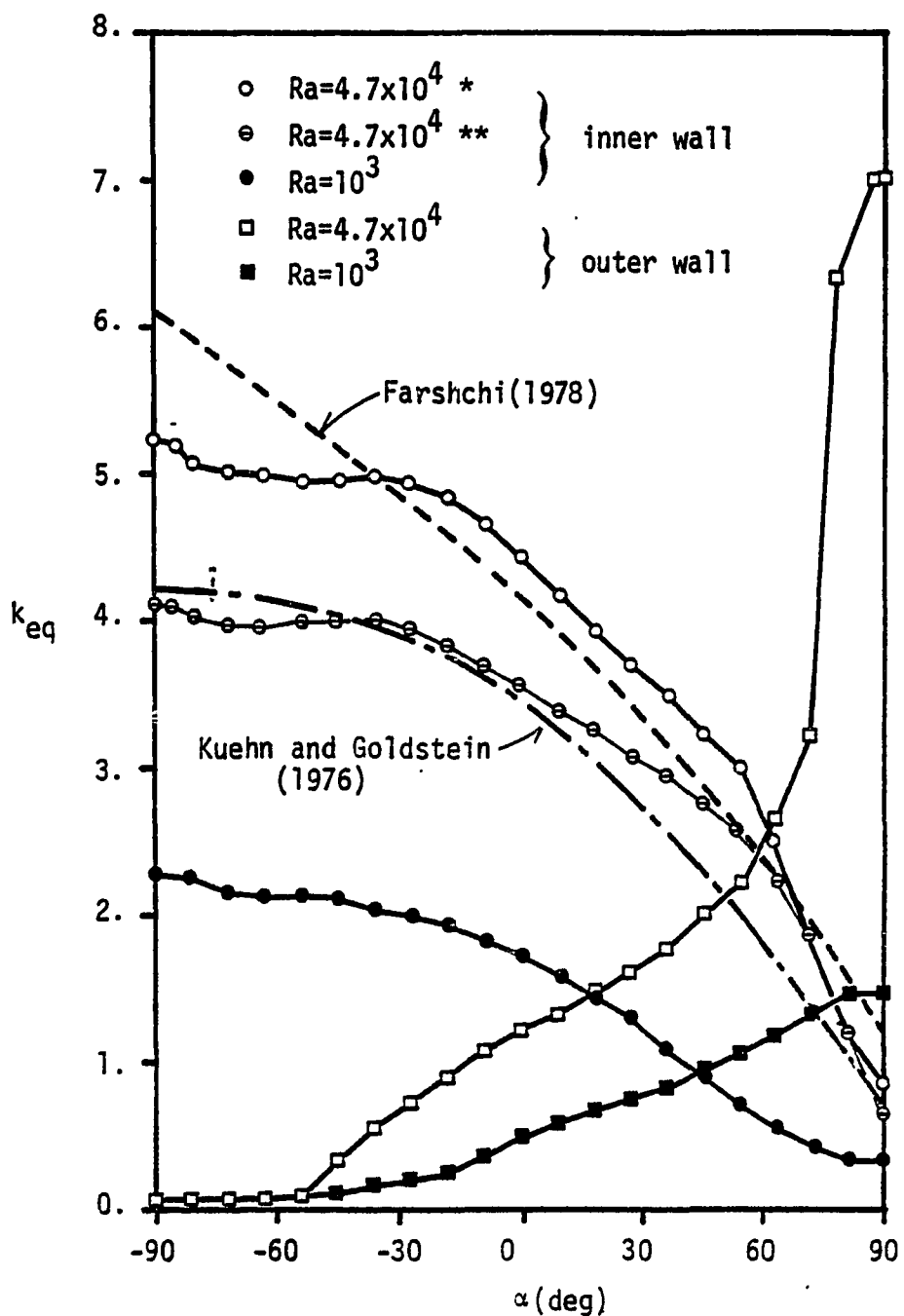


Figure 5.24 (a) Temperature distribution along half circle
 (b) Vertical velocity distribution .



* Heat transfer is calculated using temperature at $r=1.008$
 ** Heat transfer is calculated using temperature at $r=1.16$

$$k_{eq} = Nu(\alpha) \ln(r_o/r_i)$$

$$Nu(\alpha) = \left. \frac{\partial \theta}{\partial n} \right|_{at \alpha} \text{ (normal gradient)}$$

Figure 5.25 Heat transfer along inner and outer walls .

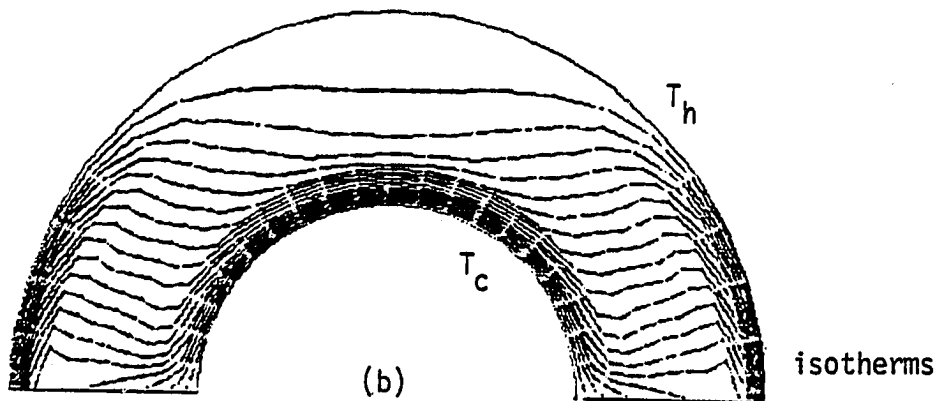
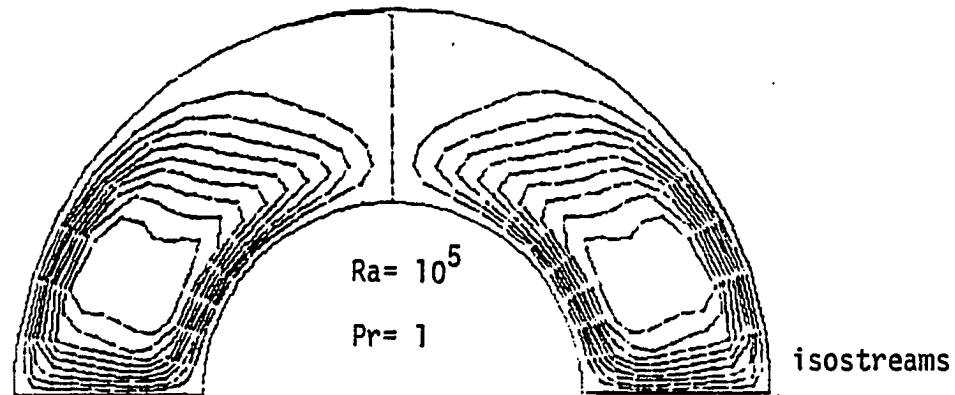
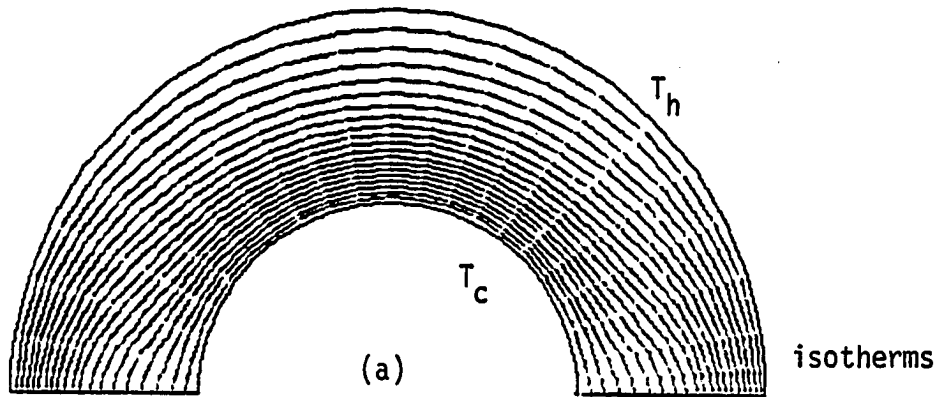
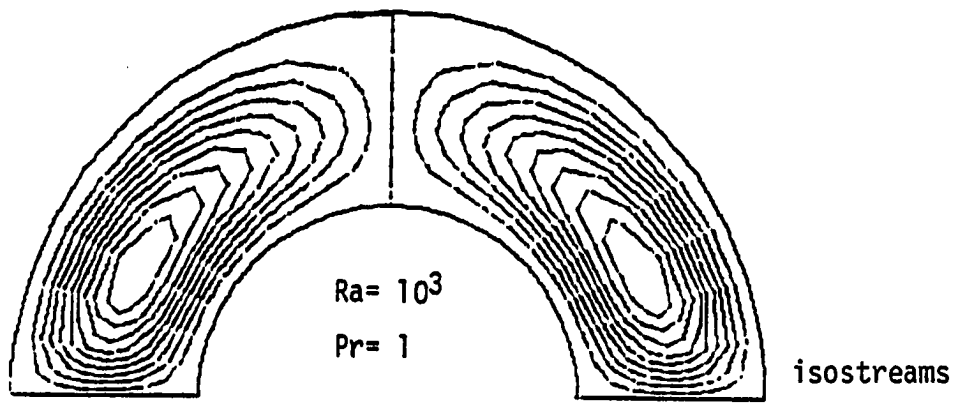


Figure 5.26 Isotherms and isostreams for half annulus placed horizontally: (a) $Ra=1000$ and (b) $Ra=100,000$.

CHAPTER VI

CONCLUSIONS AND RECOMMENDATIONS FOR FUTURE RESEARCH

Various iterative numerical schemes are constructed in order to solve two steady nonlinear problems subject to equality or inequality constraints. Three formulations to incorporate these constraints are developed as a basis for constructing numerical schemes. They are Lagrange multiplier formulation, penalty formulation, and variational inequality formulation. An iterative procedure is necessary for solving problems involving nonlinearity.

In the elastic-plastic torsion problem, an iterative scheme modifying the successive over relaxation method (SOR) is used with base on the theory of variational inequality to incorporate inequality constraint on the stress function (i.e., von Mises yielding criterion). When the inequality constraint is expressed by the explicit form in terms of the stress function (for example, in terms of fully plastic solution), the inequality condition can be taken into the iteration procedure of SOR. However, for general inequality constraints, the use of a Lagrange multiplier is necessary to release an inequality constraint on the stress function. This leads to a saddle point problem (i.e., minimization with respect to the stress function and maximization with respect to the Lagrange multiplier). The saddle

point can be obtained by two-step iteration which first solves for the stress function for a given Lagrange multiplier and then obtains the Lagrange multiplier assuming the stress function. This two-step iteration procedure is also used to satisfy the relation between total torque and the stress function when total torque is given. The optimum acceleration parameter in modified SOR can be found experimentally using the general criterion that the optimum value is the maximum value that makes the solution monotonically convergent. This practical criterion can be applied in any iterative procedure which uses an acceleration parameter.

In the natural convection problem, the penalty formulation to incorporate the incompressibility condition is shown to be efficient to solve the flow for high Rayleigh numbers compared to the stream function-vorticity formulation. In order to obtain a convergent iterative scheme for nonlinear convective terms, the use of an acceleration parameter is very effective. Also, the type of normalization influences the computational efficiency in practice. However, the penalty finite element model tends to give smaller values than those given by the stream function-vorticity model. Importantly, the penalty parameter is sensitive to neither mesh size nor Rayleigh number.

In summary, future research is recommended in the following areas:

- (1) Applications of variational inequality in engineering problems such as determination of the free surface in open channel flow, underground water flow, and determination of contact surface between elastic bodies are strongly desired.

- (2) In relation to the elastic-plastic torsion problem, hardening of material and the unloading process should be studied.
- (3) Also variational inequality can be used to solve two- or three-dimensional plasticity problems.
- (4) The use of the penalty formulation to incorporate the constraint in terms of an integral form should be studied.
- (5) Time dependent and three dimensional analysis of natural convection problems is of great interest.
- (6) Natural convection with free surface is an extremely interesting problem.

BIBLIOGRAPHY

- Arrow, K. J., Hurwicz, L., and Uzawa, H., 1958: Studies in Linear and Non-Linear Programming, Stanford Univ. Press.
- Batchelor, G. K., 1954: Heat Transfer by Free Convection Across a Closed Cavity Between Vertical Boundaries at Different Temperature. Quarterly Journal of Applied Mathematics, Vol. 12, 209-233.
- Bellman, R., 1957: Dynamic Programming, Princeton University Press, Princeton, N. J.
- Bercovier, M., 1978: Perturbations of Mixed Variational Problems, Applications to Mixed Finite Element Methods, R.A.I.R.O., Analyse Numerique/Numerical Analysis, Vol. 12, 211-236.
- Babuska, I., 1971: The Finite Element Method with Penalty, Tech. Note BN-710, The Institute for Fluid Dynamics and Applied Mathematics, University of Maryland.
- Carroll, C.W., 1961: The Created Response Surface Technique for Optimizing Nonlinear Restrained Systems. Operations Research, Vol. 9, No. 2, pp. 169-184.
- Carruthers, J. P., 1975; Crystal Growth from the Melt. Treatise on Solid State Chemistry, Vol. 5, Plenum Press, 325.
- Catton, Y., Ayyaswamy, P. S. and Clever, R. C., 1974: Natural Convection Flow in a Finite Rectangular Slot Arbitrarily Oriented with Respect to the Gravity Vector., Int. J. Heat Mass Transfer, Vol. 17, 173-184.
- Chato, J. C., 1978: Flow and Heat Transfer in Convectively Cooled Underground Electric Cable Systems: Part 1 - Temperature Distributions and Pressure Drop Correlations; Part 2 - Temperature Distributions and Heat Transfer Correlations. J. Heat Transfer, Vol. 100, 30-40.
- Cormach, P. E., Lead, L. G., and Seinfeld, J. H., 1974: Natural Convection in a Shallow Cavity with Differentially Heated End Walls, Part 2, Numerical Solutions, J. Fluid Mechanics, Vol. 65, 231-246.

- Courant, R., 1943: Variational Methods for the Solution of Problems of Equilibrium and Vibrations. Bulletin of the American Mathematical Society, Vol. 49, pp. 1-23.
- _____, 1956: Calculus of Variations and Supplementary Notes and Exercises (Mimeographed Notes), Supplementary Notes by M. Kruskal and H. Rubin, revised and amended by J. Moser, New York University.
- De Vahl, D. G., 1968: Laminar Natural Convection in an Enclosed Rectangular Cavity. Int. J. Heat Mass Transfer, Vol. 11, 1675-1693.
- Duvaut, G., and Lions, J. L., 1976: Inequalities in Mechanics and Physics, Springer-Verlag.
- Elder, J. W., 1965a: Laminar Free Convection in a Vertical Slot. J. Fluid Mechanics, Vol. 23, 77-98.
- _____, 1965b: Numerical Experiments with Free Convection in a Vertical Slot. J. Fluid Mechanics, Vol. 24, 4, 823-843.
- Farshchi, M., 1978: Boundary Layer Regime for Free Convection Flow Between Horizontal Concentric Cylinders. Master's Thesis, Aerospace, Mechanical and Nuclear Engineering, the University of Oklahoma.
- Fiacco, A. V., and McCormick, G. P., 1968: Nonlinear Programming: Sequential Unconstrained Minimization Techniques, John Wiley and Sons, Inc.
- Fichera, G., 1972: Boundary Value Problems in Elasticity with Unilateral Constraints. Handbuch der Physik, Vol. 6 a/2.
- Frisch, K. R., 1954: Principles of Linear Programming - With Particular Reference to the Double Gradient Form of the Logarithmic Potential Method. Memorandum of October 18, University Institute of Economics, Oslo.
- Gartling, D. K., 1977: Convective Heat Transfer Analysis by the Finite Element Method. Computer Meth. Appl. Mec. Eng., Vol. 12, 365-382.
- Geiringer, H. 1973: Ideal Plasticity. Handbuch der Physik, Vol. 6a/3, Springer-Verlag, New York.
- Gill, A. E., 1966: The Boundary Layer Regime for Convection in a Rectangular Cavity. J. Fluid Mechanics, Vol. 26, 3, 515-536.
- Glowinski, R. and Lanchon, H., 1973: Torsion Elastoplastique d'une Barre Cylindrique de Section Multiconnexe. Journal de Mecanique, Vol. 12, No. 1, 151-172.

- _____, Lions, J. L., and Tremolieres, R., 1976: Analyse Numerique des Inequations Variationnelles, Dunod, Paris.
- Gresho, P. and Lee, R.L., 1979: Don't Suppress the Wiggles - They're Telling You Something. (Ed.) Hughes, T.J.R., Presented at the Winter annual meeting of the American Society of Mechanical Engineers, New York.
- Hart, J. E., 1972: Stability of Thin Non-Rotating Hadley Circulation. J. Atmospheric Sci., Vol. 29, 687.
- Heinrich, J. C., Marshall, S. W., and Zienkiewicz, O. C., 1978: Penalty Function Solution of Coupled Convective and Conductive Heat Transfer. Int. Conf. Numer. Mech. in Laminar and Turbulent Flow, Swansea.
- Hellums, J. D. and Churchill, S. W., 1962: Transient and Steady State, Free and Natural Convection, Numerical Solutions. A.I. Ch. E. Journal, Vol. 8, 690-695.
- Hestenes, M. R., 1975: Optimization Theory: The Finite Dimensional Case. Wiley-Interscience, New York.
- Hiddink, J., et al., 1976: Natural Convection Heating of Liquids in Closed Containers. Appl. Sci. Res., Vol. 32, 217.
- Hughes, T. J. R., ed., 1979a: Finite Element Methods for Convection Dominated Flows. Presented at the winter annual meeting of the American Society of Mechanical Engineers, New York.
- _____, T. J. R., Liu, W. K., and Brooks, A., 1979b: Finite Element Analysis of Incompressible Viscous Flows by the Penalty Function Formulation. J. Computation Physics, Vol. 30, 1-60.
- _____, Taylor, R.L., and Levy, J.F., 1976: A Finite Element Method for Incompressible Viscous Flows. Proceedings of the Second International Symposium on Finite Element Method in Flow Problems, Italy, Santa Mergherita Ligure.
- Kikuchi, N., and Oden, J. T., 1979: Contact Problems in Elasticity. TICOM Report 79-7, The University of Texas at Austin.
- Kuehn, T.H. and Goldstein, R.J., 1976: An Experimental and Theoretical Study of Natural Convection in the Annulus Between Horizontal Concentric Cylinders. J. Fluid Mech., Vol. 74, pp. 695-719.
- Lanchon, H., 1970: Sur la Solution du Probleme de Torsion Elastoplastique d'une Barre Cylindrique de Section Multiconnexe. C. R. Acad. Sc., t. 271, series A., 1137-1140.

- _____, 1974: Torsion Elastoplastique d'un Arbre Cylindrique de Section Simplement ou Multiplement Connexe. Journal de Mécanique, Vol. 13, No. 2, 267-320.
- Leitmann, G., 1962: Optimization Techniques: With Applications to Aerospace Systems, Academic Press, New York.
- Lions, J. L., 1971: Optimal Control of System, Springer-Verlag, New York.
- _____, and Stampacchia, G., 1967: Variational Inequalities. Communications on Pure and Applied Mathematics, Vol. 20, 493-519.
- Marshall, R. S., Heinrich, J. C., and Zienkiewicz, O.C., 1978: Natural Convection in a Square Enclosure by a Finite-Element Penalty Function Method Using Primitive Fluid Variables. Numerical Heat Transfer, Vol. 1, 315-330.
- Nadai, A., 1950: Theory of Flow and Fracture of Solids, McGraw-Hill, New York.
- Oden, J. T., and Kikuchi, N., 1979: Theory of Variational Inequalities with Applications to Problems of Flow through Porous Media. TICOM Report 79-4, The University of Texas at Austin, June.
- _____, and Reddy, J. N., 1976: An Introduction to the Mathematical Theory of Finite Elements, John Wiley, New York.
- Ostrach, S., 1972: Natural Convection in Enclosures. Advances in Heat Transfer, Vol. 8, 161-227.
- Ozoe, H., Sayan, H., and Churchill, S. W., 1975: Natural Convection in an Inclined Rectangular Channel of Various Aspect Ratios and Angles -- Experimental Measurements. Int. J. Heat Mass Transfer, Vol. 18, 1425-1431.
- Pedersen, B. D., Doepken, H. C. and Dolin, P. C., 1971: Development of a Compressed Gas-Insulated Transmission Line. I.E.E.E. Winter Power Meeting. Paper 71 TP 193 PWR.
- Petuklov, B. S., 1976: Actual Problems of Heat Transfer in Nuclear Power Engineering. Int. Seminar on Future Energy Production, Hemisphere Publishing Corporation, Washington D.C., 151-163.
- Polyak, B. T., 1971: The Convergence Rate of the Penalty Function Method, Zh. vychisl. Mat. mat. fiz., Vol. 11, pp. 3-11: English translation: U.S.S.R. Computational Mathematics and Mathematical Physics, Vol. 11, pp 1-12.

- Pontryagin, L. S., Boltyanskii, V., Gamkvelidze, R., and Mishchenko, E., 1962: The Mathematical Theory of Optimal Process, Interscience Publishers, Inc., New York.
- Prager, W., and Hodge Jr., P. G., 1951: Theory of Perfect Solids. Wiley, New York.
- Reddy, J. N., 1979a: On the Finite Element Method with Penalty for Incompressible Fluid Flow Problems. The Mathematics of Finite Elements and Applications III, Whiteman, J. R., ed., Academic Press, New York, 227-235.
- _____, 1979b: Penalty Finite Element Methods for the Solution of Advection and Free Convection Flows. Finite Element Methods in Engineering, Kabaila, A. P., and Pulmano, V. A., eds., The University of New South Wales, Sydney, Australia, 583-598.
- _____, 1979c: Penalty Finite Elements: Theory and Application. Research Report No. OU-AMNE-79-6, the University of Oklahoma.
- _____, and Satake, A., 1980a: A Comparison of Various Finite-Element Models of Natural Convection in Enclosures. Journal of Heat Transfer, in press.
- _____, 1980b: On the Mathematical Theory of Penalty-Finite Elements for Navier-Stokes Equations. Third International Conference on Finite Elements in Flow Problems, Banff Center, Banff, Alberta, June 10-13, 1980.
- _____, and Mamidi, D. R., 1978: Penalty Velocity-Stream Function Finite Element Models for Free Convection Heat Transfer Problems. Recent Advances in Engineering Science, Sierakowski, R. L., ed., University of Florida, Gainesville, 381-386.
- _____, and Patil, K. H., 1977: Alternate Finite Element Formulations of Incompressible Fluid Flow with Application to Geological Folding. Wellford, L. C. Jr., ed., 129-190, Proc. Symp. Applications of Computer Methods in Eng., Vol. 1, University of Southern California, Los Angeles.
- Roache, R. J., 1972: Computational Fluid Dynamics, Hermosa Publishers, Albuquerque.
- Rubin, H. and Unger, P., 1957: Motion Under a Strong Constraining Force. Commun. Pure and Applied Mathematics, Vol. 10, 66-87.
- Sasaki, Y. K., 1976: Variational Design of Finite Difference Schemes for Initial Value Problem with an Integral Invariant. J. Comp. Physics, Vol. 21, pp. 270-278.

- Stampacchia, G., 1968: Variational Inequalities. In Theory and Applications of Monotone Operators, Ghizzetti, A., Ed., Proceeding of a NATO Advanced Study Institute held in Venice, Italy, 101-192.
- Szekely, J., and Todd, M. R., 1971: Natural Convection in a Rectangular Cavity. Transient Behavior and Two Phase Systems in Laminar Flow. Int. J. Heat Transfer, Vol. 14, 467-482.
- Tabarrok, B., and Lin, R. C., 1977: Finite Element Analysis of Free Convection Flows., Int. J. Heat and Mass Transfer, Vol. 20, 945-952.
- Tabata, M., 1976: A Numerical Method for the Variational Inequality Including the Elasto-Plastic Torsion Problem, In Theoretical and Applied Mechanics, Vol. 26, 173-178, Proceedings of the 26th Japan National Congress for Applied Mechanics, Japan National Committee for Theoretical and Applied Mechanics Science Council of Japan, University of Tokyo Press.
- Ting, T.W., 1966: Elastic-Plastic Torsion of a Square Bar. Trans Amer. Math. Soc., Vol. 123, 369-401.
- Upson, C.D., Gresho, P.H., and Lee, R.L., 1980: Finite Element Simulations of Thermally Induced Convection in an Enclosed Cavity. Informal Report, UCID-18602, Lawrence Livermore Laboratory, University of California.
- Von Mises, R., 1949: Three Remarks on the Theory of the Ideal Plastic Body. Reissner Anniversary Volume, Edwards, Ann Arbor, Mich.
- Wilkes, J. O., and Churchill, S. W., 1966: The Finite Difference Computation of Natural Convection in a Rectangular Enclosure. Amer. Inst. Chem. Eng. J., Vol. 12, 161-166.
- Young, D. M., 1971: Iterative Solution of Large Linear Systems, Academic Press, New York.
- Zienkiewicz, O. C., 1974: Constrained Variational Principles and Penalty Function Methods in Finite Element Analysis, Lecture Notes in Mathematics: Conference on the Numerical Solution of Differential Equations, edited by G. A. Watson, Springer-Verlag, Berlin, 207-214.
- _____, 1977: The Finite Element Method, Third Edition, McGraw-Hill, New York.

- _____, and Godbole, P. N., 1975: Viscous Incompressible Flow with Special Reference to Non-Newtonian (Plastic) Fluids. Finite Elements in Fluids, Vol. 1, R. H. Gallagher, J. T. Oden, C. Taylor and O. C. Zienkiewicz (eds.), Wiley-Interscience, London, pp. 25-55.
- _____, and Hinton, E., 1976: Reduced Integration, Function Smoothing and Non-conformality in Finite Element Analysis. Journal of Franklin Institute, Vol. 302, 443-461.
- _____, Taylor, R. L., and Too, J. M., 1971: Reduced Integration Techniques in General Analysis of Plates and Shells. Int. J. Num. Meth. Eng., Vol. 3, 575-586.

APPENDIX

NUMERICAL SOLUTION OF $|\nabla\phi|^2 = \tau_p^2$ in $\Omega \subset \mathbb{R}^2$

Consider the wave equation

$$\frac{\partial^2 u}{\partial t^2} - C^2 \left(\frac{\partial^2 u}{\partial x_1^2} + \frac{\partial^2 u}{\partial x_2^2} \right) = 0 \quad (\text{A.1})$$

where C is the wave speed. Let

$$u = u(t - \phi(x)) \quad (\text{A.2})$$

be the solution where $\phi(x)$ is a function to be determined. Let

$$\psi(x, t) = t - \phi(x).$$

Then, (A-1) can be written as

$$\frac{\partial^2 u}{\partial \psi^2} - C^2 \sum_{i=1}^2 \left\{ \frac{\partial^2 u}{\partial \psi^2} \left(\frac{\partial \phi}{\partial x_i} \right) - \frac{\partial u}{\partial \psi} \frac{\partial^2 \phi}{\partial x_i^2} \right\} = 0 \quad (i = 1, 2)$$

Collecting the coefficients of $\frac{\partial u}{\partial \psi}$ and $\frac{\partial^2 u}{\partial \psi^2}$,

$$\left[1 - C^2 \sum_{i=1}^2 \left(\frac{\partial \phi}{\partial x_i} \right)^2 \right] \frac{\partial^2 u}{\partial \psi^2} + C^2 \left(\sum_{i=1}^2 \frac{\partial^2 \phi}{\partial x_i^2} \frac{\partial u}{\partial \psi} \right) = 0 \quad (\text{A.3})$$

It follows then that $\psi(x, t) = \text{constant}$, are the characteristic lines, and that the coefficient of $\frac{\partial^2 u}{\partial \psi^2}$ must vanish:

$$1 - C^2 \sum_{i=1}^2 \left(\frac{\partial \phi}{\partial x_i} \right)^2 = 0 \quad \text{or} \quad |\nabla\phi|^2 = \frac{1}{C^2} \quad (\text{A.4})$$

Thus, $\phi(\underline{x}) = t - \psi(\underline{x}, t) = t + \text{constant}$ is the solution of (A.4) at point \underline{x} for a given t . Suppose that the wave starts at $t=0$ from the boundary and propagates into the domain. The initial condition is $\phi(\underline{x}) = 0$ (which describes the equation for the boundary) and therefore the constant is zero. The function $\phi(\underline{x})$ denotes the time taken by the wave to travel from the boundary to a point \underline{x} . Since the wave speed is C , we must have

$$t = \phi(\underline{x}) = d(\underline{x}, \partial\Omega)/C \quad , \quad C = 1/\tau_p \quad (\text{A.5})$$

where $d(\underline{x}, \partial\Omega)$ is the minimum distance from the boundary $\partial\Omega$ of the domain Ω to the point \underline{x} .

In the numerical scheme, the minimum distance from a given node (in the finite element mesh) to boundary (nodes) is computed, and then $\phi(\underline{x})$ is obtained only at discrete points, namely at the nodal points.